Contributions to improved risk and vulnerability assessment of critical infrastructure

by

Caroline Amy Metcalfe

Thesis submitted in fulfilment of
the requirements for the degree of
PHILOSOPHIAE DOCTOR
(PhD)

University of Stavanger

Faculty of Science and Technology
Department of Safety, Economics and Planning
2020

University of Stavanger
NO-4036 Stavanger
NORWAY
www.uis.no

ISBN: 978-82-7644-966-2
ISSN: 1890-1387
PhD: Thesis UiS No. 558

Preface

This PhD is the result of research carried out in the period September 2016 to January 2020 at the University of Stavanger, with the exception of the work undertaken at the University of Michigan, USA where I was granted the opportunity to be a visiting scholar in the period October 2017 to May 2018. The work has been made possible by funding from the Ministry of Education and Research (Kunnskapsdepartementet) in Norway. The financial support is gratefully acknowledged.

First and foremost, I would like to thank my supervisor Roger Flage. Throughout the entire process you have always provided encouragement and constructive feedback. You are very patient, always ready to provide a more positive outlook during the harder days and happy to share in the joy of the better days. It has been a great privilege to be your PhD student.

Thanks also to my co-supervisor Seth Guikema who was brave enough to let me be part of his research group for 8 months at the University of Michigan. Both you and the group were very welcoming and a great help with the research before, during and after my stay at Ann Arbor. You always know the right questions to ask which help me to refocus on the important aspects of the work and bring attention back to where it is really needed.

I would like to thank the support of my fellow PhD students in the department, both past and present for their continued support throughout my time at UiS. In particular, Kaia Stødle, who is a co-author of one of the papers and was always willing to listen when I needed to bounce ideas or coding problems off someone other than myself. Thanks to Lisbet Fjæran who has been my officemate for the past three years. You have shared in the excitement of articles coming together as well as the frustrated groans when things are not going exactly according to plan. It has been great to be in an office that is mainly filled with laughter (which maybe some of the other students may not appreciate as much as I have).

Finally, Lars Ole Grottenberg, who is always ready a for a tea break in the afternoon to help break up the days and to share a quick discussion on the pros and cons of PhD life, before putting in the last couple of hours of work.

I am also greatly appreciative of my friends and family who have been so supportive throughout the PhD and interested in hearing about the articles I have produced during this time. My parents who although are in the UK, have always been at the other end of the phone when I've needed them and have always encouraged and supported me. My friends for reminding me there is a life outside of the PhD and organising cabin trips, meeting at the gym or swimming and even talking me into signing up for the Trolljeger obstacle course. These days have been a much needed distraction and helped to ground my thoughts when getting too wrapped up in the PhD work.

Finally, Rick. You gave me a needed push to apply for the PhD, even though it meant time apart while I was in Michigan. You have always been ready to listen when needed and know when we need a Saturday spent hiking to reset. I can't put in words how thankful I am to have you by my side, not only through the PhD but every day.

Caroline Johnson

Stavanger, June 2020

Summary

The aim of this thesis is to provide contributions to the assessment of critical infrastructure risk. In particular, the thesis gains insights as to how critical infrastructure is modelled, the role of such models in risk assessment and how to assess risks related to critical infrastructure.

Various governments and scientific articles have proposed a variety of definitions of critical infrastructure. Some countries define critical infrastructure in terms of the service provided by the infrastructure. Other countries, however, define critical infrastructure in the context of societal function. In such cases, critical infrastructure comprises that which is needed to ensure a vital societal function is met. Broadly speaking, critical infrastructure is infrastructure that provides a service that is essential to some society, i.e. a country, region or organisation.

Within modern society, many critical infrastructures are reliant on each other in order to perform effectively. Such interactions between the infrastructures are referred to as dependencies. The term ‘interdependent systems’ is used to refer to a group of infrastructures that interact or depend on each other. When modelling critical infrastructure with the aim of assessing the impacts of disruptions, it is important to account for the dependencies between different infrastructures and how these can cause the effects to cascade throughout the interdependent system.

Network models are commonly used to represent infrastructure systems when simulating the effects of disruptions to infrastructure systems. A network consists of nodes and edges. When modelling infrastructure systems, the nodes represent important components within the system, and the edges, the connections or interactions between such components. Improving methods of assessing infrastructure that contain network models allows for a better assessment of the disruptions of various events that can have negative effects on infrastructure systems and, thus, the associated risk.

Paper I reviews different methods that are used to model interdependencies between different systems, where the systems are represented as networks. The different methods are summarised into categories, based on the structural form of the model; previously, interdependencies were categorised based on the functionality of the dependency. The suggested categorisation of dependencies is twofold. The first is whether the network has full or partial dependency on another; that is, do all nodes in the network have dependencies, or does only a subset have dependencies? The second is whether a node depends on one and only one or multiple nodes in another network. The categories suggested can be referred to when developing models for a simpler way to provide information on how to model the dependencies than the functional categorisations previously suggested.

Paper II investigates the topological properties of a network within an interdependent system that can be used to characterise the network's robustness when an event causes an initial disruption within a network it depends upon. A variety of network sizes and levels of dependencies were explored to provide results that are generalisable to interdependent network systems. The results suggest the important topological properties that should be considered when developing new infrastructure systems or updating existing systems to improve the robustness of the infrastructure against the cascading effects of a disruption within an interdependent system. The topological properties found to be most important are those pertaining to the level of network redundancy.

Although it is important to account for interdependencies when modelling infrastructure, it is equally important that the initiating event be modelled in a way that provides sufficient representation of the event. Paper III suggests an improved method of simulating spatial failures. Current methods simulate spatial failures by failing all components of a network within a specified area, with all components outside the affected area classed as functional. The method suggested in Paper III instead assigns a probability of failure to each component that is dependent on the component's position in relation to the hazard. This provides a more realistic method of simulating spatial failures that is still relatively simple to simulate. Within the paper, the method was applied to independent network systems only, but it can easily be adapted for simulating spatial failures to interdependent systems.

Paper IV develops a model of the dependent electric power and water system of St. Kitts. The aim of the paper is to show that the development of such a model is possible in a poor-data setting context. After developing the model, simulations of tropical storms were used to cause disruptions to the dependent system. These simulations supplied illustrations of how the model can be used to perform analyses that provide useful information when considering improvements to the system. Such analyses included identifying which components of the electric power system are most important to the water system and where best to incorporate redundancy measures such as back-up generators within the water system.

Paper V explores the feasibility of Probabilistic Risk Analysis (PRA) of infrastructure systems. Although PRA aims to provide a complete description of the associated risk, it is not a method commonly used to assess infrastructure. Due to the complexity of modern infrastructure, to carry out a PRA of such systems requires a substantial amount of both time and data. Vast amounts of data can be collected in relation to infrastructure systems, but deciding which data is relevant when performing PRA can also add to the time taken to assess the system. The shortcomings of non-PRA methods currently used to assess infrastructure performance were also discussed. Common shortcomings of non-PRA methods included not considering the likelihood of the scenarios assessed and only considering a subset of the possible scenarios that can affect infrastructure systems. This provides information on how to extend current methods in order to improve critical infrastructure risk analysis.

Table of Contents

List of papers

Paper I	Johnson, C. A., Flage, R., & Guikema, S. D. (2017). Review of network-theoretic approaches to characterise interdependencies in critical infrastructures. In M. Čepin, & R. Bris (Eds.), *Safety & Reliability, Theory and Applications*. Proceedings of the European Safety and Reliability (ESREL) Conference 2017 (Slovenia), Portorož, Slovenia, 18-22 June (pp. 765-772). CRC Press.
Paper II	Johnson, C. A., Flage, R., & Guikema, S. D. (2019). Characterising the robustness of coupled power-law networks. *Reliability Engineering & System Safety*, 191, 106560.
Paper III	Johnson, C. A., Reilly, A. C., Flage, R., & Guikema, S. D. Characterizing the robustness of power-law networks that experience spatially-correlated failures. Accepted for publication in *Journal of Risk and Reliability*.
Paper IV	Stødle, K., Johnson, C. A., Brunner, L. G., Saliani, J. N., Flage, R., & Guikema, S. D. Dependent infrastructure system modeling: A case study of real-world power and water distribution systems. Revised and resubmitted to *Reliability Engineering & System Safety*.
Paper V	Johnson, C. A., Flage, R., & Guikema, S. D. Feasibility study of PRA for critical infrastructure risk analysis. Under revision for invited resubmission to *Reliability Engineering & System Safety*.

Part I

1 Introduction

1.1 Background

With advancements in technology, societies, especially in developed countries, become increasingly reliant on critical infrastructure. It is only when something goes wrong that we become aware of how much critical infrastructure is a part of everyday life and how a significant disruption can affect the normal rhythm of a region. These disruptions can be caused by both internal and external events. Examples can be seen in infrastructure such as electric power systems, where outages are caused either by internal disruptions such as the tripping of transmission lines in Italy in 2003 (Corsi and Sabelli 2004) or by external events like the 1998 ice storm in North America (Chang et al. 2007). The recent occurrence of events that have the potential to cause large-scale disruptions has led to an increased focus on how to analyse infrastructure to aid in preparing for and protecting against such events.

Although critical infrastructure is a commonly used term, there are many definitions of what exactly is meant by critical infrastructure and which infrastructures are considered to be critical. Table 1 contains some definitions, demonstrating the range of variability in how critical infrastructure is defined. Depending on whether the definition is proposed by a government or within a scientific article, there are some differences in the focus of the definition. This is also true when considering the background or focus of the article defining critical infrastructure. A basic high-level definition of critical infrastructure which encompasses the many definitions available is an infrastructure that provides a service that is essential to some society, i.e. a country, region or organisation.

Table 1: Definitions of critical infrastructure from various sources.

Definition	Source	Source type
"Infrastructure is the basic systems and services, such as transport and power supplies, that a country or organisation uses in order to work effectively."	Cambridge Dictionary, Walter (2008, p. 741)	Dictionary
"Critical infrastructure is the systems, assets, facilities and networks that provide essential services and are necessary for the national security, prosperity and health and safety of the nation."	Public Safety and Emergency Preparedness Canada (2014, p. 2)	Government
"Critical infrastructure are the facilities and systems that are absolutely necessary to maintain the critical functions of society which in turn cover the basic needs of society and the sense of security of the population."[1]	NOU (2006:6, p. 32)	Government
"Critical infrastructure are the organisations delivering goods and services in an economy that is fundamental to the functioning of society and the economy."	Macaulay (2008, p. 8)	Literature
"Critical infrastructure are large, spatially-distributed systems with high degrees of complexity."	Johansson and Hassel (2010, p. 1335)	Literature
"Critical infrastructure are defined by their role in society: they support the services that are vital for life and sustainable economic growth."	Comes and Van de Walle (2014, p. 190)	Literature

In Norway, critical infrastructure is defined in the scope of vital societal function. The definition is seen in the third row of Table 1 as given by NOU (2006:6). The Norwegian Directorate for Civil Protection (Direktoratet for Samfunnssikkerhet og Beredskap, DSB) defines vital societal function as "functions that society could not cope without for seven days or less without this threatening the safety and/or security of

[1] This is a translation of the definition given in Norwegian by NOU (2006:6, p. 32).

the population" (DSB 2017). To put this definition into context, consider the following example. If having access to food is classified as a function that society could not cope without for seven days, the infrastructure needed in order to have access to food includes:

- transportation: in order to travel to where the food is, as well as the ability for food to be transported throughout the society,
- electricity: in order to both store and cook the food,
- communication: in order to receive information on where is food available.

These are just a few examples of critical infrastructure needed for society to have access to food. Others, such as financial institutions' ability to purchase food, could also be included, depending on the situation and the interpretation of the definition. This view enables thought of how disruptions to infrastructure may affect society but also allows the infrastructure defined as critical to change, depending on the situation.

When using critical infrastructure definitions that focus more on physical systems, deciding which infrastructures are critical also differs from country to country. Critical Five is an international forum, comprising members from government agencies from five countries that are responsible for critical infrastructure protection and resilience. The five countries are Australia, Canada, New Zealand, USA and UK. In 2014, they published a report entitled, "*Forging a Common Understanding for Critical Infrastructure: A Shared Understanding*", providing a comparison of which infrastructure is categorised as critical within the five different countries. They found that all five countries categorised the following infrastructure as critical: energy systems, communication systems, water systems (including wastewater and storm water systems), transportation and healthcare. Other infrastructure considered by some of the five countries to be critical includes banking, education, food and agriculture and government facilities (Public Safety and Emergency Preparedness Canada 2014).

Introduction

After the importance of critical infrastructure became more recognised in governmental policies and the literature of how to analyse and protect infrastructure became more widespread, the importance of the interdependencies between systems then emerged as an important aspect to be considered. Interdependence is often used to describe a group of infrastructure systems in which interactions are needed between the systems for all to function. Rinaldi et al. (2001) state that, for systems to be interdependent, the relationship between the systems needs to be bidirectional. This means that any two systems need to directly depend on each other to be considered interdependent.

Many authors have suggested different ways to categorise infrastructure interdependencies, some of which have been compared by Ouyang (2014, Table 1). The most commonly referred to categorisation is that proposed by Rinaldi et al. (2001), who suggested four types of interdependencies: physical, cyber, geographic and logical. Physical interdependencies are those where an infrastructure depends on some physical input from another. This can be electrical power, water or fuel. Cyber interdependencies cover the input of data or information from one system to another. Geographic interdependencies account for the physical proximity of infrastructures such that, if a disruption occurs within a given region, the systems, or parts of the systems within the area, will all be affected. The final category, logical, covers all other interdependencies that cannot be categorised as one of the previous three types and includes legislation, policy and human behaviour.

A simple example of how interdependencies can exacerbate the effects of a disruption can be seen from when a blackout occurred in the Italian electric power system in 2003. As mentioned previously, the tripping of transmission lines resulted in the separation of Italy from the Continent (Corsi and Sabelli 2004). This resulted in a loss of power to areas of the Internet communication network. The loss of communication caused further failures within Italian power stations, increasing the disruption of the initial outage (Buldyrev et al. 2010). If interdependencies, such as the example given here, are not taken into account, the effects of the disruptions can be underestimated.

The importance of critical infrastructure within society, as well as the costs associated with downtime and major repairs for the owners and operators, highlights why risk assessment of the systems is crucial. Understanding how different scenarios, whether they are natural disasters, intentional disruptions or cascading effects due to dependencies, can help the operators of such systems decide how best to protect against and prepare for interruptions within the infrastructure.

Probabilistic Risk Analysis (PRA) was developed in the 1970s to assess infrastructure systems, specifically nuclear power plant systems. The aim of PRA is to present a full description of the assessed system's risk, with results of all possible scenarios presented in a way that allows for easy comparison. However, the method is currently not commonly used to assess infrastructure systems, with more recently developed methods being preferred. With modern infrastructure systems becoming increasingly complex due to increased demand from society and advances in technology, PRA also becomes more complex. Even for relatively small infrastructure systems, considerable amounts of data and information are required for PRA to be performed, which may contribute to PRA's lack of popularity for assessing infrastructure systems.

There are many, more recent non-PRA, methods of modelling critical infrastructure systems, including network-based, inoperability input-output and agent-based models (Ouyang 2014). Such methods focus on the performance of the system given the occurrence of an event and can be extended to include interdependencies between infrastructure systems. The use of such models within risk assessment can be useful when planning new infrastructure or upgrades to existing systems. They provide information to those making decisions on how to better protect infrastructure from disruptive events. Therefore, it is important that the results of such models adequately communicate the risks/potential disruptions associated with infrastructure systems.

1.2 Objectives

The overall objective of this thesis is to gain insights on critical infrastructure and its modelling, and to provide guidance on how to assess and manage risk related to such infrastructure. Specifically, the thesis addresses the following sub-objectives:

- To understand the extent to which network-based approaches for modelling infrastructure interdependencies and their associated metrics are relevant for evaluating the effects of cascading disruptions.
- To understand the robustness of interdependent power-law networks to random failures and independent power-law networks to spatially correlated failures.
- To demonstrate that it is possible in a low-data setting to produce a simple model of a real-world dependent infrastructure to support risk management decision-making.
- To investigate the feasibility of probabilistic risk assessment (PRA) methodology for the analysis of infrastructure systems.

1.3 Scientific approach/Research methods

The Norwegian Research Council proposes that quality research is linked to the following three aspects (NRC 2000):

- Originality
- Solidity
- Relevance.

The presented work in this thesis covers these aspects in the following way. The work is original in that is presents new methods for assessing infrastructure performance, as well as using existing methods in a different manner. The work is solid, as it provides a clear explanation of any methods or data, is based on existing literature and has been or will be peer reviewed. It is relevant, as it provides information that aims to further the field of infrastructure risk assessment and explores some gaps within this field, as well as providing methods that are generalisable.

Kothari (2004) suggests several basic categorisations of research: descriptive vs analytical, applied vs fundamental, quantitative vs qualitative and conceptual vs empirical. The research presented is analytical, applied and fundamental, conceptual and both quantitative and qualitative. It is analytical, as is aims to describe "the world", as well as to analyse and understand such situations. This research is fundamental in that it is mainly concerned with generalisations. However, there is also an applied element of the research in which generalisations are applied to specific situations, for example, the case study of St. Kitts' electric power and water system or analysing the risk associated with a drinking water distribution system. Although the research is mainly quantitative, with the use of simulation approaches to generate relevant data and information of infrastructure systems, it is also qualitative, through its discussion of the practicalities and feasibility of methods and models within risk analysis. Finally, the research is conceptual, as it aims to generate knowledge that is related to concepts for risk analysis, namely, improvements for risk assessment within the area of critical infrastructure.

The characteristic of replicability is highlighted as being an important quality of research by Kothari (2004) and is specifically relatable to the description of models and simulations in this research. The explanation of the method used to produce the models and simulation procedures should be clearly stated, so that others can follow these descriptions and produce the same results as found in the papers.

This thesis follows the structure of a "PhD by publication" (Park 2007), which consists of two parts: a scientific contribution that consists of individually published papers (Part II of this thesis) and an introduction that places the published papers in a broader context within the area of risk analysis (Part I).

1.4 Thesis structure

This thesis has two parts. Part I describes the background, objectives, research methods, main contributions, and potential future directions of the research presented in the thesis. Among the main purposes of Part I are to motivate the performed research, to present and tie together the scientific contributions, and to frame these in the broader context of relevant related literature. Part I thus provides a summary of and context for Part II, which consists of a collection of papers that present and make up the scientific contributions of the thesis.

Specifically, Part II consists of five papers. Two of these papers are already published; one paper is published in the peer-reviewed proceedings of the European Safety and Reliability (ESREL) conference, and one paper is published in the peer-reviewed journal, *Reliability Engineering & System Safety*. Two papers have been revised and resubmitted to peer-review journals. The final paper is currently being revised to be resubmitted to a peer-reviewed journal.

The remainder of Part I is organised as follows. Section 2 summarises and contextualises the contributions of the scientific papers in Part II. Section 3 then outlines some ideas for further research, building on the scientific contributions of the thesis papers.

2 Research areas and problems

This section presents the main scientific contributions of the papers presented in Part II of the thesis. The five papers included in Part II address the thesis objectives stated in Section 1.2 in the following way:

- To understand the extent that network-based approaches for modelling infrastructure interdependencies and their associated metrics are relevant for evaluating the effects of cascading disruptions.
  - Paper I: Review of network-theoretic approaches to characterise interdependences in critical infrastructure.
- To understand the robustness of interdependent power-law networks to random failures and independent power-law networks to spatially correlated failures.
  - Paper II: Characterising the robustness of coupled power-law networks.
  - Paper III: Characterizing the robustness of power-law networks that experience spatially-correlated failures.
- To demonstrate that it is possible in a low-data setting to produce a simple model of a real-world dependent infrastructure to support risk management decision-making.
  - Paper IV: Dependent infrastructure system modeling: A case study of real-world power and water distribution systems.
- To investigate the feasibility of probabilistic risk assessment (PRA) methodology for the analysis of infrastructure systems.
  - Paper V: Feasibility study of PRA for critical infrastructure risk analysis.

When assessing critical infrastructure, the main focus in the literature is on the performance of the system or systems given some event. The event may be specified, for example an earthquake disrupting an interdependent electric power and gas system, as presented by Dueñas-Osorio et al. (2007), or more generally modelled as random failures within the system, as presented by Johansson and Hassel (2010). The first three objectives are concerned with how to improve some of the current methods for assessing the performance of infrastructure when events disrupt such systems.

Improvements to the methods of simulating disruptions within infrastructure systems, both independent and interdependent, lead to better estimations of how events can affect systems. However, when trying to improve such methods, the implementation needs to be affordable, in terms of the computational power required and the time taken to run the simulation. A balance needs to be found between the level of detail and the time- and computation expense of performing the assessment. When suggesting improvements to current methods of assessing infrastructure performance, this has been taken into account.

There is also a need to expand on assessing the effects of events to infrastructure systems, to include the likelihood of such disruptive events occurring and extending the methods to better incorporate/state the uncertainties associated with the simulated consequences. This provides a more comprehensive description of the system's risk, with more information that allows for risk mitigation measures to be implemented that are based on a broader knowledge base. An example of this is that, when only looking at the magnitude of the consequences, one disruption may cause a much larger disruption than others and should be addressed; however, when the likelihood of the event and uncertainties associated with the magnitude of consequences are also assessed, another mitigation procedure could reduce the overall risk of the system (Kaplan and Garrick 1981).

One such method that aims to provide a complete risk description is PRA. For some industries, such as nuclear power generation, offshore petroleum activities and air transportation, PRA is used to provide a description of the risk (Aven et al. 2013). However, in all other industries, PRA is not commonly used to assess infrastructure risk. Investigating the reasons why PRA is not a common tool for the assessment of infrastructure systems provides direction on where improvements can be made, in order to better infrastructure assessment.

The remainder of the section is structured as follows. Section 2.1 first describes network models and their use in representing critical infrastructure, before presenting the scientific contribution of Papers I – IV within the subsections. Section 2.2 provides some background on the method of PRA, before presenting the scientific contribution of Paper V.

2.1 Network-based approaches for modelling critical infrastructure

Network models are a popular choice to represent infrastructure systems, as the structure or topology of the system is included in the network. A network or graph is composed of nodes (or vertices) and the connections between them, which are referred to as edges (or links) (Newman 2010). The nodes represent the (important) components of the infrastructure, and the edges, the connections between the components (Ouyang 2014). In most cases, the edges represent physical connections, such as transmission or distribution lines within an electrical power system or water pipes within a water system, but they can also represent other connection types such as the need for information from one component to another.

When the network is not constructed based on a specific infrastructure system, there are three main types of networks that are commonly used to assess the effect of disruptions to network systems. The first is random networks, where the size of the network, that is the number of nodes within the network, is defined and the probability that an edge exists between each pair of nodes is the same (Barabási and Albert 1999). The second type is small-world networks, which are also referred to as Watts-

Strogatz networks (Watts and Strogatz 1998). To construct a small-world network, a regular network is first formed with v nodes, each of which is connected to its n closest neighbours. Then, with probability p, an edge is removed and replaced with one that joins two uniformly randomly chosen nodes. The final type is power-law networks, where the nodal degree distribution follows that of a power-law distribution. Both random and small-world networks produce networks that have a homogeneous nodal degree, with most nodes having approximately the same number of edges, whereas power-law networks produce non-homogeneous networks, with the majority of nodes having a low number of edges and a few nodes having a high nodal degree (Albert et al. 2000).

Power-law networks have been extended to include an exponential cutoff such that the nodal degree distribution follows that of a power-law distribution with exponential cutoff (Barabási et al. 1999). This is popular for modelling networks, as it incorporates how “expensive” it can be to add edges to a node with a high nodal degree, which is often the case in real network systems.

Network models were first used to investigate the effects of disruptions to independent networks (e.g. Callaway et al. 2000, Cohen et al. 2001, Holme et al. 2002, Motter and Lai 2002), that is networks that are self-sufficient and do not require input from other networks, before being extended to model “system of systems” models that include multiple network systems and account for interdependencies between the systems (e.g. Buldyrev et al. 2010, Gao et al. 2012, Schneider et al. 2013).

2.1.1 Independent network-based models

Although it is important to account for interdependencies when modelling infrastructure systems as networks, the initial impact of an event on each infrastructure needs to be sufficiently simulated and, in some cases, the initial disruption to network systems may occur in only one of the networks. Improving methods of simulating failures in independent networks can first be focused on, before applying the failure simulation methods to interdependent networks. The main methods of initiating disruptions in network models are random failures and spatial failures. When modelling random failures, the initial disruption is modelled by removing a percentage of the nodes (or edges) in the network that are randomly chosen; that is, each node has the same probability of failure (Holme et al. 2002). Random failure simulations can be used to assess situations where the initial disruption is caused by internal disruptions, e.g. component failure due to age or lack of maintenance.

Spatial failures allow initial disruptions that are caused by a geographic event, including earthquakes or adverse weather such as hurricanes. Spatially localised failures, as discussed in the introduction of Paper III, provide a simple starting point to model spatial failures. Localised failure methods assume that all nodes (and/or edges) within a specified area of the network are disrupted; that is, all nodes (edges) in the affected area have a probability of failing of 1, and all nodes (edges) outside the area have a failure probability of 0 (e.g. Jenelius and Mattsson 2008, Hu et al. 2016, Ouyang et al. 2019).

To extend the assessment of the impacts of spatial failures, Paper III presents a method to model spatially correlated failure events. Rather than specifying an area within the network in which all nodes fail, each node is assigned a failure probability that is dependent on its position in relation to the hazard. Different hazard scenarios were simulated with varying degrees of strength and position of the epicentre in relation to the network. The robustness of a range of power-law networks with exponential cutoff was assessed given the occurrence of spatially correlated failures. Here the robustness was measured as the fraction of nodes that were functional after the disruption occurred. The results of the disruption simulations were used to study the relationship between the topological properties of the networks and their robustness to spatially correlated failures. Topological properties of a network are properties that provide various information about the structure of the network.

When exploring the relationship between the topological properties of the network and its robustness to spatially correlated failures, in Paper III, several network topological properties were found to be significant when characterising network robustness. To find which topological and hazard properties were significant in characterising network robustness, a regression analysis was carried out, where the possible explanatory variables were the mean, minimum, maximum and standard deviation of the four topological properties presented in Table 2, as well as the two hazard properties also given in Table 2. The observed response variable in the regression analysis was network robustness to each hazard scenario, given as the fraction of functional nodes at the end of each simulation of spatially correlated failure. Table 2 gives a brief overview of the significant topological properties, as well as two properties of the spatial hazard that were also significant when characterising network robustness.

Table 2: Significant topological and hazard properties for characterising the robustness of power-law networks to spatially correlated failures, as found in Paper III.

Topological and hazard properties investigated		Brief description	Significant properties
Topology properties	Nodal degree (k)	Number of connections a node has. Gives an indication of network redundancy.	Mean k
	Betweenness centrality (Cb)	Fraction of shortest paths that pass through the node. Gives an indication of node criticality.	Mean Cb Maximum Cb
	Clustering coefficient (C)	Measure how well the neighbourhood of a node is connected, where two nodes are neighbours if an edge between them exists. Gives an indication of local redundancy.	Mean C C standard deviation
	Path length (l)	Shortest path length between each nodal pair, i.e. the path that traverses the least number of edges.	Maximum l l standard deviation
Hazard properties	Distance	Distance of the hazard epicentre from the centre of the network.	Distance
	Covariance	Measure of the spatial variance of the hazard. The greater the covariance the more concentrated the hazard.	Covariance

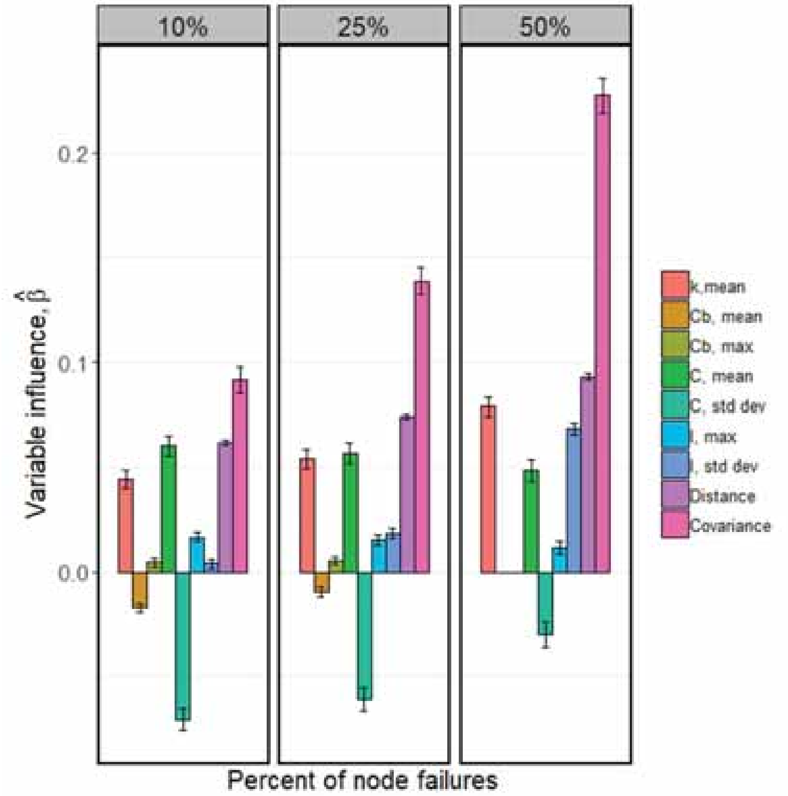

Figure 1: The influence of the significant topology measures on the robustness of the networks for 10%, 25% and 50% of node failures, as shown in Paper III (Johnson, Reilly et al. submitted p.8, Figure 1). The influence is given by the $\hat{\beta}$ value from the regression model.

Figure 1 shows the influence of the significant properties in characterising network robustness to spatially correlated failures. Variables with a positive influence indicate that the more this value increases, the more robust the network is to spatially correlated failures. Variables with a negative influence indicate that, as their value increases, the robustness of the network decreases. The distance of the hazard from the centre of the network unsurprisingly had a positive influence on network robustness, indicating that the further the hazard epicentre is from the centre of the network, the more robust the network is.

Therefore, if a hazard epicentre is known, or can be estimated, for example in earthquake scenarios, then the positioning of the network system to the epicentre should be considered when designing new systems. The results indicated that the same network topological properties were significant in characterising network robustness to spatially correlated failures, as those that were found by LaRocca and Guikema (2015) to be significant when characterising network robustness to random failures. The most influential topological properties for both random and spatially correlated failures are the mean nodal degree and mean clustering coefficient. These properties provide some indication of the global and local redundancy of the network, respectively. These results can be taken into account by infrastructure management when designing new systems or upgrading existing systems, with the aim of increasing the robustness of the system to both random and spatially correlated failures.

Paper III thus provides an alternative method of simulating spatial failures to the localised failure method. Our alternative method assesses the impacts of spatial failures on a network in a more realistic manner that is easy to implement with a low computational burden. This allows those assessing infrastructure systems to assess which areas of the system are more susceptible to spatially correlated failures, therefore indicating areas where improvements could be made to increase robustness.

2.1.2 Interdependent network-based models

With the increased attention on the assessment of critical infrastructure in relation to events that have the potential to cause large outages, the need to account for interdependencies between infrastructure systems was called into focus (e.g. Rinaldi et al. 2001, Dudenhoeffer et al. 2006, Buldyrev et al. 2010). Acquiring data about infrastructures to model the system itself is difficult, due to many being privately owned utilities that view sharing such information as a safety and security issue (Rinaldi et al. 2001, Macaulay 2008, Winkler et al. 2010). Incorporating interdependencies into infrastructure models is equally difficult, given that it requires data from multiple systems in order to provide a realistic model. Given the difficulties in modelling real systems, theoretical interdependent models were suggested in the literature, to construct models that represent a system of systems (Parshani et al. 2011, Shao et al. 2011, Havlin et al. 2015).

When referring to the different edges or connections in interdependent models, a distinction between the edges within each network and between the networks can be made. Edges within one network are referred to as intra-connections, whereas the edges between networks, which represent the interdependencies, are referred to as inter-connections. Inter-connections can be modelled to be unidirectional or bidirectional. When a dependency exists between two nodes of different networks which are both dependent on each other, the dependency is said to be bidirectional. When the dependency only exists where one node depends on input from a node in another network, the dependency is said to be unidirectional.

2.1.2.1 Categorising interdependencies in network-based models

In Paper I, different methods suggested in the literature for modelling interdependencies in network-based models were reviewed, as well as the metrics used to assess the effects of disruptions in interdependent systems. The first categorisation for how interdependencies are modelled was fully or partially dependent. In fully dependent models, each node in a network is dependent on input from another network. In partially dependent models, only a fraction of nodes in a network are dependent on nodes in other networks. These two categories were then subcategorised by single or multiple dependencies per node. In models with single dependencies, each node that is dependent on another network has one and only one inter-connection. Models with multiple dependencies allow inter-connections to form, such that each node that is dependent on another network can have multiple inter-connections. Most of the literature reviewed focused on modelling two interdependent systems, with few papers suggesting methods of extending interdependent models to systems containing more than two networks.

Although others have suggested categories of interdependencies, these categories are descriptions of the functionality of dependencies found between infrastructures. For example, Rinaldi et al. (2001) suggested four types of interdependencies: physical, cyber, geographic and logical. Others have suggested similar categories, including functional or spatial by Zimmerman (2001) and physical, geospatial, policy or informational by Dudenhoeffer et al. (2006). Paper I aims to categorise the dependencies, not on the functionality of the dependency but based on the structure of the interdependent systems. When creating an initial model to see whether it is of use to investigate the interdependent system further, it is important that the structure is a good representation of the interdependent system, regardless of dependency functionality.

Table 3 shows the methods of forming inter-connections between interdependent networks. Random attachment is when the inter-connection is randomly assigned between nodes of different networks. When the model contains only two networks that are both fully dependent with single dependencies, the networks must be the same size, i.e. contain the same number of nodes. Buldyrev et al. (2010) presented this model to demonstrate the need to account for interdependencies between networks, and so the model is simple to construct and not representative of real infrastructure interdependencies. This model was then extended such that the dependencies were formed due to some condition. Both Parshani et al. (2011) and Buldyrev et al. (2011) suggested that nodes were more likely to be dependent on other nodes with the same nodal degree. Buldyrev et al. (2011) suggested that each inter-connection be formed between two nodes with the same nodal degree. Thus, the distribution of nodal degree must be the same in both networks within the system. Parshani et al. (2011) suggested a method of forming dependencies with an inter degree-degree correlation of r_{AB}; that is the percentages of inter-connections that form dependencies between nodes with the same degree is r_{AB}.

Table 3: Methods for forming inter-connections found in the literature, as described in Paper I.

Fully or partially dependent networks	Dependencies per node	
	Single	Multiple
Fully dependent networks	Random or conditional attachment	Random or preferential attachment
Partially dependent networks	Random	Conditional preferential

For methods where each node with a dependency can have multiple inter-connections, preferential attachment is modelled such that the inter-nodal degree distribution follows a power-law distribution. The inter-nodal degree is the number of inter-connections a node has. The inter-connections are formed such that it is preferential for dependent nodes to depend on a node with a high nodal degree. In such cases, the dependencies can be formed preferentially, based on either inter-nodal degree or total nodal degree (i.e. the summation of both intra and inter-nodal degrees). Conditional preferential attachment applies when there are more than two networks within the system and accounts for the structure of the system of systems. For example, there can be one network which forms a hub for all other networks in the system. In this case, the hub network is dependent on all other networks in the system. All other networks are only dependent on the hub network.

Within the literature reviewed in Paper I, the main metric used to evaluate the effects of disruption to an interdependent network system is the giant connected component (GCC). After the disruption and cascading effects have been simulated, the system fragments into several smaller subsystems. The GCC is the subsystem which contains the greatest number of nodes (Shao et al. 2015). To allow for easy comparison between networks of different sizes, the relative GCC is often used. The relative GCC gives the percentage of nodes that are present in the GCC rather than the number, which can then be compared to the relative GCC of other networks. The relative GCC can be evaluated either individually for each network in the modelled system or for the system as a whole.

The different methods of forming interdependencies between networks allow for a variety of systems to be analysed. When modelling real systems, the most relevant method of forming dependencies can be chosen to construct the model. Some methods are easier to construct than others, e.g. fully dependent models with single dependencies, but are less representative of real systems than those that are more complex to construct. The interdependency method to be used should be chosen in relation to the time and resources available, as well as the purpose of the analysis. For an initial analysis, a less complex model may be used as a starting point, to see if a more in-depth analysis needs to be performed.

2.1.2.2 Robustness of interdependent networks

When investigating interdependent network systems, the focus of the analysis is mainly how disruptive an event is to the system, where, as previously discussed, the GCC or relative GCC is used to measure the level of disruption. Paper II investigates whether the robustness of coupled networks can be characterised by the topological properties of the network, as previously explored for independent networks by LaRocca and Guikema (2015).

The effects of network topology on the robustness of interdependent networks have previously been investigated. However, this usually involves ranking the nodes of the network according to a certain topological property and using this ranking to identify nodes to remove, in order to simulate a targeted attack on the interdependent system. Both Motter and Lai (2002) and Huang et al. (2011) used nodal degree to rank nodes before removing the highest ranked nodes to simulate targeted attacks. Zhang and Peeta (2011) investigated both nodal degree and betweenness centrality (which they referred to as “load”) as a measure of node importance, while Chai et al. (2016) also included shortest path; both authors then explored the differences in system robustness to targeted attacks for the different node rankings. Rather than focus on only one topological property, Paper II aims to characterise the robustness of coupled networks, using a collection of topological properties, providing a relationship that is generalisable to a range of coupled network structures.

In order to investigate the relationship between the robustness of networks in interdependent systems and topological properties, several different interdependent systems were explored. Each system contained two networks of equal size (i.e. equal number of nodes), ranging from 100 nodes to 1000 nodes, hereafter referred to as Network A and Network B. Both networks in the system were power-law networks with exponential cutoff. All dependencies formed between the two networks were bidirectional. Both dependent and interdependent systems were explored, to allow the results to be generalisable for a range of coupled systems. In the dependent systems, Network A was dependent on Network B, and Network B was independent, whereas, in the interdependent systems, Networks A and B were both dependent on each other. The inter-connections were formed conditionally on the closest node in the dependent system, where both networks occupied the same space and coordinates were assigned to each node.

As Network A is always dependent on Network B, Paper II explored the robustness of Network A to random failures in Network B. All initial disruptions occurred in Network B and were modelled by choosing a percentage of nodes randomly that would fail. Three levels of disruption in Network B were considered: 10%, 25% and 50%. To simulate these initial failures, the chosen nodes were removed from the network, causing the network to fragment. Systems where Network B both did and did not contain source nodes were investigated, with two different methods of simulating failures used, depending on the presence of source nodes. Source nodes are nodes which need to be functional in order for the network to function. This is representative of systems, such as electric power systems, where the source nodes represent the power plants generating electricity.

When source nodes are not present in the model, the GCC is considered the only functional cluster in the network after the initial disruption, as described above. All nodes in Network A that are dependent on non-functional nodes in Network B are also considered non-functional. This causes Network A to fragment, and only nodes in the GCC are considered functional. If Network B depends on Network A, any nodes in Network B dependent on non-functional nodes in Network A are now also non-functional. This process iterates until no additional node failures occur.

When source nodes are present in Network B, after the initial random failures (as previously described), only the clusters that contain source nodes are functional; all other nodes are non-functional. The disruptions then cascade into Network A as before, where all nodes dependent on non-functional nodes in Network B are considered non-functional, causing fragmentation within Network A. Any clusters in Network A that receive input from functional nodes in Network B are considered functional, with all other clusters considered non-functional. If Network B depends on Network A, any nodes dependent on non-functional nodes are then considered non-functional, causing further fragmentation. The process iterates again until no more node failures occur.

The level of dependency was also varied, to allow the relationship of topological properties and network robustness to be explored. For both dependent and interdependent systems, the levels of dependency were modelled as either fixed or random. For fixed levels of dependency, the percentage of nodes that were dependent on the other network in the system was predefined as either 10%, 30%, 50% or 100%. For random levels of dependency, the percentage of nodes with dependencies in each network was randomly assigned by drawing a variable from a uniform distribution with a range of 1 to 100. Table 4 shows the different levels of dependency explored.

Table 4: Summary of dependency types modelled in Paper II.

Type of dependency Network A has on Network B	Type of dependency Network B has on Network A	Percentage of source nodes in Network B
Fixed, 10%	-	-
Fixed, 30%	-	-
Fixed, 50%	-	-
Fixed, 100%	-	-
Fixed, 50%	Fixed, 50%	-
Random	-	-
Random	-	2
Random	-	5
Random	-	10
Random	Random	-
Random	Random	2
Random	Random	5
Random	Random	10

The topological properties investigated to characterise the robustness of coupled networks included the mean, minimum, maximum and standard deviation of the nodal degree, betweenness centrality, clustering coefficient and path length. The same properties were investigated in Paper III and by LaRocca and Guikema (2015), and are described in Table 2. Three additional topological properties were also included in the analysis of Paper II that accounted for the properties of the dependencies and source nodes. The first two additional properties are related to the dependencies. When the level of dependency was randomly assigned, the percentage of dependent nodes in the network was included. The mean intra-nodal degree of dependent nodes was also included as a topological property. The final additional property included in the analysis was the mean nodal degree of source nodes, which was included when source nodes were present in Network B.

Following the method used in Paper III, a regression analysis was used to find which topological properties are significant in characterising the robustness of coupled networks. A regression analysis was performed that included the topological properties of Network A but not those of Network B. This is representative of the data available when assessing real-world systems, as an infrastructure system will likely know its own structure but does not necessarily know the structure of the network systems it depends on.

Figure 2, Figure 3 and Figure 4 show the significant topological properties, as found in the regression analyses of the various coupled networks investigated in Paper II. For all the different types of coupled network systems investigated, three topological properties of Network A were always significant for characterising the robustness: mean nodal degree, mean intra-nodal degree of dependent nodes and, when applicable, the percentage of dependent nodes in the network. Mean nodal degree had a positive influence on the robustness of the network to cascading failures. This is as expected, as the mean nodal degree indicates the level of redundancy within a network: therefore, the greater the mean nodal degree, the greater the level of redundancy in the network. The mean intra-nodal degree of dependent nodes had a negative influence on the robustness. Again, this is as expected, as the disruption cascades from Network B into Network A through the dependent nodes. The greater the number of nodes within Network A that are connected to the dependent nodes, the greater the effect the disruption has on Network A. The level of dependency also had a negative influence on network robustness. This again is intuitive, as the more nodes in Network A that depend on Network B, the greater the chance of nodes in Network A being affected by the disruption that initiates in Network B.

When the level of dependency was fixed within the coupled networks, the mean clustering coefficient, nodal degree standard deviation and path length standard deviation are always significant and have a weak influence on network robustness. Mean clustering coefficient has a positive influence, whereas mean standard deviation and path length standard deviation both have a negative influence. When source nodes are present in Network B, path length standard deviation of Network A is no longer significant. Mean clustering coefficient and nodal degree path length are still significant, but the influence of each is reversed such that they have a weak negative and positive influence, respectively.

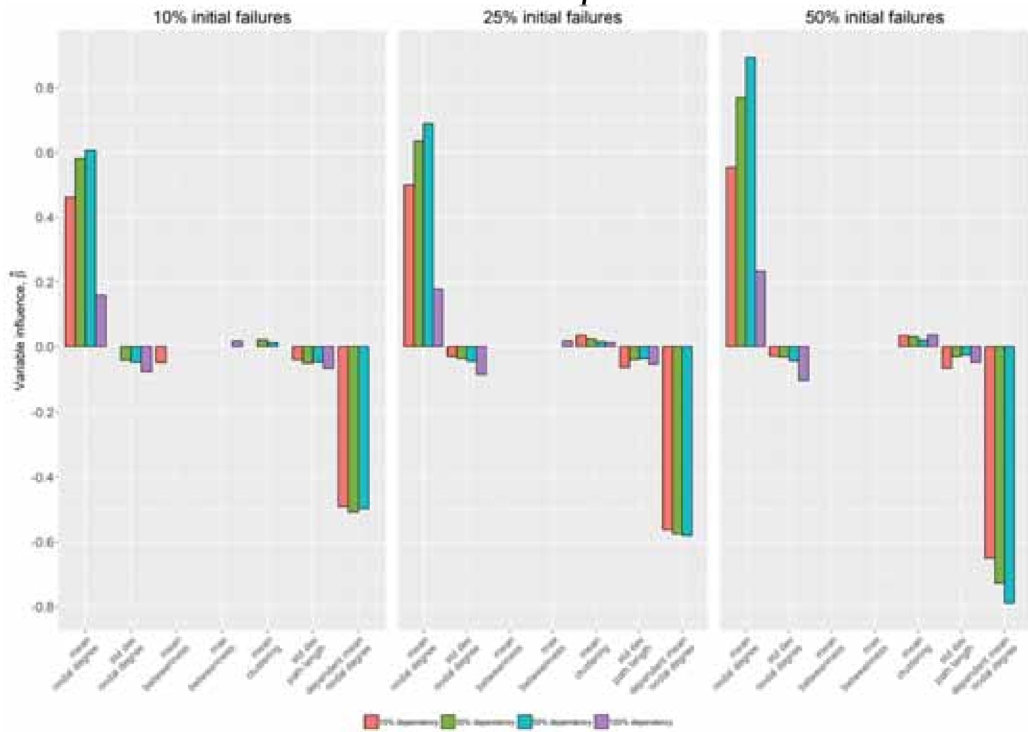

Figure 2: The influence of the significant topological measures for dependent systems where the level of dependency Network A had on Network B was fixed, as found in Paper II. The influence is given by the $\hat{\beta}$ value from the regression model.

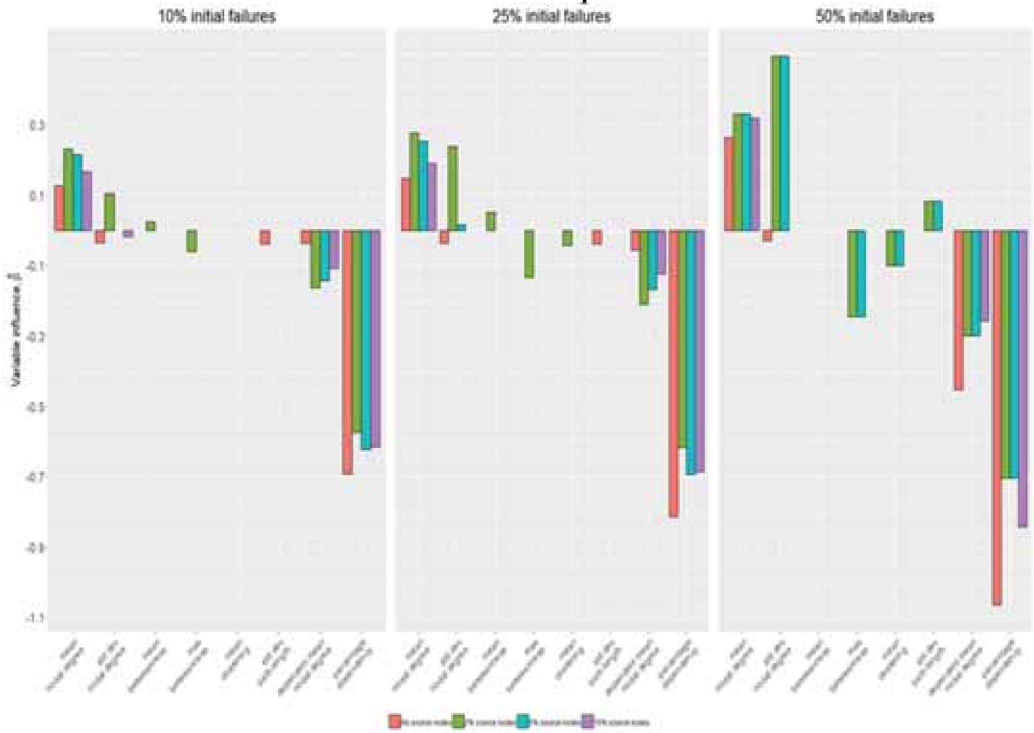

Figure 3: The influence of the significant topological measures for dependent systems where the level of dependency Network A had on Network B was random, as found in Paper II. The influence is given by the $\hat{\beta}$ value from the regression model.

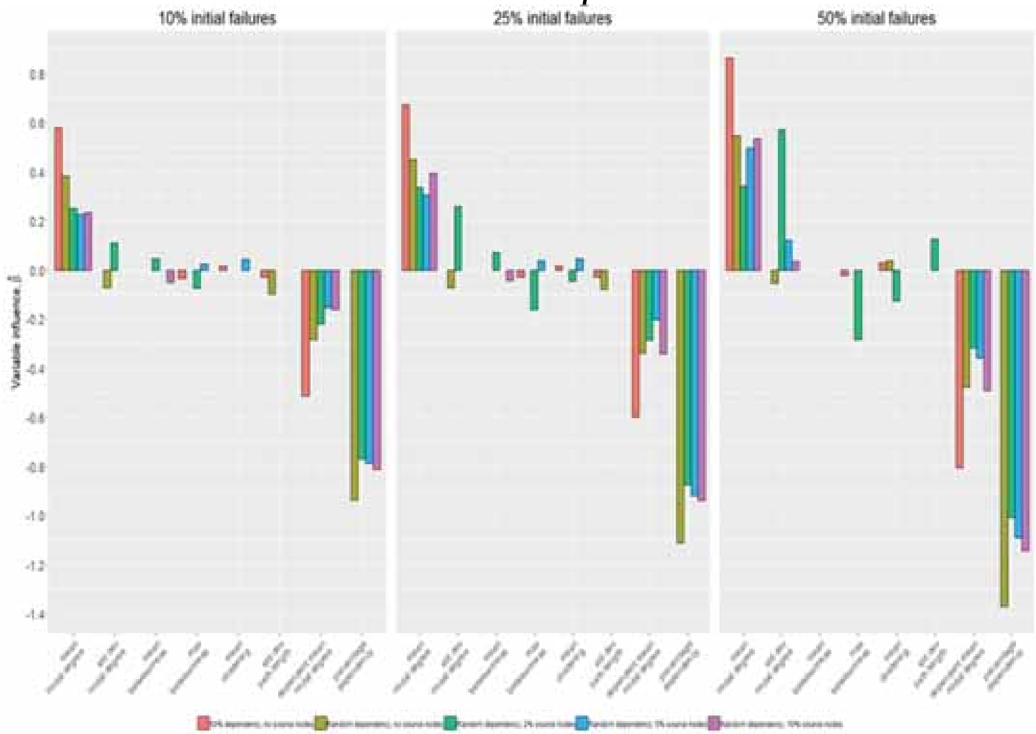

Figure 4: The influence of the significant topological measures for interdependent systems, as found in Paper II. The influence is given by the $\hat{\beta}$ value from the regression model.

Using the results of the coupled network systems analysis alongside those of LaRocca and Guikema (2015) can provide useful information for those designing or upgrading networked infrastructure systems. When designing new infrastructure systems that are dependent on others, the level of dependency should be considered. The dependency level should be as low as possible to reduce the effects of cascading disruptions that occur in the network that is depended upon. The nodes that are dependent on another network should also be considered. When nodes with a higher nodal degree are dependent on input from another network, the cascading effects are greater, although this may not be straightforward to implement, as in reality the functionality of the node determines whether the node depends on another network. In this case, providing redundancy, such as generators for nodes that are dependent on input from an electric power system, at dependent nodes with a high intra-nodal degree, can be implemented. The results are consistent over a range of different coupled network systems, suggesting that the important topological properties are the same for different structures of coupled networks, which provides a general overview of the most influential properties to consider.

2.1.2.3 Real world case studies with limited data

There have been many suggestions for modelling and analysing interdependent systems, as presented in Papers I and II. However, there are few real case studies of interdependent systems (see Dueñas-Osorio et al. 2007, Johansson and Hassel 2010, Chai et al. 2016). Such models focus on data-rich areas in developed countries, primarily the US and Europe. The aim of Paper IV is to provide a real-world interdependent infrastructure system model in a data-poor context, by presenting a model of the dependent water and electric power system of St. Kitts.

St. Kitts is one of the twin islands of the Federation of St. Kitts and Nevis, located in the eastern Caribbean Sea. St. Kitts provides a good case study, as both the power and water systems are self-contained on the island; that is, they do not require or provide input from/to external geographic areas. Due to the location of the island, tropical storms pose a significant hazard to the islands' infrastructure. Network models of the two infrastructures were first developed before being incorporated into a simulation model that estimated the effects of tropical storms on the dependent network system.

The water system was modelled using the publicly available computer program, EPANET 2.0 (Rossman 2000), and was based on data obtained from the St. Kitts Water Department. The model includes the distribution system pipes, along with supply sources and demand nodes. Supply sources consist of 30 groundwater wells, 30 surface storage tanks and six river reserves. The 30 wells are dependent on input from the electric power system to function.

The actual electric power system of St. Kitts contains 12 main trunk lines, with power generated from 10 diesel generators, located in the island's capital, Basseterre. Due to the limited information available about the electric power system, only three of the 12 main trunk lines were included in the model. These three trunk lines stretch along the coastline of the island, with one going along the peninsula to the southernmost point of the island and the other two running up to the north around each side of the island. The nine remaining trunk lines that are not included in the model service Basseterre and the surrounding area. The network model of the power system contains power poles, represented as nodes, and the transmission line as the edges between each node. Each of the three modelled trunk lines begins at Basseterre, moving away from the capital.

Figure 5 shows the schematics of the modelled water and power networks. As previously stated, the dependency between the two infrastructures is the dependency the wells in the water network have on input from the electricity network. To model this dependency, each water well is dependent on the closest power node in the network. When a power pole that a well depends on is non-functional, the dependent well is also classed as non-functional.

Due to tropical storms being a common disruption to St. Kitts, such events were used as scenario events that caused disruptions to the dependent water and electric power system of St. Kitts. A parametric wind model used in previous work (e.g. Han et al. 2009, Guikema et al. 2014) was used to simulate tropical storms within the vicinity of St. Kitts. The model estimates the maximum wind speed during a tropical storm at predefined locations on the island. These locations were one in each parish of the island, with the exception of St. George, which was given three points, as it encompasses the long southern peninsula. Using the estimated maximum wind speeds experienced in a storm, their effect on the electric power system was estimated. A fragility curve of the wooden power poles present in the simulation of disruptions was used to find the probability of damage for each modelled pole. When a power pole fails, all downstream poles also fail, as it is assumed in the model that power is not able to flow downstream of poles damaged by strong winds. The cascading effect of the disruption from the power network to the water network was then simulated. This model was then used to demonstrate how such real-world interdependent models could be used for various analyses.

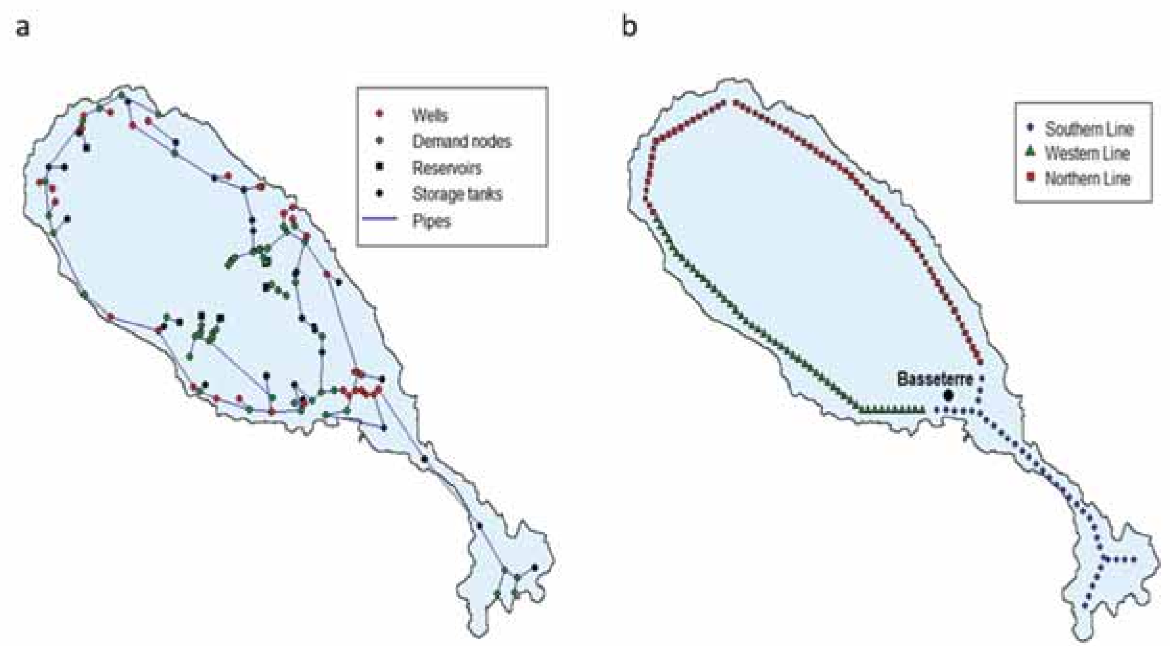

Figure 5: Schematic of a) the modelled water network and b) the modelled power network, as shown in Paper IV (Stødle et al. submitted, p. 4-5, Figures 2 and 3).

The first analysis demonstrated how to identify which components in the power system are critical to the performance of the water system. To do this, each pole was failed individually, and the effects on the water system were recorded as the number of components to experience low or negative pressures. We define low pressure to be less than 20 psi, as this is the minimum pressure standard in several US states for fire-fighting activities. This was modelled for power outages of both 12 hours and 24 hours. From Figure 6, it can be seen that, for both durations of outages, disruptions within the southern line had little effect on the water system, whereas disruptions anywhere along the northern line resulted in cascading effects within the water network.

The second analysis investigated the importance of redundancy within the water network to reduce the effects of cascading disruptions from the power network. For each well, its dependency on the power network was removed before a 72-hour power outage was simulated. This represents, for example, the inclusion of a back-up generator at the well, such that the well is able to function without input from the power network. The results of each dependency being removed one at a time were compared to the base case, where all wells were dependent on the power network and a 72-hour power outage was simulated. The reduction in negative pressures was recorded for the removal of each well dependency and can be seen in Figure 7. The results show that providing redundancy to any wells along the western side of the island increases the resilience of the water network to power outages.

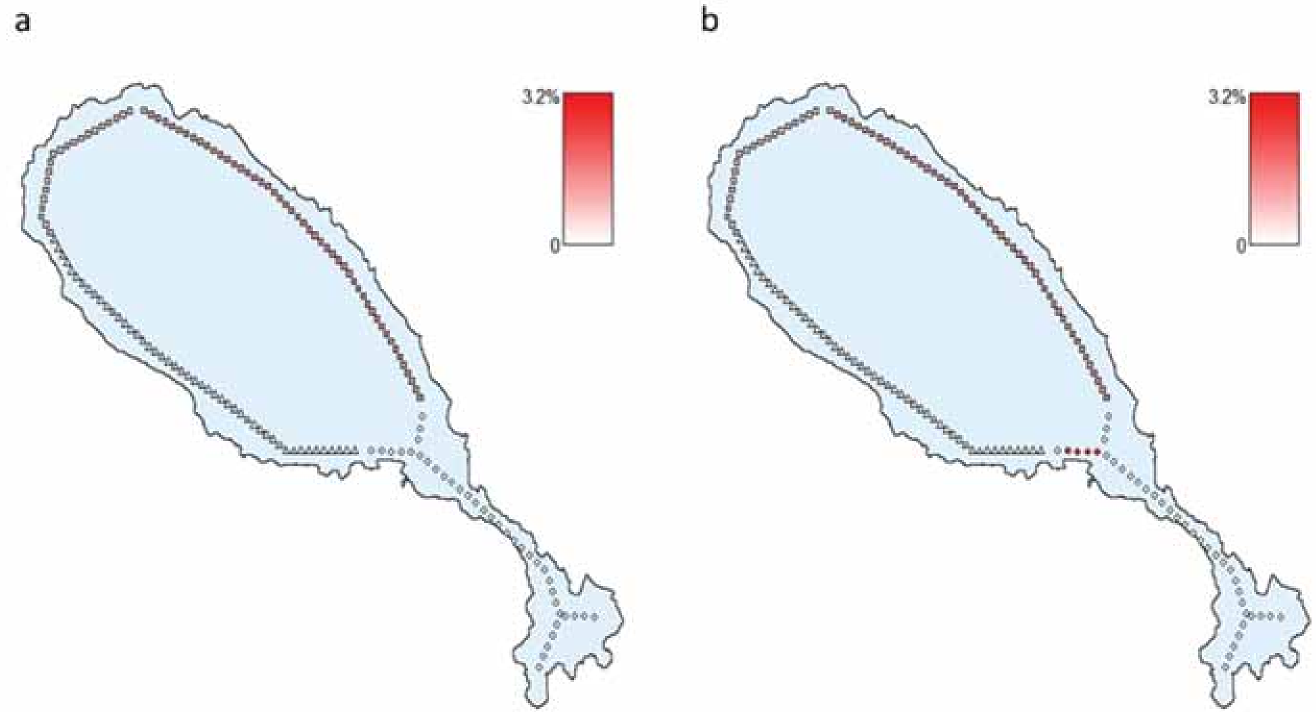

Figure 6: The percentage of water nodes obtaining negative pressure during a) a 12-hour simulation and b) a 24-hour simulation, as shown in Paper IV (Stødle et al. submitted, p. 9-10, Figures 7 and 8).

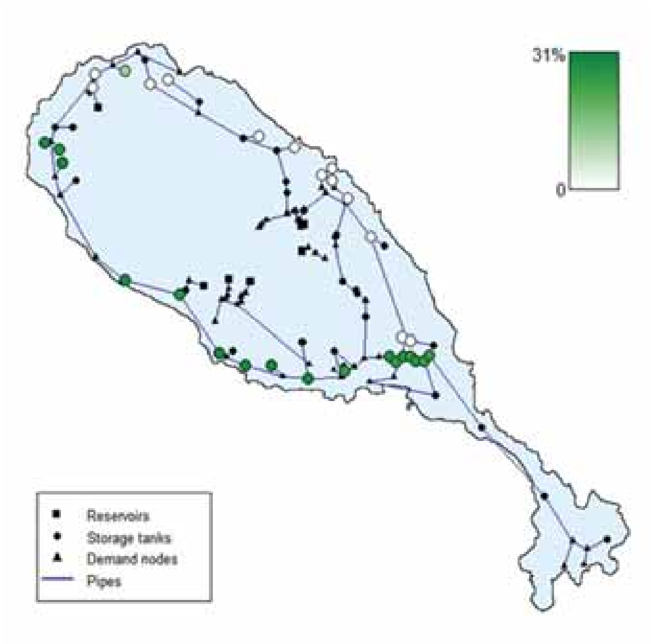

Figure 7: The percentage of reduction in the number of negative water node pressures compared to the worst-case scenario, as shown in Paper IV (Stødle et al. submitted, p. 12, Figure 10).

Although limited data was available to model the electric power network of St. Kitts, an estimate of the system was generated using publicly available information. The generation of the dependent power and water network system of St. Kitts presented in Paper IV provides an example to infrastructure management that, even with limited knowledge of the networks they depend on, simulations of cascading disruptions can still be performed to highlight areas that are more vulnerable to cascading disruptions, indicating areas that can be hardened to such disruptions.

2.2 Risk analysis approaches for critical infrastructure

Although network models allow for an analysis of the performance of infrastructure systems, they are only part of a full risk assessment of such systems. Network models allow the effects of scenarios or disruptions to infrastructure to be assessed but do not consider the likelihood of the scenario occurring and therefore do not provide a complete description of the risk. Probabilistic risk assessment (PRA) is one method that does aim to provide a complete risk description of the system. Currently however, PRA is not common in the assessment of infrastructure risk. The aim of Paper V is to discuss the feasibility of PRA for networked infrastructure systems, as well as comparing non-PRA methods of assessment, to highlight the shortcomings of these more popular methods.

PRA is comprised of three main elements: 1) scenario identification of what can go wrong, 2) a calculation of the associated likelihood of each scenario and 3) the assessment of the consequences of each scenario (Kaplan and Garrick 1981). Kaplan and Garrick (1981) are credited with first proposing the method that is now considered modern PRA. The PRA method for assessing systems was common during the 1970s within the nuclear power industry (Bedford and Cooke 2001). However, in more recent years, other methods have been more prevalent when assessing infrastructure systems. To understand why this is the case, the feasibility of PRA for critical infrastructure was investigated in Paper V. To help illustrate the process of infrastructure PRA, an analysis of one scenario was performed on the water distribution system of the virtual city of Micropolis (Brumbelow et al. 2007).

Micropolis' water distribution system was chosen for assessment, as the system is a virtual one, created by Brumbelow et al. (2007), to allow publicly available information to be used rather than needing to acquire data from real-world infrastructure systems, which often is difficult for safety and security reasons. The water distribution system of Micropolis is constructed so that it contains characteristics found in real systems, such as development over time, leading to a range of pipe materials and diameters.

Before performing a scenario assessment of Micropolis, a formulation of PRA in terms of infrastructure systems was devised. The infrastructure system is regarded as a system of components, in which, in the simplest realisation, each component is either in a functional or a non-functional state. This can be extended for components to have multiple states that represent varying levels of functionality, but, for the purpose of studying the feasibility of PRA of infrastructure, the simple case of functional vs non-functional state is sufficient. The consequence associated with a scenario, s_i, can then be expressed in terms of the component states after the scenario has occurred and can be expressed as $x_i(c_i)$, where x_i is the consequence, which is a function of $c_i = (c_i^1, c_i^2, c_i^3, \ldots, c_i^n)$, the vector of the states of the n components.

To provide an illustration of the infrastructure PRA process, a single earthquake intensity scenario was analysed. An earthquake of magnitude 6 on the Modified Morcalli Intensity (MMI) scale was simulated to affect the water distribution network of Micropolis. Given the Peak Ground Velocity (PGV) resulting from the earthquake, the probability of main pipe failures was calculated. A Monte Carlo simulation was then run, to determine which main pipes experienced failures, i.e. if their state was fully functional or performing at a reduced capacity due to the earthquake. This simulation was run for 100,000 iterations. For each iteration, the effects of the earthquake were modelled using EPANet 2.0 (Rossman 2000). If a pipe failed, a demand of 200 gallons per minute (gpm) was placed on the junction at the end of the pipe, to simulate a leakage occurring within the failed pipe. The EPANet simulation of Micropolis' water distribution system was then run over a 72-hour period, and the number of terminal nodes (end users (residential and commercial buildings) and fire hydrants) experiencing insufficient pressure during the 72 hours was recorded as the consequence of the scenario.

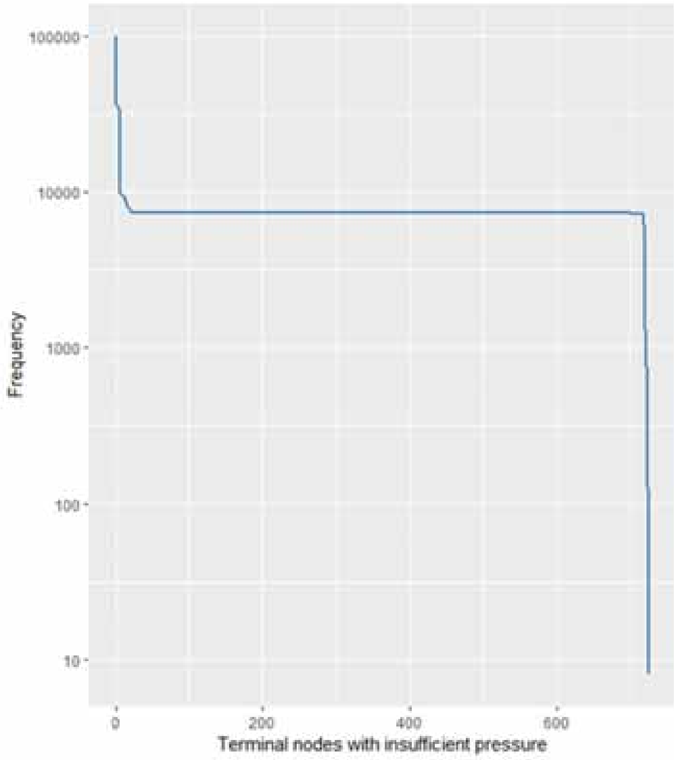

Figure 8: Cumulative frequency of terminal nodes with insufficient pressure due to an earthquake of magnitude 6 on the MMI scale, with a log scale on the y-axis, as shown in Paper V (Johnson, Flage et al. submitted, p. 13, Figure 5).

Figure 8 shows the results of the 100,000 iterations presented as an FN curve with a log scale on the y-axis. A high number of iterations (64,027) resulted in no pipe failures. The FN curve shows the frequency of the consequences for the 100,000 simulations run for an earthquake affecting the Micropolis water distribution system. When failures did occur, either a low number (between 1 and 22) or a high number (693 to 725) of terminal nodes experienced insufficient pressures, with no iterations resulting in a number of failures in the range of 23 to 692 inclusively.

This suggests there is a subset of pipe failures that have a relatively low impact on the function of the system and another subset that has a relatively large impact on the function of the system. To complete the analysis of the earthquake scenario within a PRA, the likelihood of an earthquake of magnitude 6 occurring would also need to be assessed. However, as Micropolis is a virtual city, determining the likelihood of an earthquake is not particularly meaningful.

When assessing the consequences associated with a scenario, assumptions have to be made which simplify the scenario to one that can be assessed in a reasonable timeframe. This creates a trade-off between the comprehensiveness of the analysis and the time and resources (including data) available to perform the assessment. As well as assessing single scenarios, the combination of scenarios that have the potential to occur at the same time also needs to be included in the PRA. The process of infrastructure PRA is time-consuming and requires access to large quantities of relevant data. It is only with recent technological advances that acquiring and storing system data has become achievable. However, the acquisition and storage of such data can still be expensive, and the relevance is hard to determine without a process of trial and error to see what should be stored and processed.

Other methods that are more prevalent in assessing infrastructure systems include *N-k* analysis (including *N-1* analysis), network models, both theoretic and flow-based, and statistical learning theory. *N-1* analysis is popular within the electric power sector of the US, as regulations state that generation and transmission systems should be able to function with the loss of one element (U.S. Department of Energy 2015). *N-k* analysis is an extension of *N-1* that assesses the functionality of a system when *k* components are non-functional (Chen and McCalley 2005). For network models, both theoretic and flow-based, a subset of nodes or edges is removed, to study the effects of loss of functionality in such components (Motter and Lai 2002, LaRocca and Guikema 2015, Ouyang 2016, Johnson et al. 2019). Both *N-k* (including *N-1* analysis) and network-based models assess the performance of the systems, given certain components are non-functional, allowing the consequences of the scenario to be seen. However, neither method includes a likelihood assessment of the scenario that results in the assessed component failures.

Statistical learning theory is another popular method for assessing the impacts of natural events on critical infrastructure. Using knowledge available about the infrastructure, its surrounding environment and the natural hazard, statistical models are built that estimate the impact the hazard has on the infrastructure (Guikema 2009). Han et al. (2009) present such a model that estimates the impact of hurricanes on an electric power system in terms of number of customers without power. As with *N-k* analysis and network models, the likelihood of the scenario is not included in the model, as such methods have been developed to provide quick feedback when there is an indication of a natural hazard occurring in the near future.

All three of these methods are less complex than PRA but only assess the infrastructure for a subset and not all possible scenarios. These methods also do not consider the likelihood of the initial scenarios (that they model) occurring. Although PRA is not feasible in an infrastructure setting, the elements of PRA that are not yet covered by the more prevalent non-PRA methods used to assess infrastructure should be incorporated into infrastructure assessments.

3 Further work

This section proposes further work that ensues from the papers presented in Part II of the thesis.

The first suggestion for further work would be to use the method of simulating spatially correlated failures, as proposed in Paper III, to create disruptions to the coupled network systems assessed in Paper II. This would allow an exploration of the significant topological properties of the coupled network system that characterise the robustness of the network to spatial failures. These could then be compared to the results of random failures found in Paper II, to see whether the same topological properties are significant or whether other properties should be considered in relation to spatial failures. The findings of this work could provide information to those designing or upgrading infrastructure systems.

Another extension of Paper II would be to investigate different categories of dependency types between the coupled systems. All the coupled network systems in Paper II had only single dependency; that is, if a node was dependent on another network, it had a maximum of one and only one dependency. Varying the number of dependencies that a node has on another network may produce different topological properties to be significant in characterising the robustness of the network. This could be explored for both random failures, as simulated in Paper II, and spatially correlated failures, as simulated in Paper III. This again may provide useful information on which topological properties are the most important to consider when designing or updating infrastructure systems.

In Paper IV, an attempt to validate the model of the dependent electric power and water system of St. Kitts was made, using Hurricane Maria, which hit St. Kitts in September 2017. However, due to a lack of publicly available data, finding the actual effects that the hurricane had on the two infrastructures was difficult. Therefore, from Paper IV, possible further work would be to validate the dependent electric power and water model developed in the paper, if actual outage data for an event relating to the dependent system could be acquired. If a more thorough validation of the model were possible, this could provide suggestions on how to better improve the dependent model.

Paper V highlights the complications involved in performing a PRA for modern infrastructure systems, as well as some of the shortcomings associated with more common non-PRA methods currently used to assess infrastructure performance with regard to risk. Developing a method that better incorporates the aims of PRA to improve current methods of assessing critical infrastructure risk could be an interesting extension of Paper V. A further improvement of such a framework would be to find a way in which black swan events (that is, surprising, high-impact events) could be better incorporated into the risk assessment of critical infrastructure.

References

Albert, R., Jeong, H. & Barabási, A.-L. 2000. *Error and attack tolerance of complex networks*. Nature, 406, 378.

Aven, T., Baraldi, P., Flage, R. & Zio, E. 2013. *Uncertainty in risk assessment: the representation and treatment of uncertainties by probabilistic and non-probabilistic methods*, John Wiley & Sons.

Barabási, A.-L. & Albert, R. 1999. *Emergence of scaling in random networks*. Science, 286, 509-512.

Barabási, A.-L., Albert, R. & Jeng, H. 1999. *Mean-field theory for scale-free random networks*. Physica A, 272, 173-187.

Bedford, T. & Cooke, R. 2001. *Probabilistic risk analysis: Foundations and methods*, Cambridge University Press.

Brumbelow, K., Torres, J., Guikema, S., Bristow, E. & Kanta, L. 2007. *Virtual cities for water distribution and infrastructure system research*. *World Environmental and Water Resources Congress.*

Buldyrev, S. V., Parshani, R., Paul, G., Stanley, H. E. & Havlin, S. 2010. *Catastrophic cascade of failures in interdependent networks*. Nature, 464, 1025.

Buldyrev, S. V., Shere, N. W. & Cwilich, G. A. 2011. *Interdependent networks with identical degrees of mutually dependent nodes*. Physical Review E, 83, 016112.

Callaway, D. S., Newman, M. E., Strogatz, S. H. & Watts, D. J. 2000. *Network robustness and fragility: Percolation on random graphs*. Physical Review Letters, 85, 5468.

Chai, W. K., Kyritsis, V., Katsaros, K. V. & Pavlou, G. 2016. *Resilience of interdependent communication and power distribution networks against cascading failures*. *IFIP Networking Conference (IFIP Networking) and Workshops, 2016.* IEEE.

Chang, S. E., McDaniels, T. L., Mikawoz, J. & Peterson, K. 2007. *Infrastructure failure interdependencies in extreme events: power* *outage consequences in the 1998 Ice Storm*. Natural Hazards, 41, 337-358.

Chen, Q. & McCalley, J. D. 2005. *Identifying high risk N-k contingencies for online security assessment*. IEEE Transactions on Power Systems, 20, 823-834.

Cohen, R., Erez, K., Ben-Avraham, D. & Havlin, S. 2001. *Breakdown of the internet under intentional attack*. Physical Review Letters, 86, 3682.

Comes, T. & Van de Walle, B. 2014. *Measuring disaster resilience: The impact of hurricane Sandy on*

Corsi, S. & Sabelli, C. 2004. *General blackout in Italy Sunday September 28, 2003, h. 03:28:00*. IEEE Power Engineering Society General Meeting, 2004.

DSB 2017. *Vital functions in society*. Tønsberg. https://www.dsb.no/globalassets/dokumenter/rapporter/kiks-ii_english_version.pdf Accessed on 25 September 2019.

Dudenhoeffer, D. D., Permann, M. R. & Manic, M. 2006. *CIMS: A framework for infrastructure interdependency modeling and analysis. Proceedings of the 38th conference on winter simulation.* Winter Simulation Conference.

Dueñas-Osorio, L., Craig, J. I. & Goodno, B. J. 2007. *Seismic response of critical interdependent networks*. Earthquake Engineering & Structural Dynamics, 36, 285-306.

Gao, J., Buldyrev, S. V., Stanley, H. E. & Havlin, S. 2012. *Networks formed from interdependent networks*. Nature Physics, 8, 40.

Guikema, S. D. 2009. *Natural disaster risk analysis for critical infrastructure systems: An approach based on statistical learning theory*. Reliability Engineering & System Safety, 94, 855-860.

Guikema, S. D., Nateghi, R., Quiring, S. M., Staid, A., Reilly, A. C. & Gao, M. 2014. *Predicting hurricane power outages to support storm response planning*. IEEE Access, 2, 1364-1374.

Han, S.-R., Guikema, S. D., Quiring, S. M., Lee, K.-H., Rosowsky, D. & Davidson, R. A. 2009. *Estimating the spatial distribution of power* *outages during hurricanes in the Gulf coast region*. Reliability Engineering & System Safety, 94, 199-210.

Havlin, S., Stanley, H. E., Bashan, A., Gao, J. & Kenett, D. Y. 2015. *Percolation of interdependent network of networks*. Chaos, Solitons & Fractals, 72, 4-19.

Holme, P., Kim, B. J., Yoon, C. N. & Han, S. K. 2002. *Attack vulnerability of complex networks*. Physical Review E, 65, 056109.

Hu, F., Yeung, C. H., Yang, S., Wang, W. & Zeng, A. 2016. *Recovery of infrastructure networks after localised attacks*. Scientific Reports, 6, 24522.

Huang, X., Gao, J., Buldyrev, S. V., Havlin, S. & Stanley, H. E. 2011. *Robustness of interdependent networks under targeted attack*. Physical Review E, 83, 065101.

Jenelius, E. & Mattsson, L.-G. 2008. *The vulnerability of road networks under area-covering disruptions*. INFORMS annual meeting, Washington DC, USA.

Johansson, J. & Hassel, H. 2010. *An approach for modelling interdependent infrastructures in the context of vulnerability analysis*. Reliability Engineering and System Safety, 95, 1335-1344.

Johnson, C. A., Flage, R. & Guikema, S. D. 2019. *Characterising the robustness of coupled power-law networks*. Reliability Engineering & System Safety, 191, 106560.

Johnson, C. A., Flage, R. & Guikema, S. D. submitted. *Feasibility study of PRA for critical infrastructure risk analysis*. Manuscript submitted for publication.

Johnson, C. A., Reilly, A. C., Flage, R. & Guikema, S. D. submitted. *Characterizing the robustness of power-law networks that experience spatially-correlated failures*. Manuscript submitted for publication.

Kaplan, S. & Garrick, B. J. 1981. *On the quantitative definition of risk*. Risk Analysis, 1, 11-27.

Kothari, C. R. 2004. *Research methodology: Methods and techniques*, New Age International.

LaRocca, S. & Guikema, S. D. 2015. *Characterizing and predicting the robustness of power-law networks*. Reliability Engineering & System Safety, 133, 157-166.

Macaulay, T. 2008. *Critical infrastructure: Understanding its component parts, vulnerabilities, operating risks, and interdependencies*, CRC Press.

Motter, A. E. & Lai, Y.-C. 2002. *Cascade-based attacks on complex networks*. Physical Review E, 66, 065102.

Newman, M. 2010. *Networks: An introduction*, Oxford University Press.

NOU 2006:6 *Når sikkerheten er viktigst: Beskyttelse av landets kritiske infrastrukturer og kritiske samfunnsfunksjoner*. https://www.regjeringen.no/contentassets/c8b710be1a284bab8aea8fd955b39fa0/no/pdfs/nou200620060006000dddpdfs.pdf Accessed on 25 September 2019.

NRC 2000. *Kvalitet i norsk forskning - En oversikt over begreper, metoder og virkemidler*. [online] https://www.forskningsradet.no/siteassets/publikasjoner/1203528275725.pdf Accessed on 20 January 2020.

Ouyang, M. 2014. *Review on modeling and simulation of interdependent critical infrastructure systems*. Reliability Engineering & System Safety, 121, 43-60.

Ouyang, M. 2016. *Critical location identification and vulnerability analysis of interdependent infrastructure systems under spatially localized attacks*. Reliability Engineering & System Safety, 154, 106-116.

Ouyang, M., Tian, H., Wang, Z., Hong, L. & Mao, Z. 2019. *Critical infrastructure vulnerability to spatially localized failures with applications to Chinese railway system*. Risk Analysis, 39, 180-194.

Park, C. 2007. *Redefining the doctorate*. [online] https://eprints.lancs.ac.uk/id/eprint/435/1/RedefiningTheDoctorate.pdf Accessed on 17 January 2020.

Parshani, R., Rozenblat, C., Ietri, D., Ducruet, C. & Havlin, S. 2011. *Inter-similarity between coupled networks*. EPL (Europhysics Letters), 92, 68002.

Public Safety and Emergency Preparedness Canada 2014. *Forging a common understanding for critical infrastructure: shared narrative*. Public Safety Canada, Ottawa. http://publications.gc.ca/collections/collection_2017/sp-ps/PS4-221-2014-eng.pdf Accessed on 25 September 2019.

Rinaldi, S. M., Peerenboom, J. P. & Kelly, T. K. 2001. *Identifying, understanding and analyzing critical infrastructure interdependencies*. IEEE Control Systems, 21**,** 11-25.

Rossman, L. 2000. *EPANET 2 Users Manual*. https://epanet.es/wp-content/uploads/2012/10/EPANET_User_Guide.pdf Accessed on 21 January 2020.

Schneider, C. M., Yazdani, N., Araújo, N. A., Havlin, S. & Herrmann, H. J. 2013. *Towards designing robust coupled networks*. Scientific Reports, 3**,** 1969.

Shao, J., Buldyrev, S. V., Havlin, S. & Stanley, H. E. 2011. *Cascade of failures in coupled network systems with multiple support-dependence relations*. Physical Review E, 83**,** 036116.

Shao, S., Huang, X., Stanley, H. E. & Havlin, S. 2015. *Percolation of localized attack on complex networks*. New Journal of Physics, 17**,** 023049.

Stødle, K., Johnson, C. A., Brunner, L. G., Saliani, J. N., Flage, R. & Guikema, S. D. submitted. *Dependent infrastructure system modeling: A case study of real-world power and water distribution systems*. Manuscript submitted for publication.

US` Department of Energy 2015. *United States Electricity Industry Primer*. https://www.energy.gov/sites/prod/files/2015/12/f28/united-states-electricity-industry-primer.pdf Accessed on 21 January 2020.

Walter, E. 2008. *Cambridge advanced learner's dictionary*, Cambridge University Press.

Watts, D. J. & Strogatz, S. H. 1998. *Collective dynamics of 'small-world' networks*. Nature, 393**,** 440-442.

Winkler, J., Dueñas-Osorio, L., Stein, R. & Subramanian, D. 2010. *Performance assessment of topologically diverse power systems* *subjected to hurricane events*. Reliability Engineering & System Safety, 95, 323-336.

Zhang, P. & Peeta, S. 2011. *A generalized modeling framework to analyze interdependencies among infrastructure systems*. Transportation Research Part B: Methodological, 45, 553-579.

Zimmerman, R. 2001. *Social Implications of infrastructure network interactions*. Journal of Urban Technology, 8, 97-119.

Part II

Paper I

Review of network-theoretic approaches to characterise interdependencies in critical infrasturctures.

Authors: Caroline A Johnson, Roger Flage and Seth D Guikema

Published in: M. Čepin, & R. Bris (Eds.), *Safety & Reliability, Theory and Applications*. Proceedings of the European Safety and Reliability (ESREL) Conference 2017 (Slovenia), Portorož, Slovenia, 18-22 June (pp. 765-772). CRC Press.

Paper II

Characterising the robustness of power-law networks.

Authors: Caroline A Johnson, Roger Flage and Seth D Guikema

Published in: *Reliability Engineering & System Safety*, 191, 106560.

Reliability Engineering and System Safety 191 (2019) 106560

Contents lists available at ScienceDirect

Reliability Engineering and System Safety

journal homepage: www.elsevier.com/locate/ress

Characterising the robustness of coupled power-law networks

Caroline A. Johnson[a,*], Roger Flage[a], Seth D. Guikema[b]

[a] University of Stavanger, P.O. Box 8600 Forus, 4036 Stavanger, Norway
[b] University of Michigan, USA

ARTICLE INFO

Keywords:
Network topology
Power-law networks
Interdependent networks
Coupled networks
Network robustness

ABSTRACT

Many networks exhibit a power-law configuration, where the number of connections each node has follows a power-law distribution, including the Internet, terrorist cells, species relationships and infrastructure. Given the prevalence of power-law networks, studying the effects of disruptions on their performance is of interest. Previous work has investigated the influence of network topology on the effects of random node failures for independent networks. Many networks depend on others to function and thus, exploring the influence of network topology on the effects of failures in interdependent networks is of interest. The present paper extends the previous work to coupled power-law network systems. For a set of randomly generated coupled systems, each containing two networks, we investigate the significant topological factors for different dependency types. Failures in the coupled networks are simulated and the effects on the system performance are analysed by performing a beta regression. The results are consistent across the dependency types, with the most influential topological factors being mean nodal degree and factors relating to the dependency type. The results are also compared with those of the independent networks and their potential relevance to the design of interdependent networks is indicated, for example, their use within an infrastructure setting.

1. Introduction

It is well established that to model and evaluate the robustness (or vulnerability) of critical infrastructure, the dependencies that exist between infrastructure systems need to be accounted for [7,32,34]. Over the years, there have been many methods suggested for how to model dependencies between infrastructures, including the use of agent based and network based approaches [29]. Network models are based on a network representation of the important components of each infrastructure, represented as nodes, and the connections between the components within the same network, as well as between the different networks, represented as edges. The edges between nodes of different networks represent the dependencies between the different infrastructures.

Infrastructure networks are a special case of the broader class of interdependent networks. For example, the metabolic pathways of different species in an ecosystem can be interdependent (e.g., one species depends on an output from another species as an input). Similarly, economies, when represented as networks of consumers and producers, are strongly interdependent across regions within a country and across different countries.

There have been many differing methods suggested for modelling the dependencies between infrastructures using network models. Some examples of the different methods are given by Parshani et al. [31], Gaogao et al. [19] Jiang et al. [20], and Cheng and Cao [10]. The main structural differences between the models can be characterised by whether the infrastructures are fully or partially dependent (i.e., if each node has at least one dependency to a node in the other network or only a fraction of the nodes do) and if components with dependencies have single or multiple dependencies (each dependent node has one or more than one dependency) [17].

For both independent and interdependent networks, percolation theory has been used to find analytical solutions to disruptions across an array of different network types and dependency methods [7,10,18]. Such papers show the number or fraction of nodes removed in the initial disruption that lead to complete collapse of the investigated system. This can be used as a measure of the system's robustness and to compare the robustness of different system models [18,20]. However, this measure does not convey information about what happens to network performance at lower levels of node removals and does not directly provide information about the relative importance of different topological properties of the network in terms of their influence on network robustness.

Network flow models are an extension of the network models that

* Corresponding author.
E-mail address: caroline.a.johnson@uis.no (C.A. Johnson).

https://doi.org/10.1016/j.ress.2019.106560
Received 26 September 2018; Received in revised form 9 May 2019; Accepted 28 June 2019
Available online 02 July 2019

include the addition of load to the nodes and/or edges of the network. The load represents the amount of commodity present at each node and or/edge. Each node and/or edge is also assigned a maximum capacity. When a disruption occurs the load of any failed nodes and edges is redistributed throughout the remaining functional network components. The reassignment of the load can lead to additional failures if the load of nodes or edges exceeds their maximum capacity [14,38].

Scala et al. [35] investigated the inclusion of physical flow to both independent and interdependent networks, with a focus on how edge overload affected the robustness of the networks. They used a mean field model to redistribute the load of failed edges throughout the system, that is, they assumed when an edge failed its load was redistributed evenly throughout the existing edges within the network.

The addition of commodity flow within networks is useful when looking into the cascading mechanisms between specific infrastructure network types, such as electric power and telecommunication. The interaction between the types of infrastructure can be explored to see how the redistribution of commodity flow can influence the cascading effects of disruptions [22,38]. One conclusion from the literature is that the inclusion of network flow shows an increased level of cascading effects [42], while others argue that including “smart” interactions (which occur due to buffers within real dependent infrastructure systems) between the two networks decreases the cascading effects within the interdependent power-communication system [22].

The use of network flow models is effective when studying a specific system, such as one including an electric power system. However, when investigating the effects of dependencies between general infrastructure networks, the type of infrastructure is not specified, and thus the flow of the commodity cannot be included. Instead the structure of the networks can be explored. The effects of network structure, or topology, on the robustness of independent networks have previously been investigated [3,23]. Different topological factors can be calculated, which capture particular structural features of a network.

Four of these topological factors are nodal degree, path length, betweenness centrality and clustering coefficient. Nodal degree specifies the number of edges connected to each node. Path length provides the shortest path between each nodal pair within a network. Here the shortest path is considered as the path that traverses the least number of edges. Betweenness centrality indicates the extent to which a node lies on the shortest path between two other nodes within the network [27]. Clustering coefficient (also referred to as transitivity) indicates the how likely it is for the neighbours of a node to also be neighbours, where if an edge exists between two nodes, then they are neighbours. Clustering coefficient gives an indication of local redundancy within a network.

Alipour et al. [3] used topological based and reliability based measures to identify weak nodes within power transmission networks. The topology based measures included factors such as nodal degree and betweenness centrality. The reliability based measures incorporates what the author refers to as the reliability of the edges within the system. To do this, a weight is assigned to each edge that represents the probability that the edge is functional. The topological factors are then calculated including the weights of the edges. They also compared the robustness of the independent power transmission networks to random and targeted attacks, using efficiency as a measure of robustness. Efficiency is defined as the inverse of the average of the shortest paths between each nodal pair within the network. The targeted attacks were simulated by removing the most central nodes of the network. The most central nodes are defined as those who had the highest cumulative rank score in relation to the reliability based measure, i.e., the greater the value of each reliability based measure a node has the lower it is ranked.

LaRocca and Guikema [23] provide a general overview of the topological factors that have a significant influence on the robustness of independent networks when random failures occur. The focus of the paper was the robustness of networks, of which the nodal degree followed a power-law distribution with exponential cut-off. Here, robustness was defined as the percentage of functional nodes after disruptions. Their findings show that the following topological factors are significant when characterising the robustness of independent networks: mean nodal degree, mean betweenness centrality, mean clustering coefficient, standard deviation of clustering coefficient and standard deviation of path length. However, the influence of the topology on the robustness of interdependent networks has not been explored. In this paper, characterising the robustness of networks with topological factors is extended to the case of coupled network systems.

LaRocca et al. [24] compared the use of network topology and network flow models to simulate electric power networks. They concluded that using only network topology as performance measures for particular power networks under specific disruption scenarios provides poor estimates of system performance, relative to when commodity flow is taken into account. However, they also find that an average of some performance measures, such as largest connected subgraph, may capture the average behaviour of the system when random failures occur. If investigating the effects of disruption to a specific system that includes at least one infrastructure for which the flow of the commodity can be modelled, then the use of a physical flow model is more appropriate than a network theoretic model. However, this paper aims to give an overview for any type of networks within a coupled system and thus does not include physical flow. The inclusion of flow limits the connections within an individual network to all be of the same type of connection, e.g. physical if the flow of a commodity (e.g. power of water) or of information. By not including physical flow, the connections within the model can represent different types of connections, rather than just one.

To extend the work of LaRocca and Guikema [23] the present paper aims to provide a general overview of which topological factors are important when random disruptions occur in coupled network systems for a variety of different dependency types. The various dependency types allow for the investigation of both dependent and interdependent coupled systems. The 2000 coupled network systems are generated such that each system consists of two networks, both of which are scale-free networks that follow a power-law distribution with exponential cut-off. The two networks present in each coupled system are referred to as Network A and Network B. The dependencies between the two networks are directional (or unidirectional), i.e., if node i in Network A depends on node j in Network B, node j does not necessarily depend on node i in Network A.

In our analysis, the robustness of Network A is explored when random disruptions occur within the coupled system. Robustness here is considered as the percentage of functional nodes after a disruption occurs. The analysis aims to advance the understanding of how the robustness is affected within a short time frame after the initial disruption. All initial failures occur within Network B, thus investigating the first order effects of a disruption on Network A. A first order effect refers to the effect of a disruption that initiates in Network B and affects Network A through the dependencies Network A has on Network B [34]. After the disruptions are simulated within the coupled system, a beta regression is performed to provide an overview of which topological factors are significant in characterising the robustness of Network A. A comparison of the significant topological factors across the different types of dependencies modelled is made, as well as a comparison to the significant factors reported for independent networks in LaRocca and Guikema [23].

The remainder of this paper is structured as follows: Section 2 provides an overview of the different network related terminology used throughout the paper. The methods used to generate and analyse the coupled network systems are outlined in Section 3, with the results of the regression analysis are presented in Section 4. A discussion of the findings is given in Section 5, followed by the conclusion in Section 6.

2. Network terminology

Networks consisting of nodes and edges can be used to construct a simplified representation of an infrastructure system. The nodes represent important components of the system and the edges represent the connections between such components. The network or graph can be denoted as $G = \{V, E\}$, where V is the set of vertices or nodes in the network and E is the set of edges, which form connections between the nodes. The size of the network, N, is equal to the number of vertices [5]. The edges in a network can either be directed or undirected. When the edges are directed, the direction of each edge is specified and can only be traversed in the specified direction. When the edges are undirected, the edges can be traversed in either direction. For simplicity, the networks generated to be included the coupled systems in this paper are undirected.

Barabási and Albert [4] first observed that the nodal degree of some networks can be described as following a power-law distribution, given by:

$$P(k) \sim k^{-\gamma}$$

such that $P(k)$ is the probability that a node is connected to k neighbours and γ is some constant. It has since been suggested that the power-law distribution with exponential cut-off is more accurate as it takes into account the physical cost of adding additional edges to a node, providing an upper limit to the number of edges a node can have. The power-law distribution with exponential cut-off is given as:

$$P(k) \sim k^{-\gamma} e^{-(k/K)}$$

where K is the cut-off at which it becomes too costly to add additional edges to a node [2, 26].

It has recently been questioned if power-law networks are as prevalent in the real world as the mountain of literature stating this would have us believe. Broido and Clauset [6] investigated if the best fitting power-law distribution for the nodal degree of 3662 simple graphs (constructed from 928 real-world networks) was better than alternative (non-scale-free) distributions. They use the term scale-free networks to refer to networks which nodal degree follows a power-law distribution. Likelihood ratio tests were compared for the best fitting model from four alternative degree distributions. One such distribution they compared was the power-law with exponential cut-off, where 56% of the results favoured the power-law distribution with exponential cut-off. This result led Broido and Clauset [6, p. 5] to state "a majority of networks favor the power law with cutoff model, indicating that finite-sized effects may be common". This topic of discussion will likely gain much attention in the near future, and may lead to a different underlying degree distribution to be proposed. However, for the time being, the power-law distribution with exponential cut-off is one of the better methods to use when constructing simulated networks.

2.1. Network topology

The structure or topology of a network can be described using different network parameters. Four such parameters that are particularly useful for characterising the network structure are: nodal degree, betweenness centrality, clustering coefficient and path length. Each of these four topological parameters can be calculated for any network [23].

2.1.1. Nodal degree

The degree, k, of any node in an undirected network is the number of edges connected to the node. The mean nodal degree of the network is expressed as

$$k = \frac{1}{N} \sum_{i \in V} k_i$$

where V is the set of nodes in the network, and k_i is the degree of node i.

2.1.2. Path length

The length of the shortest path for each pair of nodes within a network is calculated as the least number of edges traversed to get from one node in the pair to the other. The shortest path from node i to node j in a network is denoted as p_{ij}. For undirected graphs $p_{ij} = p_{ji}$. For the remainder of the paper, the set of shortest paths between each nodal pair in a network is denoted as L.

2.1.3. Betweenness centrality

For each node i in the network, the betweenness centrality is defined as:

$$Bc_i = \sum_a \sum_b \frac{p_{aib}}{p_{ab}}, \quad a \neq b \neq i,$$

where p_{aib} is the number of shortest paths from node a to node b that pass through node i, and p_{ab} is the total number of shortest paths from node a to node b.

2.1.4. Clustering coefficient

The clustering coefficient of a node specifies how connected its neighbours are to each other and is an indication of local redundancy in the network. The neighbours of a node is the set of nodes to which it is connected to. For node i, which has k_i neighbours, the clustering coefficient is defined as:

$$Cc_i = \frac{2E_i}{k_i(k_i - 1)}$$

where E_i is the number of edges between the neighbours of node i.

2.2. Giant connected component and source node clusters

When disruptions occur to a network, the network can fragment into several clusters. The largest connected cluster present after the network fragments is referred to as the Giant Connected Component (GCC). The relative size of the GCC is the percentage of nodes within the GCC [9,10,36]. The relative size of the GCC can be used as a measure of network performance after disruption has occurred [17,22]. We acknowledge that this is an imperfect measure of network robustness, especially given that it does not account for source and sink nodes or for the physics of network flows. However, this simple, widely-used measure, provides an initial view of the influence of topological factors on the topological robustness of a network.

Source nodes can also be included into a network. Source nodes represent components of the network that must be functioning in order for the network to be functional. When a disruption occurs within a network containing source nodes, only the clusters that contain source nodes are considered functional.

2.3. Network dependencies

Connections between different networks can also be formed to generate a system of dependent networks. These connections represent the dependencies that exist between different infrastructure networks, for example the dependency a water network has on an electricity network to power electric pumps [13]. To distinguish between the edges within each network and between the networks the terms intra-connections and inter-connections are used. Intra-connections refer to the connections or edges between two nodes within the same network. Inter-connections refer to the connections or edges between two different networks, i.e. the dependencies between the networks.

For the remainder of the article, all intra-connections are assumed to be undirected and all inter-connections are assumed to be directed. This is representative of situations such as a drinking water network and its dependency on a power network. The water within the network can flow in both directions, such that the intra-connections are undirected. However, some components of the water network, such as the pumps, rely on electricity to function and thus the dependency is directional from the power network to the water network. Another example is a transportation network and its dependency on a power network. Within the transportation network traffic flows in both directions, whereas the dependency is directed from the power network to the transportation network, for example, to signals within the transportation network that requires electricity. The power network can also be dependent on the transportation network, for example, the transportation of fuel (e.g., coal) or spare parts, but not necessarily on the component that depends on the power network, such as the signals.

For coupled system where the networks have partial dependency (i.e., only a percentage of the nodes in the network depend on another), the influence of additional variables on the robustness of the system are considered. These variables are the percentage of nodes in the network which are dependent on another network, denoted *Dp*, and the intra-nodal degree (number of intra-connections a node has) of these dependent nodes, which is denoted as *Dk*. When source nodes are included in the coupled systems, the influence of the additional variable of the source nodes' intra-nodal degree is also considered, and denoted as *Sk*.

3. Methods

A total of 4000 networks were generated following the process outlined in Section 3.1 before being sorted into pairs to give 2000 coupled network systems. The two networks within each system are referred to as Network A and Network B. Different types of dependencies between the two networks were explored and are described in Section 3.2.1. For each dependency type, failure scenarios were simulated within the 2000 coupled systems and the robustness of Network A was recorded. More information on simulating the failure scenarios is given in Section 3.3. To characterise the robustness of Network A from the topological factors of the coupled network system a beta regression analysis was performed as described in Section 3.4.

3.1. Generating networks

The 4000 networks were generated using the preferential attachment variation algorithm presented by LaRocca and Guikema [23]. This algorithm assigns the degree of each node from the power-law distribution with exponential cut-off before assigning intra-connections preferentially, based on nodal degree. All intra-connections are assumed to be undirected.

An assortment of simulated networks was produced using combinations of different network sizes and parameter groups for the nodal degree distribution. Five different power-law distributions with exponential cut-off were used to assign the nodal degree of the networks. The parameter groups of the five power-law distributions used are shown in Table 1. These distributions are the same as those used previously by LaRocca and Guikema [23] and were chosen as they represented nodal degree distributions exhibited by real-world networks studied in Albert and Barabási [2]. Twenty different network sizes ranging from 100 to 1000 nodes were chosen from a uniform distribution and can be seen in Table 2. Therefore, for each combination of network size and nodal degree distribution 40 networks were generated.

Table 1
Power-law parameters used for generating networks.

Power-law distribution parameters γ	K
1.1	40
1.7	200
2.0	900
2.1	400
2.4	2000

Table 2
Summary of generated networks.

Number of nodes	Number of degree distributions	Number of networks	Number of nodes	Number of degree distributions	Number of networks
100	5	40	485	5	40
133	5	40	509	5	40
142	5	40	536	5	40
232	5	40	547	5	40
249	5	40	690	5	40
350	5	40	697	5	40
361	5	40	752	5	40
448	5	40	862	5	40
464	5	40	896	5	40
467	5	40	1000	5	40

After generating the networks, the mean, minimum, maximum and standard deviation of the four topological factors of each network was calculated. A summary can be seen in Table 3.

3.2. Generating coupled network systems

The 4000 networks generated were then paired such that each pair of networks, referred to as Network A and Network B, were the same size and of the same parameter group for the nodal degree distribution. Each pair was used to form a coupled network system, resulting in 2000 systems. The two networks within each coupled system were assumed to occupy the same spatial area. The layout of each network was decided using the layout.graphopt function in the igraph R package [12]. This assigned each node a Cartesian (x, y) coordinate.

The inclusion of source nodes within the coupled network systems was also explored to see if their presence caused a change in which topological factors were significant to network robustness. When source nodes were present in the coupled system, a random subset of nodes in Network B were chosen to represent these source nodes. The size of the subset was varied at 2%, 5% and 10% of the network's size. These relatively low percentages of source nodes are representative of systems such as infrastructure where the large majority of nodes are demand points and demand is met by a relatively small number of major source nodes; for example, natural gas networks [15, 33, 37], electric power systems [1, 39–41] and water distribution systems [21, 25, 28]. The analysis could be extended to networks with much higher percentages of source nodes, but this is not explored in this paper.

3.2.1. Forming dependencies

For each type of dependency, Network A is always dependent on Network B, however Network B was either independent (did not depend on Network A) or was dependent on Network A. For each dependency type, a subset of nodes in Network A is randomly chosen to depend on Network B. This subset is denoted as A_D. Each node in A_D depends on the closest node in Network B (based on Euclidean distance). This allows multiple nodes in A_D to be dependent on the same node in Network B. The method of forming dependencies based on geographic proximity is used by Dueñas-Osorio et al. [13] when modelling the interdependent power and water system of Shelby County, Tennessee and Ouyang et al. [30] to simulate coupled power and water systems with features similar to those of real infrastructure.

For dependency types that include Network B depending on Network A, the dependencies Network A has on Network B are first formed, using the method described in the previous paragraph. Next a random subset of nodes in Network B is chosen to depend on Network A. This subset is denoted as B_D. Each node in B_D is dependent on the closest node in Network A (based on Euclidean distance) that is not present in the subset A_D. This allows for multiple nodes in B_D to depend on the same node in Network A.

Table 3
Summary of the topological characteristics of the generated networks, separated into Network A and Network B.

Parameter	Within-network measure	Network A Mean	Min	Max	Std dev	Network B Mean	Min	Max	Std dev
Network size (N)		496	100	1000	253.5	496	100	1000	253.5
Degree (k)	Mean	5.35	2.34	12.94	2.35	5.37	2.49	12.44	2.37
	Minimum	1.00	1.00	1.00	0.00	1.00	1.00	1.00	0.00
	Maximum	372	39	999	241	374	42	998	241
	Std dev	20.50	6.77	37.18	6.24	20.62	6.83	36.94	6.23
Betweenness centrality (Bc)	Mean	706	95	2948	535	700	95	2953	528
	Minimum	0.00	0.00	0.00	0.00	0.00	0.00	0.00	0.00
	Maximum	214,499	1766	995,119	236,109	216,959	1752	993,561	236,791
	Std dev	9049	368	31,468	7608	9131	344	31,419	7633
Clustering coefficient (Cc)	Mean	0.31	0.04	0.66	0.11	0.31	0.03	0.69	0.12
	Minimum	0.00	0.00	0.00	0.00	0.00	0.00	0.00	0.00
	Maximum	1.00	0.90	1.00	0.00	1.00	1.00	1.00	0.00
	Std dev	0.40	0.11	0.49	0.08	0.40	0.10	0.49	0.08
Path length (L)	Mean	2.36	1.96	4.00	0.53	2.35	1.95	3.98	0.52
	Minimum	1.00	1.00	1.00	0.00	1.00	1.00	1.00	0.00
	Maximum	4.75	2.00	14.00	2.20	4.74	2.00	17.00	2.32
	Std dev	0.46	0.06	1.38	0.33	0.46	0.06	1.90	0.33

Table 4
Summary of dependency types considered.

Type of dependency Network A has on Network B	Type of dependency Network B has on Network A	Percentage of source nodes in Network B
Fixed, 10%	–	–
Fixed, 30%	–	–
Fixed, 50%	–	–
Fixed, 100%	–	–
Fixed, 50%	Fixed, 50%	–
Random	–	–
Random	–	2
Random	–	5
Random	–	10
Random	Random	–
Random	Random	2
Random	Random	5
Random	Random	10

The size of the dependent subsets A_D and B_D vary for each dependency type. An overview of the size of the dependent subsets is given in Table 4. When the percentage of dependency is referred to as fixed, this means that each of the 2000 coupled systems have the same fixed percentage of dependent nodes. When Network B was independent, 10%, 30%, 50% and 100% of dependency levels (of Network A on Network B) were considered. These levels were picked such that a range of levels that could be observed by infrastructure systems were covered. When both Network A and B were dependent on each other, a fixed percentage of 50% was considered, though this could be extended in future work. When the percentage is referred to as random, the percentage of nodes to be chosen for the subset(s) A_D (and B_D) is randomly assigned to Network A (and Network B) in each of the 2000 coupled network systems. The percentage of dependent nodes is assigned using a uniform distribution with a range from 1/N% to 100%, where N is the size of the network, for each dependent network. This provides a range of dependency from only one node being dependent in a network to the network being fully dependent.

3.3. Simulating failures

Each failure scenario was simulated by randomly choosing a subset of nodes in Network B to fail. The percentage of nodes randomly chosen to initially fail in Network B was investigated at the 10%, 25% and 50% level. These failed nodes were then removed from the network and the cascading effect throughout the coupled system was observed. For each dependency type, 100 failure scenarios were run for each of the 2000 coupled network systems. The percentage of nodes functional in Network A was averaged over the 100 failure scenarios run on each coupled network system and recorded. Two different methods were used to simulate the cascading effects of the initial disruption. When the coupled network systems did not contain source nodes, only nodes in the GCC of Network A were considered as functional. When source nodes were present in the coupled network system, only nodes that could be reached from source nodes after disruption were considered as functional. A more in-depth explanation to the two methods used to simulate the cascade effects are given in Sections 3.3.1 and 3.3.2.

3.3.1. Giant connected component (source nodes not present)

When source nodes were not present in the coupled system, only nodes present in the GCC were considered as functional. The initial disruption removed a percentage of nodes in Network B, causing the network to fracture into clusters. Of these clusters, only the largest, the GCC, is considered as functional and thus all nodes outside the GCC are also considered as failed. Any nodes in A_D that depend on failed nodes in Network B also fail and are removed from Network A. This causes Network A to fragment into clusters. As with Network B, only the largest cluster, the GCC, of Network A is considered functional and all nodes outside of the GCC are also considered as failed. Any nodes in B_D that depend on nodes in Network A which have failed are also considered failed. This process iterates until an equilibrium is reached (no additional node failures occur). In the dependency types where Network B is independent, B_D will be an empty set and thus the failures of Network A will not affect Network B and the system will reach equilibrium after any nodes outside of the GCC of Network A are considered as failed.

3.3.2. Source node clusters (source nodes present)

When source nodes are present in the coupled system, the initial failures occur within Network B, the failed nodes are removed and the network fragments as with the method described in Section 3.3.1. However, with the inclusion of source nodes, only the clusters which contain source nodes will be considered as functional and all nodes outside of these clusters are also considered as failed. As before, any nodes in $A_D$which depend on failed nodes in Network B fail and Network A fragments into clusters. The set of functioning dependent nodes in Network A is denoted as A_{Df}. Now only clusters that have input from Network B are functional. This means that only clusters containing the nodes in A_{Df} are functional. Nodes outside of these functional clusters are also considered as failed. Any nodes in B_D that depend on failed nodes in Network A are now considered as failed, causing further fragmentation to Network B. As before, this process iterates until the

Table 5

Significant covariates when Network A is dependent on Network B and Network B is independent and the effect of change of these covariates. The sign indicates if the covariate has a positive or negative influence on the percentage of nodes considered functional in Network A after random failures in Network B. The colour indicates the covariate coefficient value with the darker the colour indicating the further the value is from 0.

Type of dependency Network A has on Network B		Fixed, 10%			Fixed, 30%			Fixed, 50%			Fixed, 100%			Random			Random			Random			Random		
Percentage of source nodes in Network B		0			0			0			0			0			2			5			10		
Percentage of initial failures in Network B		10	25	50	10	25	50	10	25	50	10	25	50	10	25	50	10	25	50	10	25	50	10	25	50
Topology of Network A only in regression model	*k*, mean A	+	+	+	+	+	+	+	+	+	+	+	+	+	+	+	+	+	+	+	+	+	+	+	+
	k, std dev A		-	-	-	-	-	-	-	-	-	-	-	-	-	-	+	+	+		+	+	-		
	Bc, mean A	-											+				+	+	+						
	Bc, max A										+	+					-	-	-			-			
	Cc, mean A		+	+	+	+	+	+	+	+		+	+					-	-			-			
	L, std dev A	-	-	-	-	-	-	-	-	-	-	-	-	-	-				+						
	Dp, A													-	-	-	-	-	-	-	-	-	-	-	-
	Dk, mean A	-	-	-	-	-	-	-	-	-				-	-	-	-	-	-	-	-	-	-	-	-
Topology of Networks A and B in regression model	*k*, mean A	+	+	+	+	+	+	+	+	+	+	+	+	+	+	+	+	+	+	+	+	+	+	+	+
	Bc, max A																-	-	-			-			
	Cc, mean A		+	+																					
	L, std dev A	-	-	-	-	-		-	-		-	-		-	-		-	-	-			-			
	Dp, A													-	-	-	-	-	-	-	-	-	-	-	-
	Dk, mean A	-	-	-	-	-	-	-	-	-				-	-	-	-	-	-	-	-	-	-	-	-
	k, std dev B	-	-	-	-	-	-	-	-	-	-	-	-	-	-	-	+	+	+		+	+	-		
	Bc, mean B	-																+	+						+
	Cc, mean B				+	+	+	+	+	+		+	+						-						+
	L, std dev B										-	-					+	+	+			+			
	Sk, mean B																	+	+						

system reaches an equilibrium. Again, in the dependency types where Network B is independent, the set B_D will be empty and the failures will not cascade back into Network B.

3.4. Regression model

After simulating the various failure scenarios, regression analyses were performed on the recorded outcomes. The analyses present the significant topological measures of the coupled network system that affect the robustness of Network A. For each method of forming dependencies, and each percentage of initial node failures in Network B, two regression analyses were completed, one that included the topological factors of Network A only and one including the topological factors of both Networks A and B. In real-world situations the two different infrastructures are commonly owned by different private companies that do not share infrastructure data for safety and security reasons. Therefore, if the owner or management of Network A wanted a general overview of the most important topological factors to consider in relation to robustness of random failure events they would be able to have an good overview of their own structure but would likely have little or no information regarding the topological structure of the network they are dependent on.

The dependent variable for the regression was the average percentage of nodes in Network A considered functional after a random disruption occurs in Network B over the 100 failure scenarios. The beta regression model was chosen as the dependent variable was in the range (0, 1). The beta regression model was proposed by Ferrari and Cribari-Neto [16] for instances when the dependent variable follows a beta distribution. The beta density they suggest for the regression model is a parameterisation of the beta density to account for a regression structure where the dependent variable is an average of the response and is given as

$$f(y;\mu;\phi) = \frac{\Gamma(\phi)}{\Gamma(\mu\phi)\Gamma((1-\phi)\mu)} y^{\mu\phi-1}(1-y)^{(1-\mu)\phi-1},\ 0 < y\langle 1,\ \phi \rangle 0$$

and the mean and variance of y are

$$E(y) = \mu$$

and

$$Var(y) = \frac{V(\mu)}{1+\phi}.$$

The parameter estimation is performed using the maximum likelihood method. For our analysis the logit link function was used.

When only the topology of Network A is considered, the independent variables were the mean, minimum, maximum and standard deviation of the four topology factors (shown in Table 3) as well as the percentage of dependency and mean nodal degree of dependent nodes, when applicable. When considering the topology of Network A and Network B the independent variables also included the mean, minimum, maximum and standard deviation of the four topological factors for Network B, as well as the percentage of dependency, mean nodal degree of dependent nodes and mean nodal degree of source nodes, when applicable.

Any of the within network topological factors that have a standard deviation of zero in Table 3 were removed from the data set as they do not impact the results. After removing variables with a standard deviation of zero, the Variance Inflation Factor (VIF) method was used to remove multicollinear variables. The VIF of each variable gives an indication of how well each variable can be explained by a combination of the other variables. A VIF of 1 indicates the variable is not explainable with the others, with a larger VIF indicating a larger degree of redundancy with the other variables. The variable with the largest VIF was removed iteratively until all variables had a VIF value of less than 10. For the regression models which only included the topological factors of Network A and for the model including the topological factors of both Networks A and B, the following variables of Network A were

Table 6
Significant covariates when Network A and Network B are interdependent and the effect of change of these covariates. The sign indicates if the covariate has a positive or negative influence on the percentage of nodes considered functional in Network A after random failures in Network B. The colour indicates the covariate coefficient value with the darker the colour the further the value is from 0.

Type of interdependency Networks A and B have		Fixed, 50%			Random			Random			Random			Random		
Percentage of source nodes in Network B		0			0			2			5			10		
Percentage of initial failures in Network B		10	25	50	10	25	50	10	25	50	10	25	50	10	25	50
Topology of Network A only in regression model	*k*, mean A	+	+	+	+	+	+	+	+	+	+	+	+	+	+	+
	k, std dev A	-	-	-	-	-	-	+	+	+			+			+
	Bc, mean A							+	+	+				-	-	
	Bc, max A							-	-	-	+	+				
	Cc, mean A	+	+	+			+		-	-	+	+				
	L, std dev A	-	-	-	-	-				+						
	Dp, A				-	-	-	-	-	-	-	-	-	-	-	-
	Dk, mean A	-	-	-	-	-	-	-	-	-	-	-	-	-	-	-
Topology of Networks A and B in regression model	*k*, mean A	+	+	+	+	+	+	+	+	+	+	+	+	+	+	+
	Bc, max A							-	-	-			-			
	Cc, mean A			+			+				+					
	L, std dev A	-	-		-	-		-	-	-			-			
	Dp, A				-	-	-	-	-	-	-	-	-	-	-	-
	Dk, mean A	-	-	-	-	-	-	-	-	-	-	-	-	-	-	-
	k, std dev B	-	-	-	-	-	-	+	+	+		+	+			+
	Bc, mean B								+	+				-	-	-
	Cc, mean B	+	+	+				-	-	-		+				
	L, std dev B	-			-	-			+	+			+			+
	Dp, B				-	-	-	-	-	-	-	-	-	-	-	-
	Dk, mean B	-	-			-		+	+						+	+
	Sk, mean B							+	+	+						

removed due to multicollinearity: maximum nodal degree, betweenness centrality standard deviation, clustering coefficient standard deviation, mean path length and maximum path length. Additionally, for the regression model including topological factors from both Networks A and B the variables maximum nodal degree and mean betweenness centrality of Network A were removed due to multicollinearity as well as the following variables from Network B: mean nodal degree, maximum nodal degree, maximum betweenness centrality, betweenness centrality standard deviation, clustering coefficient standard deviation, mean path length and maximum path length.

After removing variables due to multicollinearity, the remaining variable were normalised before fitting a beta regression model using the betareg R package [11]. After fitting the initial beta regression model, the least significant variable was removed iteratively, until all remaining variables were significant at the $\alpha = 0.05$ level. The results of the regression analysis are shown in Section 4.

4. Results

The results of the beta regression analyses are shown in Tables 5 and 6. Table 5 contains the results for regression analyses relating to the dependent coupled systems (i.e., Network A depends on Network B and Network B is independent). Table 6 contains the results for the regression analyses relating to the interdependent coupled systems (i.e. Networks A depends on Network B and Network B depends on Network A). The full results of the beta regression models are given in Appendix A.

Each column of Tables 5 and 6 represents the result of the regression analysis for a dependency type and percentage of initial failures occurring in Network B. For example, the first column in Table 5 shows the results for when, in each of the 2000 coupled network systems, 10% of nodes in Network A are dependent on Network B, Network B has no source nodes and 10% of nodes in Network B are randomly chosen to fail initially. If a topological factor was significant in a beta regression model, then the cell in the corresponding column is shaded and contains either a positive or negative sign. The sign indicates if the topological factor has a positive of negative influence on the robustness of Network A, and the shading indicates how strong of an influence it has, the darker the shading the more influential the factor is (i.e., the further the covariate coefficient is from 0). Table 7 shows the values associated with the levels of shading for both Tables 5 and 6 (the same scale has been used to shade both Tables 5 and 6). If a factor has a positive influence on the robustness of Network A, this indicates the greater the values of the topological factor the more robust Network A is. When a factor has a negative influence on the robustness of Network A this means the greater the value of the topological factor the less robust Network A is.

Table 7
Reference for the covariate coefficient values represented in Tables 5 and 6.

Coefficient Value	-1.4	-1.2	-1	-0.8	-0.6	-0.4	-0.2	0	0.2	0.4	0.6	0.8	1
Colour													

4.1. General observations

The level or percentage of dependency Network A had on Network B (Dp, A) was always significant (when included in the applicable regression models) and has a great negative on the robustness of Network A. Given that all initial failures occur in Network B, it seems intuitive that the more dependent Network A is on Network B, the greater the cascading effects will be in Network A. The mean intra-nodal degree of dependent nodes in Network A (Dk, mean A) consistently has a negative effect on the robustness of Network A. The structure of power-law networks is described as containing hubs [8]. The greater the mean nodal degree of dependent nodes, the more likely it is for the central nodes of the hubs to be dependent on Network B. When one of the central nodes of a hub fails, the network is more likely to fragment into many clusters that contain only a small number of nodes. Therefore, the higher the intra-nodal degree of dependent nodes in Network A, the greater the chance that a central node of a hub fails, and thus the less robust the network is when initial failures occur in Network B.

The mean nodal degree of Network A (k, mean A) is significant in every regression model with a positive influence on the robustness of Network A. This is expected as the greater the mean nodal degree, the more edges or connections are present in the network. This increases the chance of alternative pathways within the networks, increasing the redundancy of the network.

4.2. Dependent coupled systems

Table 5 shows the results for the dependent coupled systems, that is when Network A depends on Network B and Network B is independent. The top section of Table 5 shows the regression results when only the topological factors of Network A were included as covariates in the regression model. The bottom section of Table 5 shows the results when both the topological factors of Networks A and B were included in the regression model.

4.2.1. Topological factors of Network A only

When Network A has a fixed partial dependency on Network B, the first three columns in Table 5, the two most influential topological factors are the mean nodal degree (k, mean A) and the mean intra-nodal degree of dependent nodes (Dk, mean A). The mean nodal degree has a positive influence on the robustness of Network A, whereas the mean intra-nodal degree of dependent nodes has a negative influence. For Network A fully dependent on Network B (100% dependency), as shown in column four, it can be seen that the mean nodal degree (k, mean A) still has a positive influence on the robustness of Network A, but is less influential compared to when Network A is partially dependent. The standard deviation of both nodal degree and path length (k, std dev A and L, std dev A) have a weak negative influence on the robustness of Network A for all fixed dependency types. The mean clustering coefficient (Cc, mean A) has a weak positive influence on the robustness of Network A.

When the level of dependency is randomly assigned to each of the 2000 coupled systems, the percentage of dependent nodes in Network A (Dp, A) becomes the most influential factor, with a negative influence on the robustness of the network. The mean nodal degree and mean intra-nodal degree of dependent nodes (k, mean A and Dk, mean A) consistently have a positive and negative influence, respectively, on the robustness of Network A, however to a lesser extent than when the dependency level is fixed.

4.2.2. Topological factors of Network A and Network B

The topological factors with the greatest influence when the topological factors of both networks are included in the regression model are consistent of those when only the factors of Network A are considered. For fixed levels of dependency the mean nodal degree of Network A (k, mean A) has the greatest positive influence on the robustness of Network A and the mean intra-nodal degree of dependent nodes in Network A (Dk, mean A) has the greatest negative influence. When the level of dependency is randomly assigned to each coupled system again the percentage of dependency (Dp, A) becomes the most influential factor, with a negative influence on the robustness of Network A. The nodal degree standard deviation of Network A (k, std dev A) is no longer significant, however path length standard deviation of Network A (L, std dev A) is sometimes significant, mainly when the initial percentage of node failures is 10% and 25%, again with a negative influence on the robustness of Network A.

When source nodes are not present in the model the nodal degree standard deviation of Network B (k, std dev B) is significant with a weak negative influence on the robustness of Network A. When source nodes are present the nodal degree standard deviation of Network B (k, std dev B) is sometimes significant, mostly with a weak positive influence on the robustness of Network B. However, the inclusion of source nodes within the coupled system does not change which topological factors are the most influential on the robustness of the network.

4.3. Interdependent coupled systems

Table 6 shows the result for interdependent coupled systems, that is when Network A and B both depend on each other. The top section of Table 6 shows the regression results when only the topological factors of Network A are included in the regression model. The bottom section of Table 6 shows the results when the topological factors of both networks were included in the regression model.

4.3.1. Topological factors of Network A only

The first column in Table 6 shows the results when both Network A and Network B had a fixed level of dependency at 50%. Similar to the results for fixed levels of dependency in Table 5, the mean nodal degree and mean intra-nodal degree of dependent nodes in Network A (k, mean A and Dk, mean A) have the greatest influence on the robustness of Network A. Again, the mean nodal degree (k, mean A) has a positive influence and the mean intra-nodal degree of dependent nodes (Dk, mean A) has a negative influence. The remaining columns in Table 6 show the results when the level of dependency was randomly assigned to Networks A and B separately, with the level of dependency for Network A (Dp, A) included in the regression model. Again, this now becomes the most influential factor, with a negative influence on the robustness of Network A. The influence of the mean nodal degree and mean intra-nodal degree (k, mean A and Dk, mean A) are still influential with a positive and negative influence, respectively.

For a fixed 50% dependency and random dependency when no source nodes are present both the standard deviation of the nodal degree and path length (*k*, std dev A and *L*, std dev A) have a weak negative influence on the robustness of Network A. When source nodes are present the influence of both nodal degree standard deviation and path length standard deviation (*k*, std dev A and *L*, std dev A) have a weak influence, when significant, but now both have a positive influence on the robustness of Network A.

4.3.2. Topological factors of Network A and Network B

Comparing the bottom section on Table 6 with that of Table 5, the results look similar, with the main difference being that now that Network B depends on Network A the percentage of dependency Network B has on Network A (*Dp*, B) is now included in the model, and is significant with a negative influence on the robustness of Network A. The mean intra-nodal degree of the dependent nodes in Network B (*Dk*, mean B) is significant in some of the regression models, however the influence it has is not as great as the mean intra-nodal degree of the dependent nodes in Network A (*Dk*, mean A).

Nodal degree standard deviation of Network A (*k*, std dev A) is no longer significant for any regression models. However, path length standard deviation of Network A (*L*, std dev A) is still sometimes significant, with a weak negative influence when significant. Nodal degree standard deviation of Network B (*k*, std dev B) is often significant, with a weak influence on the robustness of Network A. When source nodes are not present in Network B this influence is negative, but becomes positive when source nodes are present in Network B.

5. Discussion

In the analysis presented, the first order effects of a disruption within a coupled system have been explored for different structures of coupled systems. Across the various methods of forming dependencies (both dependent and interdependent systems) as well as two different methods of simulating failures, the majority of the results were consistent.

The most influential factors across all the coupled network structures investigated are the mean nodal degree of Network A, the mean intra-nodal degree of dependent nodes in Network A and, when applicable, the percentage of dependency Network A has on Network B. It is worth noting that of the three most influential factors, two were in relation to the dependency Network A has on Network B. However, this analysis only covers scenarios where initial failures occurred in Network B and so these results are to be expected.

The analysis which included the topological factors of Network B (in addition to those of Network A) concluded some addition factors were significant, but have only minor influence on the robustness of Network A. This suggests that even for interdependent networks, the most important topological factors when characterising the robustness are those relating to the network's own structure.

The most influential factor was the percentage of dependency Network A had on Network B. This has a negative effect on the robustness of a network in relation to first order effects. All initial disruptions occurred within Network B, and so, the more nodes in Network A depending on Network B, the more likely it is for failures to cascade into Network A. Increased percentage of dependency increases the number of paths available for the disruption to cascade from Network B to Network A.

The mean nodal degree of Network A has a positive influence on the network's robustness, however, the mean nodal degree of dependent nodes in Network A has a negative influence. The positive influence of the mean nodal degree can be attributed to the fact that the higher the mean nodal degree a network has, the more intra-connections are present, increasing the likelihood of available paths between the nodes, and so, increasing the redundancy of the network. The negative influence of the mean intra-nodal degree of dependent nodes in Network A is intuitive. Any dependent node in Network A fails if the node it depends on fails. If the dependent nodes have a high intra-degree, when they fail they have a greater potential to affect the robustness of Network A.

Some factors were significant over the different system structures, but their effect on the robustness of the network changed. For example, when source nodes are present in Network B, the standard deviation of the nodal degree of Network A has a positive influence. However, when neither network within the coupled system contains source nodes, the standard deviation of Network A's nodal degree has a negative effect on its robustness. The mean clustering coefficient of Network A also changes from having a positive influence when source nodes not are present in Network B, to a negative influence when source nodes are present in the coupled system.

The change in the influence of the clustering coefficient may be due to the different methods of assessing which nodes are functional for the different coupled system structures. When source nodes are not present within the system, the GCC method is used to assess which nodes are functional after disruption. When this method is used the more connections between a neighbourhood of nodes, the less likely the neighbourhood is to fragment when disruptions occur, leaving a cluster with a high population. However, when source nodes are present, a node is only functional if there is a path available from any source node to that node. If neighbourhoods of nodes are highly connected, they may be reliant on only a small number of nodes in the neighbourhood to receive input from the source nodes. When these nodes fail, the other members of the neighbourhood will no longer have a path from a source node to itself, causing the entire neighbourhood to fail.

When comparing the results of the coupled system analysis to those found by LaRocca and Guikema [23], some factors which were significant for independent networks were no longer significant for dependent networks. Other factors remained significant but the influence of the factors on the robustness of the network changed. LaRocca and Guikema [23] found that the mean clustering coefficient was the most influential topological factor for independent networks when 10% and 25% of nodes initially failed. When 50% and 75% nodes initially failed in an independent network the mean nodal degree was the most influential factor. However, when looking at the robustness of a network in a coupled system, the influence of the mean nodal degree is always more influential that the mean clustering coefficient. This suggests that for first order disruptions the overall redundancy of the network is more important than the local redundancy.

These results can be used alongside those of LaRocca and Guikema [23] to provide some direction on which topological factors should be given more focus on when planning improvements or developing new networks. The influence of the significant topological factors shown by LaRocca and Guikema [23] for failures within a network and those presented in this paper for first order disruptions can be used together to plan the structure of networks, such as infrastructure, so that it is robust to disruptions that both directly affect it and, through dependencies, indirectly affect it.

If a new network is being designed, attention should be given to the level of dependency. Our results show that for each dependency type we investigated, the higher the level of dependency, the less robust the network is to first order disruptions. This suggests that the level of dependency a network has should be low as possible.

The nodes which have dependencies should also be carefully considered. Our results show that the greater the nodal degree of the components that are dependent on another network, the less robust the network is to first order disruptions. This suggests that dependent nodes should have the fewest number of intra-connection possible. However, in reality, the components which have dependencies are guided by functionality. In this case, the results can be considered when deciding how to increase redundancy within the network. For example, in a water supply network, the dependency on the power network is through pumps within the network. The nodal degree of the dependent pumps could be taken into consideration when deciding where to improve redundancy, such as the addition of a back-up generator.

This extension of LaRocca and Guikema [23] to interdependent networks has covered a range of coupled network structures to provide a generalised overview of the important topological factors for characterising robustness of a dependent network, however, there are numerous ways of modelling dependencies between networks, as well as multiple failure scenarios. The results give a general overview of the important topological factors for a network present in a coupled infrastructure system, where each dependent node has one and only one dependency, concerning the first order effects of a random disruption.

The results presented in this paper highlight to networks, such as infrastructure, that even though they depend on another infrastructure, the most influential factors are primarily those attributed within their own structure, or topology. Therefore, changes to their own structure can help to increase their robustness to random failures in the dependent networks. Although when applicable, the percentage of dependency was the most influential topological factor, the dependency of one infrastructure on another is defined by the need for the input (or the utility) that the infrastructure produces and thus is not easy to change to increase the robustness of the dependent infrastructure. Therefore, the more important topological factors to consider when designing or improving infrastructure are nodal degree and the intra-nodal degree of the dependent networks. The topology of components (or nodes) with dependencies on other networks are shown to be important and thus gives an indication that providing some redundancy into the infrastructure, such as back-up generators for those dependent on the power network, for example, could improve their own robustness.

6. Conclusion

In conclusion we find that the most influential topological factors associated with the robustness of coupled power-law networks with exponential cut-off are those related to the dependency the network has on the network in which the disruption originates. These factors are the percentage of dependency and the mean nodal degree of the dependent nodes in the coupled power-law network system. However, in networks such as infrastructure the dependency an infrastructure has on another, and which components need input from another infrastructure is determined by the operational needs of the network and thus is difficult to change. The mean nodal degree of the network has also shown to be very influential on the robustness of the network, with the greater the mean degree the more robust the network was to first order effects of a disruption. Although a variety of dependency types have been explored, the results remained consistent over the different coupled network structures. The results provide a general overview of the most influential topological factors for a coupled network system and can be used as a basis of which topological factors should be considered by, for example, infrastructure owners or management when developing or improving their infrastructure.

Supplementary materials

Supplementary material associated with this article can be found, in the online version, at doi:10.1016/j.ress.2019.106560.

Appendix A

Tables A.1–A.6 show the full beta regression results for the various regression analyses performed as part of the current paper.

Table A.1
Full beta regression results for fixed dependency types when topology of Network A only are included in the regression analysis.

Dependency type	10% initial failures Topology measure	Co-efficient	Std error	p value	25% initial failures Topology measure	Co-efficient	Std error	p value	50% initial failures Topology measure	Co-efficient	Std error	p value
Network A fixed 10%	Intercept	3.904	0.007	0.000	Intercept	2.991	0.007	0.000	Intercept	2.328	0.007	0.000
dependency	k, mean A	0.460	0.010	0.000	k, mean A	0.500	0.013	0.000	k, mean A	0.554	0.014	0.000
Network B	Bc, mean A	−0.049	0.008	0.000	k, std dev A	−0.030	0.007	0.000	k, std dev A	−0.029	0.008	0.000
independent	L, std dev A	−0.041	0.011	0.000	Cc, mean A	0.036	0.009	0.000	Cc, mean A	0.034	0.010	0.000
	Dk, mean A	−0.491	0.006	0.000	L, std dev A	−0.064	0.014	0.000	L, std dev A	−0.066	0.016	0.000
					Dk, mean A	−0.562	0.006	0.000	Dk, mean A	−0.652	0.007	0.000
Network A fixed 30%	Intercept	2.712	0.005	0.000	Intercept	1.741	0.005	0.000	Intercept	0.964	0.006	0.000
dependency	k, mean A	0.581	0.013	0.000	k, mean A	0.634	0.012	0.000	k, mean A	0.769	0.015	0.000
Network B	K, std dev A	−0.042	0.006	0.000	K, std dev A	−0.037	0.006	0.000	K, std dev A	−0.032	0.007	0.000
independent	Cc, mean A	0.021	0.007	0.003	Cc, mean A	0.023	0.007	0.001	Cc, mean A	0.031	0.008	0.000
	L, std dev A	−0.052	0.012	0.000	L, std dev A	−0.041	0.011	0.000	L, std dev A	−0.031	0.013	0.020
	Dk, mean A	−0.509	0.009	0.000	Dk, mean A	−0.576	0.008	0.000	Dk, mean A	−0.729	0.010	0.000
Network A fixed 50%	Intercept	2.168	0.004	0.000	Intercept	1.129	0.004	0.000	Intercept	0.232	0.005	0.000
dependency	k, mean A	0.607	0.013	0.000	k, mean A	0.689	0.012	0.000	k, mean A	0.894	0.015	0.000
Network B	K, std dev A	−0.049	0.005	0.000	K, std dev A	−0.046	0.004	0.000	K, std dev A	−0.045	0.006	0.000
independent	Cc, mean A	0.012	0.006	0.040	Cc, mean A	0.015	0.005	0.005	Cc, mean A	0.020	0.007	0.002
	L, std dev A	−0.048	0.010	0.000	L, std dev A	−0.038	0.009	0.000	L, std dev A	−0.026	0.011	0.015
	Dk, mean A	−0.498	0.011	0.000	Dk, mean A	−0.581	0.010	0.000	Dk, mean A	−0.790	0.012	0.000
Network A fixed 100%	Intercept	1.396	0.003	0.000	Intercept	0.184	0.003	0.000	Intercept	−1.176	0.004	0.000
dependency	k, mean A	0.158	0.006	0.000	k, mean A	0.178	0.006	0.000	k, mean A	0.233	0.007	0.000
Network B	K, std dev A	−0.078	0.007	0.000	K, std dev A	−0.086	0.007	0.000	K, std dev A	−0.102	0.006	0.000
independent	Bc, max A	0.017	0.007	0.013	Bc, max A	0.017	0.007	0.010	Bc, mean A	0.021	0.008	0.009
	L, std dev A	−0.067	0.006	0.000	Cc, mean A	0.012	0.004	0.005	Cc, mean A	0.037	0.006	0.000
					L, std dev A	−0.054	0.007	0.000	L, std dev A	−0.049	0.010	0.000
Network A fixed 50%	Intercept	1.941	0.005	0.000	Intercept	0.932	0.005	0.000	Intercept	0.092	0.006	0.000
dependency	k, mean A	0.634	0.016	0.000	k, mean A	0.746	0.016	0.000	k, mean A	0.977	0.018	0.000
Network B fixed 50%	K, std dev A	−0.061	0.006	0.000	K, std dev A	−0.053	0.006	0.000	K, std dev A	−0.051	0.007	0.000
dependency	Cc, mean A	0.019	0.007	0.006	Cc, mean A	0.027	0.007	0.000	Cc, mean A	0.036	0.008	0.000
	L, std dev A	−0.081	0.012	0.000	L, std dev A	−0.058	0.012	0.000	L, std dev A	−0.026	0.013	0.045
	Dk, mean A	−0.528	0.013	0.000	Dk, mean A	−0.641	0.013	0.000	Dk, mean A	−0.887	0.015	0.000

Table A.2
Full beta regression results for fixed dependency types when the topology of both Network A and Network B are included in the regression analysis.

	10% initial failures				25% initial failures				50% initial failures			
Dependency type	Topology measure	Co-efficient	Std error	p value	Topology measure	Co-efficient	Std error	p value	Topology measure	Co-efficient	Std error	p value
Network A fixed 10%	Intercept	3.904	0.007	0.000	Intercept	2.991	0.007	0.000	Intercept	2.328	0.007	0.000
dependency	k, mean A	0.467	0.011	0.000	k, mean A	0.492	0.013	0.000	k, mean A	0.547	0.014	0.000
Network B	L, std dev A	−0.065	0.012	0.000	Cc, mean A	0.038	0.009	0.000	Cc, mean A	0.037	0.009	0.000
independent	Dk, mean A	−0.491	0.006	0.000	L, std dev A	−0.053	0.013	0.000	L, std dev A	−0.056	0.014	0.000
	k, std dev B	−0.017	0.008	0.029	Dk, mean A	−0.563	0.006	0.000	Dk, mean A	−0.652	0.007	0.000
	Bc, mean B	−0.032	0.010	0.001	k, std dev B	−0.026	0.007	0.000	k, std dev B	−0.025	0.007	0.000
Network A fixed 30%	Intercept	2.712	0.005	0.000	Intercept	1.741	0.005	0.000	Intercept	0.964	0.006	0.000
dependency	k, mean A	0.568	0.012	0.000	k, mean A	0.622	0.011	0.000	k, mean A	0.746	0.011	0.000
Network B	L, std dev A	−0.034	0.010	0.001	L, std dev A	−0.024	0.009	0.011	Dk, mean A	−0.729	0.010	0.000
independent	Dk, mean A	−0.509	0.009	0.000	Dk, mean A	−0.576	0.008	0.000	k, std dev B	−0.025	0.006	0.000
	k, std dev B	−0.037	0.005	0.000	k, std dev B	−0.032	0.005	0.000	Cc, mean B	0.044	0.006	0.000
	Cc, mean B	0.030	0.006	0.000	Cc, mean B	0.034	0.006	0.000				
Network A fixed 50%	Intercept	2.168	0.004	0.000	Intercept	1.129	0.004	0.000	Intercept	0.232	0.005	0.000
dependency	k, mean A	0.593	0.013	0.000	k, mean A	0.678	0.012	0.000	k, mean A	0.874	0.012	0.000
Network B	L, std dev A	−0.030	0.008	0.000	L, std dev A	−0.023	0.007	0.001	Dk, mean A	−0.789	0.012	0.000
independent	Dk, mean A	−0.497	0.011	0.000	Dk, mean A	−0.580	0.010	0.000	k, std dev B	−0.039	0.005	0.000
	k, std dev B	−0.043	0.004	0.000	k, std dev B	−0.041	0.004	0.000	Cc, mean B	0.029	0.005	0.000
	Cc, mean B	0.019	0.005	0.000	Cc, mean B	0.019	0.005	0.000				
Network A fixed 100%	Intercept	1.396	0.003	0.000	Intercept	0.184	0.003	0.000	Intercept	−1.176	0.004	0.000
dependency	k, mean A	0.146	0.005	0.000	k, mean A	0.162	0.006	0.000	k, mean A	0.210	0.004	0.000
Network B	L, std dev A	−0.029	0.006	0.000	L, std dev A	−0.017	0.006	0.007	k, std dev B	−0.078	0.004	0.000
independent	k, std dev B	−0.058	0.004	0.000	k, std dev B	−0.064	0.004	0.000	Cc, mean B	0.044	0.004	0.000
	L, std dev B	−0.026	0.006	0.000	Cc, mean B	0.016	0.004	0.000				
					L, std dev B	−0.020	0.006	0.002				
Network A fixed 50%	Intercept	1.941	0.005	0.000	Intercept	0.932	0.005	0.000	Intercept	0.092	0.006	0.000
dependency	k, mean A	0.659	0.018	0.000	k, mean A	0.758	0.017	0.000	k, mean A	0.958	0.015	0.000
Network B fixed 50%	L, std dev A	−0.047	0.010	0.000	L, std dev A	−0.039	0.010	0.000	Cc, mean A	0.024	0.011	0.022
dependency	Dk, mean A	−0.529	0.013	0.000	Dk, mean A	−0.639	0.013	0.000	Dk, mean A	−0.886	0.015	0.000
	k, std dev B	−0.059	0.006	0.000	k, std dev B	−0.046	0.005	0.000	k, std dev B	−0.044	0.006	0.000
	Cc, mean B	0.021	0.007	0.003	Cc, mean B	0.033	0.006	0.000	Cc, mean B	0.023	0.011	0.033
	L, std dev B	−0.030	0.011	0.007	Dk, mean B	−0.030	0.011	0.006				
	Dk, mean B	−0.032	0.011	0.005								

Table A.3
Full beta regression results for when Network A has random dependency types, Network B is independent and the topology of Network A only is included in the regression analysis. .

	10% initial failures				25% initial failures				50% initial failures			
Dependency group	Topology measure	Co-efficient	Std error	p value	Topology measure	Co-efficient	Std error	p value	Topology measure	Co-efficient	Std error	p value
Network A random	Intercept	2.347	0.009	0.000	Intercept	1.319	0.009	0.000	Intercept	0.397	0.010	0.000
dependency	k, mean A	0.128	0.013	0.000	k, mean A	0.147	0.013	0.000	k, mean A	0.264	0.011	0.000
Network B	k, std dev A	−0.035	0.009	0.000	k, std dev A	−0.037	0.010	0.000	k, std dev A	−0.029	0.010	0.002
independent	L, std dev A	−0.039	0.013	0.003	L, std dev A	−0.040	0.014	0.005	Dp, A	−1.064	0.011	0.000
	Dp, A	−0.693	0.008	0.000	Dp, A	−0.814	0.009	0.000	Dk, mean A	−0.453	0.020	0.000
	Dk, mean A	−0.037	0.007	0.000	Dk, mean A	−0.057	0.007	0.000				
Network A random	Intercept	2.430	0.008	0.000	Intercept	1.312	0.008	0.000	Intercept	0.178	0.010	0.000
dependency	k, mean A	0.230	0.013	0.000	k, mean A	0.277	0.016	0.000	k, mean A	0.332	0.023	0.000
Network B	k, std dev A	0.105	0.015	0.000	k, std dev A	0.238	0.017	0.000	k, std dev A	0.495	0.026	0.000
independent with 2%	Bc, mean A	0.025	0.010	0.015	Bc, mean A	0.052	0.016	0.001	Bc, mean A	0.076	0.024	0.001
source nodes	Bc, max A	−0.061	0.016	0.000	Bc, max A	−0.134	0.018	0.000	Bc, max A	−0.246	0.022	0.000
	Dp, A	−0.576	0.008	0.000	Cc, mean A	−0.042	0.013	0.002	Cc, mean A	−0.102	0.017	0.000
	Dk, mean A	−0.162	0.011	0.000	Dp, A	−0.618	0.008	0.000	L, std dev A	0.083	0.027	0.002
					Dk, mean A	−0.211	0.012	0.000	Dp, A	−0.705	0.010	0.000
									Dk, mean A	−0.300	0.016	0.000
Network A random	Intercept	2.512	0.008	0.000	Intercept	1.446	0.008	0.000	Intercept	0.431	0.009	0.000
dependency	k, mean A	0.214	0.011	0.000	k, mean A	0.254	0.012	0.000	k, mean A	0.353	0.014	0.000
Network B	Dp, A	−0.622	0.008	0.000	k, std dev A	0.016	0.007	0.033	k, std dev A	0.143	0.019	0.000
independent with 5%	Dk, mean A	−0.143	0.012	0.000	Dp, A	−0.695	0.008	0.000	Bc, max A	−0.066	0.019	0.001
source nods					Dk, mean A	−0.169	0.012	0.000	Cc, mean A	−0.034	0.010	0.001
									Dp, A	−0.832	0.009	0.000
									Dk, mean A	−0.251	0.013	0.000
Network A random	Intercept	2.533	0.009	0.000	Intercept	1.482	0.008	0.000	Intercept	0.516	0.009	0.000
dependency	k, mean A	0.166	0.011	0.000	k, mean A	0.191	0.011	0.000	k, mean A	0.318	0.013	0.000
Network B	k, std dev A	−0.019	0.007	0.010	Dp, A	−0.687	0.008	0.000	Dp, A	−0.843	0.010	0.000
independent with 10%	Dp, A	−0.616	0.008	0.000	Dk, mean A	−0.125	0.011	0.000	Dk, mean A	−0.258	0.014	0.000
source nodes	Dk, mean A	−0.108	0.011	0.000								

Table A.4
Full beta regression results for when Networks A and B have random dependency type and the topology of Network A only is included in the regression analysis.

Dependency group	10% initial failures				25% initial failures				50% initial failures			
	Topology measure	Co-efficient	Std error	p value	Topology measure	Co-efficient	Std error	p value	Topology measure	Co-efficient	Std error	p value
Network A random	Intercept	1.969	0.012	0.000	Intercept	0.994	0.011	0.000	Intercept	0.148	0.011	0.000
dependency	k, mean A	0.384	0.022	0.000	k, mean A	0.453	0.022	0.000	k, mean A	0.548	0.017	0.000
Network B random	k, std dev A	−0.072	0.012	0.000	k, std dev A	−0.071	0.012	0.000	k, std dev A	−0.054	0.011	0.000
dependency	L, std dev A	−0.096	0.018	0.000	L, std dev A	−0.078	0.018	0.000	Cc, mean A	0.040	0.011	0.000
	Dp, A	−0.935	0.012	0.000	Dp, A	−1.111	0.012	0.000	Dp, A	−1.369	0.013	0.000
	Dk, mean A	−0.284	0.019	0.000	Dk, mean A	−0.338	0.018	0.000	Dk, mean A	−0.475	0.017	0.000
Network A random	Intercept	2.043	0.013	0.000	Intercept	0.952	0.012	0.000	Intercept	−0.164	0.013	0.000
dependency	k, mean A	0.254	0.024	0.000	k, mean A	0.338	0.026	0.000	k, mean A	0.343	0.032	0.000
Network B random	k, std dev A	0.111	0.021	0.000	k, std dev A	0.260	0.026	0.000	k, std dev A	0.571	0.036	0.000
dependency with 2%	Bc, mean A	0.046	0.014	0.001	Bc, mean A	0.072	0.023	0.001	Bc, mean A	0.078	0.032	0.014
source nodes	Bc, max A	−0.075	0.023	0.001	Bc, max A	−0.161	0.026	0.000	Bc, max A	−0.283	0.030	0.000
	Dp, A	−0.768	0.012	0.000	Cc, mean A	−0.045	0.019	0.020	Cc, mean A	−0.125	0.023	0.000
	Dk, mean A	−0.219	0.023	0.000	Dp, A	−0.874	0.013	0.000	L, std dev A	0.127	0.037	0.001
					Dk, mean A	−0.285	0.022	0.000	Dp, A	−1.005	0.015	0.000
									Dk, mean A	−0.317	0.023	0.000
Network A random	Intercept	2.054	0.013	0.000	Intercept	1.038	0.012	0.000	Intercept	0.077	0.012	0.000
dependency	k, mean A	0.228	0.018	0.000	k, mean A	0.309	0.019	0.000	k, mean A	0.499	0.020	0.000
Network B random	Bc, max A	0.026	0.011	0.023	Bc, max A	0.038	0.012	0.002	k, std dev A	0.122	0.012	0.000
dependency with 5%	Cc, mean A	0.044	0.011	0.000	Cc, mean A	0.047	0.012	0.000	Dp, A	−1.090	0.014	0.000
source nodes	Dp, A	−0.787	0.012	0.000	Dp, A	−0.919	0.013	0.000	Dk, mean A	−0.359	0.021	0.000
	Dk, mean A	−0.153	0.018	0.000	Dk, mean A	−0.202	0.019	0.000				
Network A random	Intercept	2.139	0.012	0.000	Intercept	1.148	0.011	0.000	Intercept	0.254	0.011	0.000
dependency	k, mean A	0.235	0.016	0.000	k, mean A	0.394	0.019	0.000	k, mean A	0.536	0.018	0.000
Network B random	Bc, mean A	−0.050	0.012	0.000	Bc, mean A	−0.042	0.012	0.001	k, std dev A	0.037	0.011	0.001
dependency with 10%	Dp, A	−0.810	0.012	0.000	Dp, A	−0.939	0.012	0.000	Dp, A	−1.143	0.013	0.000
source nodes	Dk, mean A	−0.159	0.014	0.000	Dk, mean A	−0.339	0.020	0.000	Dk, mean A	−0.488	0.020	0.000

Table A.5
Full beta regression results for when Network A has random dependency types, Network B is independent and the topology of Network A and Network B is included in the regression analysis.

Dependency group	10% initial failures				25% initial failures				50% initial failures			
	Topology measure	Co-efficient	Std error	p value	Topology measure	Co-efficient	Std error	p value	Topology measure	Co-efficient	Std error	p value
Network A random	Intercept	2.347	0.009	0.000	Intercept	1.319	0.009	0.000	Intercept	0.397	0.010	0.000
dependency	k, mean A	0.122	0.012	0.000	k, mean A	0.142	0.013	0.000	k, mean A	0.264	0.011	0.000
Network B	L, std dev A	−0.031	0.012	0.012	L, std dev A	−0.032	0.013	0.017	Dp, A	−1.064	0.011	0.000
independent	Dp, A	−0.693	0.008	0.000	Dp, A	−0.814	0.009	0.000	Dk, mean A	−0.453	0.020	0.000
	Dk, mean A	−0.037	0.007	0.000	Dk, mean A	−0.057	0.007	0.000	k, std dev B	−0.032	0.010	0.001
	k, std dev B	−0.035	0.008	0.000	k, std dev B	−0.036	0.009	0.000				
Network A random	Intercept	2.431	0.008	0.000	Intercept	1.312	0.008	0.000	Intercept	0.179	0.010	0.000
dependency	k, mean A	0.221	0.016	0.000	k, mean A	0.240	0.017	0.000	k, mean A	0.306	0.023	0.000
Network B	Bc, max A	−0.061	0.015	0.000	Bc, max A	−0.122	0.017	0.000	Bc, max A	−0.210	0.021	0.000
independent with 2%	L, std dev A	−0.050	0.015	0.001	L, std dev A	−0.077	0.017	0.000	L, std dev A	−0.122	0.021	0.000
source nodes	Dp, A	−0.575	0.008	0.000	Dp, A	−0.615	0.008	0.000	Dp, A	−0.701	0.010	0.000
	Dk, mean A	−0.162	0.011	0.000	Dk, mean A	−0.210	0.012	0.000	Dk, mean A	−0.295	0.016	0.000
	k, std dev B	0.126	0.016	0.000	k, std dev B	0.234	0.018	0.000	k, std dev B	0.458	0.024	0.000
	L, std dev B	0.084	0.016	0.000	Bc, mean B	0.058	0.018	0.001	Bc, mean B	0.089	0.025	0.000
					L, std dev B	0.121	0.022	0.000	Cc, mean B	−0.052	0.016	0.001
					Sk, B	0.018	0.009	0.034	L, std dev B	0.228	0.027	0.000
									Sk, B	0.037	0.010	0.000
Network A random	Intercept	2.512	0.008	0.000	Intercept	1.446	0.008	0.000	Intercept	0.431	0.009	0.000
dependency	k, mean A	0.214	0.011	0.000	k, mean A	0.254	0.012	0.000	k, mean A	0.324	0.018	0.000
Network B	Dp, A	−0.622	0.008	0.000	Dp, A	−0.695	0.008	0.000	Bc, max A	−0.061	0.017	0.000
independent with 5%	Dk, mean A	−0.143	0.012	0.000	Dk, mean A	−0.169	0.012	0.000	L, std dev A	−0.048	0.017	0.004
source nodes					k, std dev B	0.016	0.007	0.024	Dp, A	−0.832	0.009	0.000
									Dk, mean A	−0.250	0.013	0.000
									k, std dev B	0.149	0.018	0.000
									L, std dev B	0.088	0.018	0.000
Network A random	Intercept	2.534	0.008	0.000	Intercept	1.482	0.008	0.000	Intercept	0.516	0.009	0.000
dependency	k, mean A	0.167	0.011	0.000	k, mean A	0.191	0.011	0.000	k, mean A	0.296	0.015	0.000
Network B	Dp, A	−0.616	0.008	0.000	Dp, A	−0.687	0.008	0.000	Dp, A	−0.842	0.010	0.000
independent with 10%	Dk, mean A	−0.109	0.011	0.000	Dk, mean A	−0.125	0.011	0.000	Dk, mean A	−0.256	0.013	0.000
source nodes	k, std dev B	−0.021	0.007	0.005					Bc, mean B	0.039	0.014	0.005
									Cc, mean B	0.037	0.012	0.002

Table A.6
Full beta regression results for when Networks A and B have random dependency types and the topology of Network A and Network B is included in the regression analysis.

	10% initial failures				25% initial failures				50% initial failures			
Dependency group	Topology measure	Co-efficient	Std error	p value	Topology measure	Co-efficient	Std error	p value	Topology measure	Co-efficient	Std error	p value
Network A random	Intercept	2.045	0.010	0.000	Intercept	1.031	0.010	0.000	Intercept	0.159	0.010	0.000
dependency	k, mean A	0.421	0.018	0.000	k, mean A	0.486	0.021	0.000	k, mean A	0.551	0.017	0.000
Network B random	L, std dev A	−0.050	0.016	0.002	L, std dev A	−0.043	0.017	0.013	Cc, mean A	0.039	0.011	0.000
dependency	Dp, A	−0.974	0.010	0.000	Dp, A	−1.121	0.010	0.000	Dp, A	−1.362	0.012	0.000
	Dk, mean A	−0.319	0.016	0.000	Dk, mean A	−0.362	0.015	0.000	Dk, mean A	−0.486	0.016	0.000
	k, std dev B	−0.073	0.010	0.000	k, std dev B	−0.069	0.010	0.000	k, std dev B	−0.055	0.010	0.000
	L, std dev B	−0.065	0.016	0.000	L, std dev B	−0.036	0.017	0.037	Dp, B	−0.168	0.010	0.000
	Dp, B	−0.293	0.008	0.000	Dp, B	−0.249	0.009	0.000				
					Dk, mean B	−0.025	0.013	0.048				
Network A random	Intercept	2.120	0.010	0.000	Intercept	0.997	0.011	0.000	Intercept	−0.145	0.013	0.000
dependency	k, mean A	0.325	0.021	0.000	k, mean A	0.364	0.025	0.000	k, mean A	0.362	0.030	0.000
Network B random	Bc, max A	−0.049	0.017	0.003	Bc, max A	−0.132	0.021	0.000	Bc, max A	−0.221	0.026	0.000
dependency with 2%	L, std dev A	−0.040	0.017	0.016	L, std dev A	−0.088	0.021	0.000	L, std dev A	−0.106	0.027	0.000
source nodes	Dp, A	−0.839	0.010	0.000	Dp, A	−0.916	0.011	0.000	Dp, A	−1.011	0.014	0.000
	Dk, mean A	−0.244	0.019	0.000	Dk, mean A	−0.302	0.019	0.000	Dk, mean A	−0.326	0.021	0.000
	k, std dev B	0.094	0.016	0.000	k, std dev B	0.236	0.024	0.000	k, std dev B	0.479	0.030	0.000
	Cc, mean B	−0.036	0.011	0.002	Bc, mean B	0.058	0.026	0.024	Bc, mean B	0.124	0.031	0.000
	Dp, B	−0.297	0.009	0.000	Cc, mean B	−0.048	0.016	0.003	Cc, mean B	−0.086	0.020	0.000
	Dk, mean B	0.020	0.010	0.040	L, std dev B	0.071	0.027	0.008	L, std dev B	0.173	0.033	0.000
	Sk, B	0.022	0.009	0.014	Dp, B	−0.274	0.010	0.000	Dp, B	−0.245	0.013	0.000
					Dk, mean B	0.023	0.010	0.024	Sk, B	0.058	0.013	0.000
					Sk, B	0.032	0.010	0.002				
Network A random	Intercept	2.141	0.010	0.000	Intercept	1.090	0.010	0.000	Intercept	0.098	0.011	0.000
dependency	k, mean A	0.235	0.014	0.000	k, mean A	0.307	0.016	0.000	k, mean A	0.448	0.025	0.000
Network B random	Cc, mean A	0.031	0.009	0.001	Dp, A	−0.967	0.011	0.000	Bc, max A	−0.051	0.023	0.027
dependency with 5%	Dp, A	−0.867	0.010	0.000	Dk, mean A	−0.214	0.016	0.000	L, std dev A	−0.068	0.022	0.002
source nodes	Dk, mean A	−0.171	0.015	0.000	k, std dev B	0.023	0.010	0.021	Dp, A	−1.103	0.013	0.000
	Dp, B	−0.326	0.009	0.000	Cc, mean B	0.029	0.010	0.004	Dk, mean A	−0.359	0.019	0.000
					Dp, B	−0.293	0.010	0.000	k, std dev B	0.175	0.024	0.000
									L, std dev B	0.121	0.024	0.000
									Dp, B	−0.223	0.011	0.000
Network A random	Intercept	2.222	0.010	0.000	Intercept	1.198	0.009	0.000	Intercept	0.275	0.010	0.000
dependency	k, mean A	0.234	0.012	0.000	k, mean A	0.422	0.016	0.000	k, mean A	0.537	0.020	0.000
Network B random	Dp, A	−0.874	0.009	0.000	Dp, A	−0.979	0.010	0.000	Dp, A	−1.153	0.012	0.000
dependency with 10%	Dk, mean A	−0.164	0.010	0.000	Dk, mean A	−0.392	0.016	0.000	Dk, mean A	−0.531	0.018	0.000
source nodes	Bc, mean B	−0.042	0.009	0.000	Bc, mean B	−0.031	0.010	0.002	k, std dev B	0.081	0.017	0.000
	Dp, B	−0.313	0.008	0.000	Dp, B	−0.277	0.009	0.000	Bc, mean B	−0.063	0.020	0.001
					Dk, mean B	0.021	0.009	0.024	L, std dev B	0.082	0.026	0.001
									Dp, B	−0.215	0.011	0.000

References

[1] Albert R, Albert I, Nakarado GL. Structural vulnerability of the North American power grid. Phys Rev E 2004;69(2):025103.
[2] Albert R, Barabási A-L. Statistical mechanics of complex networks. Rev Mod Phys 2002;74(1):47.
[3] Alipour Z, Monfared MAS, Zio E. Comparing topological and reliability-based vulnerability analysis of Iran power transmission network. Proc Inst Mech Eng Part O: J Risk Reliab 2014;228(2):139–51.
[4] Barabási A-L, Albert R. Emergence of scaling in random networks. Science 1999;286:509–12.
[5] Barabási A-L, Albert R, Jeong H. Mean-field theory for scale-free random networks. Physica A 1999;272(1–2):173–87.
[6] Broido AD, Clauset A. Scale-free networks are rare. Nat Commun 2019;10(1).
[7] Buldyrev SV, Parshani R, Paul G, Stanley HE, Havlin S. Catastrophic cascade of failures in interdependent networks. Nature 2010;464(7291):1025–8.
[8] Buldyrev SV, Shere NW, Cwilich GA. Interdependent networks with identical degrees of mutually dependent nodes. Phys Rev E 2011;83(1):016112.
[9] Chai WK, Kyritsis V, Katsaros KV, Pavlou G. Resilience of interdependent communication and power distribution networks against cascading failures. Proceedings of the IFIP Networking Conference (IFIP Networking) and Workshops, 2016. IEEE; 2016.
[10] Cheng Z, Cao J. Cascade of failures in interdependent networks coupled by different type networks. Physica A 2015;430:193–200.
[11] Cribari-Neto F, Zeileis A. Beta regression in R. J Stat Softw 2010;34:24.
[12] Csardi G, Nepusz T. The igraph software package for complex network research. *Int J* Complex Syst 2006;1695(5):1–9.
[13] Dueñas-Osorio L, Craig JI, Goodno BJ. Seismic response of critical interdependent networks. Earthq Eng Struct Dyn 2007;36(2):285–306.
[14] Dueñas-Osorio L, Vemuru SM. Cascading failures in complex infrastructure systems. Struct Saf 2009;31(2):157–67.
[15] Fang J, Zeng Q, Ai X, Chen Z, Wen J. Dynamic optimal energy flow in the integrated natural gas and electrical power systems. IEEE Trans Sustain Energy 2017;9(1):188–98.
[16] Ferrari S, Cribari-Neto F. Beta regression for modelling rates and proportions. J Appl Stat 2004;31(7):799–815.
[17] Fu G, Dawson R, Khoury M, Bullock S. Interdependent networks: vulnerability analysis and strategies to limit cascading failure. Eur Phys J B 2014;87(7):148.
[18] Gao J, Buldyrev SV, Havlin S, Stanley HE. Robustness of a network of networks. Phys Rev Lett 2011;107(19):195701.
[19] Dong G, Tian L, Zhou D, Du R, Xiao J, Stanley HE. Robustness of n interdependent networks with partial support-dependence relationship. EPL (Europhys Lett) 2013;102(6):68004.
[20] Jiang J, Li W, Cai X. The effect of interdependence on the percolation of interdependent networks. Physica A 2014;410:573–81.
[21] Jolly MD, Lothes AD, Bryson LS, Ormsbee L. Research database of water distribution system models. J Water Resour Plann Manag 2013;140(4):410–6.
[22] Korkali M, Veneman JG, Tivnan BF, Bagrow JP, Hines PD. Reducing cascading failure risk by increasing infrastructure network interdependence. Sci Rep 2017;7(1):44499.
[23] LaRocca S, Guikema SD. Characterizing and predicting the robustness of power-law networks. Reliab Eng Syst Saf 2015;133:157–66.
[24] LaRocca S, Johansson J, Hassel H, Guikema S. Topological performance measures as surrogates for physical flow models for risk and vulnerability analysis for electric power systems. Risk Anal 2015;35(4):608–23.
[25] Lippai I. Colorado springs utilities case study: water system Calibration/ optimization. Proceedings of the Pipeline Division Specialty Conference. 2005.
[26] Mossa S, Barthélémy M, Stanley HE, Nunes Amaral LA. Truncation of power law behavior in "Scale-Free" network models due to information filtering. Phys Rev Lett 2002;88(13):138701.
[27] Newman M. Networks: an introduction. Oxford University Press; 2010.
[28] Ostfeld A, Uber JG, Salomons E, Berry JW, Hart WE, Phillips CA, Watson JP, Dorini G, Jonkergouw P, Kapelan Z, di Pierro F, Khul S-T, Savic D, Eliades D, Polycarpou

M, Ghimire SR, Barkdoll BD, Gueli R, Huang JJ, McBean EA, James W, Krause A, Leskovec J, Isovitsch S, Xu J, Guestrin C, VanBriesen J, Small M, Fischbeck P, Preis A, Propato M, Piller O, Trachtman GB, Wu ZY, Walski T. The battle of the water sensor networks (BWSN): a design challenge for engineers and algorithms. J Water Resour Plann Manag 2008;134(6):556–68.

[29] Ouyang M. Review on modeling and simulation of interdependent critical infrastructure systems. Reliab Eng Syst Saf 2014;121:43–60.

[30] Ouyang M, Hong L, Mao ZJ, Yu MH, Qi F. A methodological approach to analyze vulnerability of interdependent infrastructures. Simul Modell Pract Theory 2009;17(5):817–28.

[31] Parshani R, Buldyrev SV, Havlin S. Interdependent networks: reducing the coupling strength leads to a change from a first to second order percolation transition. Phys Rev Lett 2010;105(4):048701.

[32] Parshani R, Rozenblat C, Ietri D, Ducruet C, Havlin S. Inter-similarity between coupled networks. EPL (Europhys Lett) 2011;92(6):68002.

[33] Praks P, Kopustinskas V, Masera M. Probabilistic modelling of security of supply in gas networks and evaluation of new infrastructure. Reliab Eng Syst Saf 2015;144:254–64.

[34] Rinaldi SM, Peerenboom JP, Kelly TK. Indentifying, understanding and analyzing critical infrastructure interdependencies. IEEE Control Syst 2001;21:11–25.

[35] Scala A, De Sanctis Lucentini PG, Caldarelli G, D'Agostino G. Cascades in interdependent flow networks. Physica D 2016;323-324:35–9.

[36] Hong S, Zhu J, Braunstein LA, Zhao T, You Q. Cascading failure and recovery of spatially interdependent networks. J Stat Mech Theory Exp 2017;2017(10):103208.

[37] Song J, Ok SY. Multi-scale system reliability analysis of lifeline networks under earthquake hazards. Earthq Eng Struct Dyn 2010;39:259–79.

[38] Tang L, Jing K, He J, Stanley HE. Complex interdependent supply chain networks: cascading failure and robustness. Physica A 2016;443:58–69.

[39] Thacker S, Hall JW, Pant R. Preserving key topological and structural features in the synthesis of multilevel electricity networks for modeling of resilience and risk. J Infrastruct Syst 2017;24(1):04017043.

[40] Thacker S, Pant R, Hall JW. System-of-systems formulation and disruption analysis for multi-scale critical national infrastructures. Reliab Eng Syst Saf 2017;167:30–41.

[41] Winkler J, Dueñas-Osorio L, Stein R, Subramanian D. Performance assessment of topologically diverse power systems subjected to hurricane events. Reliab Eng Syst Saf 2010;95(4):323–36.

[42] Zhao Z, Zhang P, Yang H. Cascading failures in interconnected networks with dynamical redistribution of loads. Physica A 2015;433:204–10.

Paper III

Characterising the robustness of power-law networks that experience spatially-correlated failures.

Authors: Caroline A Johnson, Allison C Reilly, Roger Flage and Seth D Guikema

Accepted for publication in *Journal of Risk and Reliability*.

Characterizing the Robustness of Power-Law Networks that Experience Spatially-Correlated Failures

Caroline A. Johnson[a*], Allison C. Reilly[b], Roger Flage[a] & Seth D. Guikema[c]
[a] University of Stavanger, Norway
[b] University of Maryland, USA
[c] University of Michigan, USA
[*] Corresponding author: University of Stavanger, P.O. Box 8600 Forus, 4036 Stavanger, Norway. E-mail: caroline.a.johnson@uis.no.

Abstract:

Knowing the ability of networked infrastructure to maintain operability following a spatially distributed hazard (e.g., an earthquake or a hurricane) is paramount to managing risk and planning for recovery. Leveraging topological properties of the network, along with characteristics of the hazard field, may be an expedient way of predicting network robustness compared to more computationally-intensive simulation methods. Prior work has shown that the topological properties are insightful for predicting robustness, considered here to be measured by the relative size of the largest connected subgraph after failures, especially for networks experiencing *random* failures. While this does not equate to full engineering-based performance, it does provide an indication of the robustness of the network. In this work, we consider the effect that spatially-correlated failures have on network robustness using only spatial properties of the hazard and topological properties of networks. The results show that the spatial properties of the hazard together with the mean nodal degree, mean clustering coefficient, clustering coefficient standard deviation and path length standard deviation are the most influential factors in characterizing the network robustness. Using the results, recommendations are made for infrastructure management/owners to consider when improving existing systems, or designing new infrastructure. Recommendations include examining the known possible locations of potential hazards in relation to the system and considering the level of redundancy within the system.

1. Introduction

Large-scale disasters can quickly destroy key components of networked infrastructure, leading to widespread service interruptions. The likelihood that these components fail is highly correlated to their location relative to the hazard. Take the case of Florida Power and Light (FPL), an electric-utility company serving large portions of Florida's coastline, following Hurricane Irma in 2017. Over 2,000 utility poles were felled by strong winds despite extensive system hardening, contributing to 4.5 million customers losing power [1]. Failures in numerous other networked infrastructures (e.g., communication systems, transportation systems) are similarly dependent on the spatial distribution of hazards, including earthquakes and precipitation events. Being able to quickly model a network's ability to withstand spatially-correlated component failures is key for managing the risk facing the network and for developing strategies that enhance network robustness.

Unfortunately, after many disasters, situational awareness of specific infrastructure component performance is poor for some types of infrastructure. For example, after an earthquake, it may take days for water utilities to determine which pipes are broken and in need of repair. Leveraging topological properties of these networks – which are computationally quick to measure – and integrating these properties with spatial information about the hazard may present an expedient way of estimating network robustness quickly after a disaster, helping utilities target their damage inspection efforts better.

The goal of the present paper is to study the relationship among topological properties of networks, spatial properties of hazards, and network robustness. Here, robustness is defined as the fraction of nodes contained within the largest connected component after the failure event relative to the size of the original network. Often after major disasters, the condition of networks are unknown, and computing robustness measures is computationally taxing – thus potentially slowing recovery planning. Knowing the relationship of the topological properties to network robustness allows for a quick assessment of network robustness even for events that cause large-scale disruptions.

Presently, the influence of topology characteristics on network robustness for spatially-correlated failures is unknown. Further, there are no methods for modeling network robustness using network topology characteristics and spatial properties of the hazard. This paper aims to model the robustness of power-law networks in anticipation of a spatially-correlated failure event using a network's topological properties. We also aim to develop an efficient heuristic for understanding robustness of networks subjected to spatially-correlated failures based on easy to compute network topological properties and properties of the hazard. LaRocca and Guikema [2] previously explored the relationship of topological properties and network robustness for random failures, building from previous work in the literature (e.g., 3-16). However, investigating spatially-correlated failures provides information that is more relevant to events such as natural hazards. Earthquakes, tropical storms, fires, and other hazards affect networks in a spatial manner, and this fact is not considered at all in the LaRocca and Guikema [2] work. Therefore, exploring the relationship of topological properties of the network, spatial properties of the hazard and network robustness provides insight into how the robustness of the network can be estimated with regards to spatial events making this work much more practically relevant than that of LaRocca and Guikema [2]. If a relationship is found between the topological properties of a network, the spatial properties of the hazard, and the network's robustness, it can provide a heuristic to aid recovery planning.

The networks used in the analysis presented in this paper are constructed to have a power-law nodal degree distributions with exponential cutoff. The use of power-law networks as estimations of real networks was first proposed by Barabási and Albert [4]. They suggested that real networks have two main developmental properties of growth and preferential attachment, which result in a power-law distribution for the nodal degree of a network. Amaral et al. [5] investigated adding constraints to the power-law distribution of networks. They suggested adding various cutoffs, including exponential cutoffs, to the power-law distribution to better represent some real network systems. These cutoffs represent situations such as where the cost of additional edges to a node become too costly, or where the age of the node is taken into account, with older nodes being less preferable than modern nodes [5, 6]. Recently Broido and Clauset [15] have raised the issue of how well power-law distributions represent real network systems. They [15] tested the fit of the power-law distribution and four alternative distributions, including the power-law distribution with exponential cutoff, for 927 networks. They concluded that 43% of the networks demonstrated no evidence of having scale-free structure (networks with a power-law distribution) and that the power-law distribution with exponential cutoff has superior fit compared to other distributions.

Our work assumes that the failures are spatially-correlated and thus nodes closer to the hazard center have a greater probability of failure. We assume that the failures result from an exogenous threat (e.g., an earthquake, a hurricane or a tornado) to the system. This differs from Daqing et al. [17] who investigated spatial correlation of internal cascading failures resulting from functional overload (see: Motter [18] and Simonsen et al. [19] for more information on internal cascading failures due to functional overload). When spatially-correlated failures do occur due to an exogenous threat, it is difficult to know exactly where failures have occurred within the network, but based on the intensity of the hazard, it may be possible to estimate that fraction of the network that has been affected. Therefore, a reasonable goal is to understand the largest subgraph that remains of the network.

Authors within the area of network graph theory have developed multiple methods to represent spatially-localized failures within networks [10]. One method is to randomly choose a "root" node (or edge) to be the center of the hazard area and then fail the nodes/edges closest to the root node/edge until a percentage of the nodes/edges have been removed from the graph [11-13]. The largest connected component is then used to indicate which nodes/edges are functional. Other methods involve partitioning the network by either geographic regions such as municipalities [14, 16] or imposing a grid over the space in which the network is embedded [7-9] and failing all nodes within a particular region or grid space, or imposing a hazard area, such as a circle, over the network such that the nodes within fail [20].

While the aforementioned work on methods to represent localized-failures offers a quick and simple starting point to analyzing spatial failures, this body of knowledge assumes that failures are deterministic. That is, for all spatially-localized failures, the probability that a component in the network fails is either equal to one, if in hazard area, or zero, if not. This assumption allows for a quick analysis of the robustness of the network to spatial failures, but is a very simplistic method for analyzing hazards such as earthquakes or hurricanes. In actuality, when hazards do occur and disrupt a network, the probability that infrastructure components fail depends on their proximity to the hazard's intensity field. It is not a certainty that components closest to the hazard's most intense region fail, nor that components far from the intense portions of the hazard field will remain operational.

Stochastic simulation approaches can be used to indicate the distribution of the network's operability after spatially-correlated disruptions, but can quickly become computationally expensive, especially for large networks [21-25]. Previous authors who have applied simulation methods to this problem have focused on a specific component of the network, such as bridges in a transportation network, and run failure scenarios that focus on the disruption to the particular component. Guikema and Gardoni [21] and Haghighi et al. [26] focus on the failure of bridges within a road network for earthquake events. Although these simulations are not computationally expensive, they focus on the simulation of failure probabilities for a small subset of the network's components for one hazard event. If these models were to include the effects of the hazard to other components of the network, or investigate the distribution over hazard possibilities, the computational requirements can become large.

Winkler et al. [27] simulated the effects of hurricanes on power systems by investigating link failures within the network. Although this method allows for all edges, and not just a subset, to fail, the hazard and network properties were constant for each of the 50 failure scenarios. The computational cost was feasible as the runtime to the order of $O(Nm)$ operations, where m is the number of edges in the network and N is the number of failure sequences. However, if the effects of the hazard strength or different hazard scenarios were to be explored, the computational costs increase with a runtime to the order of $O(HNm)$, were H is the number of different hazard strengths or scenarios investigated.

Adachi and Ellingwood [28] investigated the effects of earthquakes on a water network using closed-form upper and lower bounds of component failure probability to estimate the damage to the system. The probability of component failure is dependent on the Peak Ground Velocity (PGV), which is a measure of ground motion due to an earthquake. The lower bound is calculated as the probability of component failure when the PGV values at each component are statistically independent, while the upper bounds are calculated as the component failure probability when the PGV values are perfectly correlated. To demonstrate the feasibility of the method they apply it to Shelby County in Tennessee that is subject to disruptions from the New Madrid Seismic Zone.

The objective of our work is distinct yet complementary to Hines et al. [29], who examined whether topological properties are good indicators of network reliability relative to power flow models for electric power systems. Using a collection of vulnerability measures that cover network theoretic and flow-based approaches, they analyze the outcomes of random and targeted attacks (looking at four different means of targeted attack). They discover that which is expected to be the "worst" failure vector (i.e., set of nodes to fail) strongly depends on which topology measure is used. This finding explains the conflicting results presented by Albert et al. [30] and Wang and Rong [31]. They [30, 31] use distinct topology measures to examine how targeted removal of minor nodes in a power system may have disproportionate effect on system survivability. However, their conclusions on the survivability of the system were contradictory. These results provide further warning that topology measures are simply indicators of the potential survivability of a network to failure.

In this work, we seek to understand how a suite of topology measures might characterize network robustness – based on connectivity – after spatially-correlated node failures. Although we consider only the topology of the network and not the full physical-flow, the results are useful in providing a quick analysis of a spatially-correlated failure, even for large networks containing up to 1,000 nodes that otherwise are computationally expensive to analyze with simulation methods.

Section 2 introduces the topology measures used to characterize the network robustness. Section 3 provides an overview of the methods used to simulate the networks, generate failure scenarios and analyze the robustness of the network given these failure scenarios. The results of the analysis are given in Section 4 which is followed by a discussion in Section 5. Finally, Section 6 contains the conclusion of the paper.

2. Topology measures

A network or graph is denoted as $G = [V, E]$ where V is the set of vertices or nodes and E is the set of edges. The number of nodes in a network is equal to the number of elements in V, such that $N = |V|$. The degree of each node, i, in V is the number of edges that are incident to it and denoted as k_i. Graphs can provide a simplified representation of a network system, such as infrastructure systems. The nodes represent the important components, and edges represent the connections that exist between the components. Although edges typically represent physical connections between the components, they can also represent other connections, such as cyber or the sharing of information

The structure of networks can be described using several topology measures. These measures provide indication of the configuration of the nodes within the network. In this paper, four topology measures are used to characterize the robustness of power-law networks when spatially-correlated failures occur. A brief overview of each of the four topology measures is provided in this section.

2.1. Nodal degree distribution

The nodal degree of node i, denoted k_i, is the number of edges that are incident to that node. The average nodal degree of the network, denoted $\langle k \rangle$, is then

$$\langle k \rangle = \frac{1}{N} \sum_{i \epsilon V} k_i$$

where N is the size of the network (the number of nodes in the network).

The distribution that the nodal degree of a network follows has been given much attention [3, 6, 32]. As stated in Section 1, many have compared the distribution of real network systems to that of the power-law distribution and suggested that the nodal degree of such systems are well characterized by a power-law distribution where the probability of a node having a degree of exactly k is

$P(k) \sim k^{-\gamma}$,

where γ is some constant. More recently it has been suggested that a power-law distribution with exponential cutoff is more appropriate as this incorporates the cost of adding many edges to a node [33, 34]. The probability of a node having a degree of exactly k when an exponential cutoff is included is

$P(k) \sim k^{-\gamma} e^{-\left(\frac{K}{k}\right)}$,

where K is the cutoff at which is becomes too costly to add more edges to a node. The nodal degree can be a measure of network redundancy, as the higher the nodal degree, the more edges or connections are present in the network. This work generates power-law networks with exponential cutoffs.

2.2. Path length

The path length of a nodal pair within the network is the length of the shortest path which connects the two nodes. The length of the path is calculated as the number of edges traversed. The path length for the pair of nodes i and j is denoted as d_{ij}. The mean path length of a network is then calculated as

$$l = \frac{1}{N(N-1)} \sum_{i \epsilon V} \sum_{j \epsilon V} d_{ij}$$

where N is the size of the network. The set of path lengths for each node pair in a network is denoted by L for the remainder of the paper.

2.3. Betweenness centrality

Betweenness centrality gives a measure of each node's centrality by describing what fraction of all shortest paths, for all node combinations the network, pass through that node. It is formally computed by

$$Cb_i = \sum_{s \epsilon V} \sum_{t \epsilon V} \frac{p_{sit}}{p_{st}}, \quad s \neq i \neq t$$

where p_{sit} is the number of shortest paths from node s to node t that pass through node i, and p_{st} is the total number of shortest paths from node s to node t. The betweenness centrality of each node gives an indication as to how critical it is in keeping the network connected.

2.4. Clustering coefficient

For each node in the network, the clustering coefficient measures of how well connected its neighbors are. Two nodes are neighbors if an edge exists between them. The clustering coefficient for a node i in an undirected network is

$$C_i = \frac{2E_i}{k_i(k_i-1)},$$

where E_i is the number of edges that exist between the neighbors of node i and k_i is the number of edges, or neighbors, node i has.

3. Methods

3.1. Simulation

While real network data are ideal, the number of networks for which real data are available is insufficient for conducting statistical analyses. Thus, this work uses the 2,000 randomly-generated networks produced in LaRocca and Guikema [2] to provide insights between network topologies and network failures. Briefly, these synthetic networks possess power-law degree distributions with exponential cutoffs and distribution parameters consistent with real-world scale-free networks [6]. The networks' sizes are uniformly distributed and range from 100 to 1,000 nodes. In total, 20 network sizes are used. The differently-sized networks are each assigned five pairs of exponential cutoff degree distribution parameters. These parameters are based on findings from Albert and Barabási [6] and are presented in Table 1. For each network size-pair combination, 20 synthetic networks are generated using a variation of preferential attachment [2], thus creating 2,000 networks.

Table 1. *The five pairs of exponential cutoff degree distribution parameters used to generate networks.*

γ	κ
1.1	40
2.0	900
2.1	400
2.4	2,000
1.7	200

The mean, standard deviation, minimum and maximum values for the four topological properties (degree, betweenness centrality, clustering coefficient, and path length) are calculated over the 2,000 networks and are presented in Table 2. These values have been shown to be consistent with other real networks, including food webs, movie actors, and metabolic reactions [2].

Table 2. *Summary of the topology measures of the networks and spatial properties of the hazard scenarios.*

Parameter	Within-network measure	Mean	Std deviation	Minimum	Maximum
Network size (N)		505	272	100	1,000
Degree (k)	Mean	5.13	2.24	2.34	11.19
	Minimum	1.00	0.00	1.00	1.00
	Maximum	307	220	24	989
	Std deviation	17.75	5.73	4.50	31.68
Betweenness centrality (Cb)	Mean	746	452	105	2,287
	Minimum	0.00	0.00	0.00	0.00
	Maximum	192,468	229,924	1,808	992,170
	Std deviation	8,433	7,495	316	31,375
Clustering coefficient (C)	Mean	0.29	0.09	0.07	0.61
	Minimum	0.00	0.00	0.00	0.00
	Maximum	1.00	0.00	0.00	0.00
	Std deviation	0.39	0.07	0.13	0.48
Path length (L)	Mean	2.47	0.26	2.00	3.30
	Minimum	1.00	0.00	1.00	1.00
	Maximum	4.686	0.962	3.00	8.00
	Std deviation	0.54	0.13	0.12	1.09
Hazard field properties					
Distance from epicenter to graph center		0.80	0.29	0.01	1.66
Hazard field covariance		0.28	0.19	0.00	0.89

The synthetic power-law networks are then translated to geometric graphs using the Graph function in the software system SageMath [35], such that the topological properties are maintained and the number of intersecting edges is minimized. This translates the network to a 2×2 graph where the domain of the graphs is between 0 and 2 and the range is between -1 and 1. The domain specifies the possible values of the x-axis of the graph and the range the possible values of the y-axis. The graphs' spatial centers are identified by averaging nodal locations.

Next, 50 hazard scenarios, H, are generated. A hazard scenario, $h \in H$, could be representative of an earthquake, a hurricane, or any other spatially-distributed hazard with a single epicenter. The hazard is modeled as a bivariate normal distribution. The distribution is parameterized using uniformly-generated random coordinates within the graph's domain and range to represent the hazard's epicenter and a 2 x 2 randomly-generated positive semi-definite covariance matrix to represent the hazard's spatial variance.

We then repeatedly and independently simulate 50 node failure sequences, F, for each hazard scenario, h. The likelihood of a node failure is assumed proportional to its spatial positioning in the bivariate normal distribution. More specifically, for each hazard field, each node is assigned a probability of failure that is proportional to its position in the hazard field. These probabilities are then normalized so that they sum to one and create their own cumulative density function. This density function is then sampled using a Bernoulli trail, and the node that corresponds to the Bernoulli sample is removed from the network. This is repeated until pN^{n_0} nodes are removed, where N^{n_0} is the number of initial nodes in the network n, and $p = [0.25, 0.5, 0.75]$ is the sequence of percentage of nodes removed. This creates one failure sequence, f, for the hazard scenario. This process is then repeated 50 times to represent 50 failure sequences, $f \in F$, for each hazard field. This is procedure is illustrated in Figure 1. Afterward, we count, N_{hf}^{pn}, the number of nodes in the largest connected subgraph that remain for a given network n, hazard scenario h, failure sequence f, and fraction of the nodes that fail, p. Network robustness is measured by

$$S_{hf}^{pn} = \frac{N_{hf}^{pn}}{N^{n_0}},$$

giving the relative size of the largest connected subgraph after p failures, and is a measure of network resistance to node failures [36]. We elected to add the final step of removing pN^{n_0} nodes via a Bernoulli trial as opposed to using solely the bivariate normal distribution to predict failures. This allows for a systematic comparison of the importance of topology measures as a function of the fraction of nodes, p, that are removed and for easier interpretation of the model later.

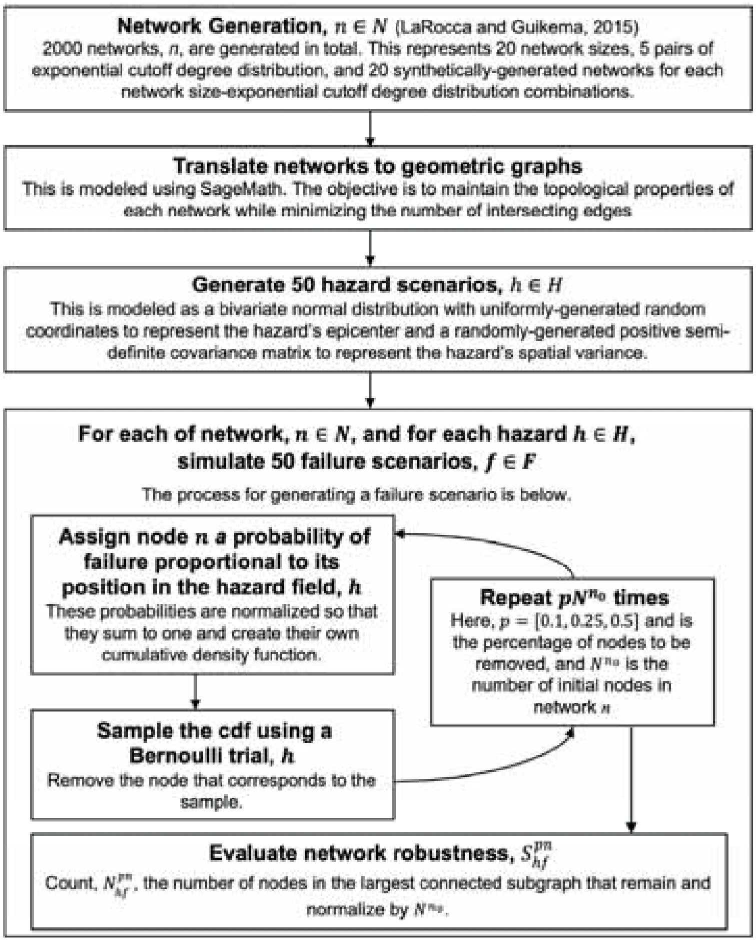

Figure 1: A flowchart of the method.

3.2. Regression

Our goal is to model network robustness as measured by S_{hf}^{pn} using the topological measures described in Section 2 and the spatial proximity of the network to the hazard. As S_{hf}^{pn} is confined to [0, 1], we use a Beta regression model with a standard logit-link function[1] [37]. Beta regression models have some superior properties for handling unit data compared to their logistic regression counterparts. The first property is their explicit treatment of heteroskedasticity via a reparameterization of the Beta family density function. Data confined to the unit interval typically possess heteroskedasticity, with more variation closer to the mean than the extremes. Another beneficial property is their interpretability, in that parameters can be directly interpreted in relation to the mean of the response variable without model transformation [38]. The Ferrari and Cribari-Neto [37] approach for Beta regression model depends on a reparameterization of the Beta density function:

$$f(y;\mu,\phi) = \frac{\Gamma(\phi)}{\Gamma(\mu\phi)\Gamma\big((1-\mu)\phi\big)} y^{\mu\phi-1}(1-y)^{(1-\mu)\phi-1}, 0 < y < 1$$

The mean and variance of the reparameterization are:

$$E(y) = \mu$$

$$var(y) = \frac{\mu(1-\mu)}{1+\phi}$$

Therefore μ is the mean of the response variable, y. Notice that the variance of the response variable is a function of its expected value, μ, and thus heteroskedasticity is explicitly present. The parameter ϕ is often called the precision parameter and reflects the variance of the response variable where, for a fixed μ, the variance decreases as ϕ increases. When performing the Beta regression to determine the significant topological characteristics the response variable, y, is the relative size of the largest connected component, S_{hf}^{pn}. The Beta distribution is linked to the response variables through a link function. In this paper we use the standard logit link function:

$$Ln\left(\frac{y}{1-y}\right) = \beta_0 + \sum_p \beta_p x_p$$

Our initial dataset includes 18 explanatory variables, 16 of which relate to network topology. The topological characteristics are the mean, standard deviation, minimum and maximum values for degree, betweenness centrality, clustering coefficient, and path length for a given network. The final two explanatory variables relate to the hazard. The first is a Euclidean measure of distance between the center of the graph and the center of the hazard field. The second is the hazard field's covariance (i.e., the off-diagonals from the semi-definite covariance matrix). All variables with a standard deviation of 0 are excluded. These variables are minimum degree, minimum betweenness centrality, minimum clustering coefficient, maximum clustering coefficient, and minimum path length. Further, we remove variables with high degrees of correlation. In this case, we remove maximum degree, standard deviation of degree, standard deviation of betweenness centrality, and mean path length. The data reduction is consistent with LaRocca and Guikema [2]. In total, 9 explanatory variables remain: mean nodal degree, mean betweenness centrality, maximum betweenness centrality, mean clustering coefficient, standard deviation of clustering coefficient, maximum path length, standard deviation of path length, distance from hazard epicenter to the center of the network and the covariance of the hazard field.

[1] Other link functions are available. The logit link function offered the best fit as measured by its pseudo-R^2.

We consider a sequence of three levels of node removals (10%, 25%, and 50%), and as such, we build three distinct regression models. A Beta regression model is fit to our data via maximum likelihood estimation using the R package 'BetaReg' [38, 39]. Covariates that lack statistical significance at $\alpha = 0.05$ are iteratively removed one-by-one based on the highest p-value and the model is refit. This is repeated until the variables that remain are all statistically significant at $\alpha = 0.05$.

The predictive accuracy of our model is evaluated using repeated random holdout validation. 80% of the data are randomly selected to serve as training data and the remainder are saved to serve as validation data. The training data are fit to a Beta regression model. This model is used to predict S_{hf}^{pn} for the explanatory data in the validation dataset. The predicted value of S_{hf}^{pn} is then compared to the simulated outcome of S_{hf}^{pn}. This validation step is repeated 100-times for each of the three levels of node removals. The results follow.

4. Results

4.1. Influence of topology measures and hazard properties on relative graph size

Figure 2a and 2b show the mean size of the relative largest connected component, S_{hf}^{pn}, and the MAE values for each level of node removals, respectively. In Figure 2a it can be seen that at the 10% level of node removals that the average size of the relative largest connected component is 85%, which then decreases to just below 65% for the 25% level of node removals and finally is just under 35% for the 50% level of node removals. Figure 2b shows that the greater the level of node removals, the higher the MAE value is, suggesting that the model is better at predicting the robustness of the network when fewer nodes initially fail. However, the MAE values for all three levels of node removals are low compared to the relative size of the largest connected component. This suggests that the regression model accurately predicts the out of sample relative size of the largest connected component for spatially-correlated failures.

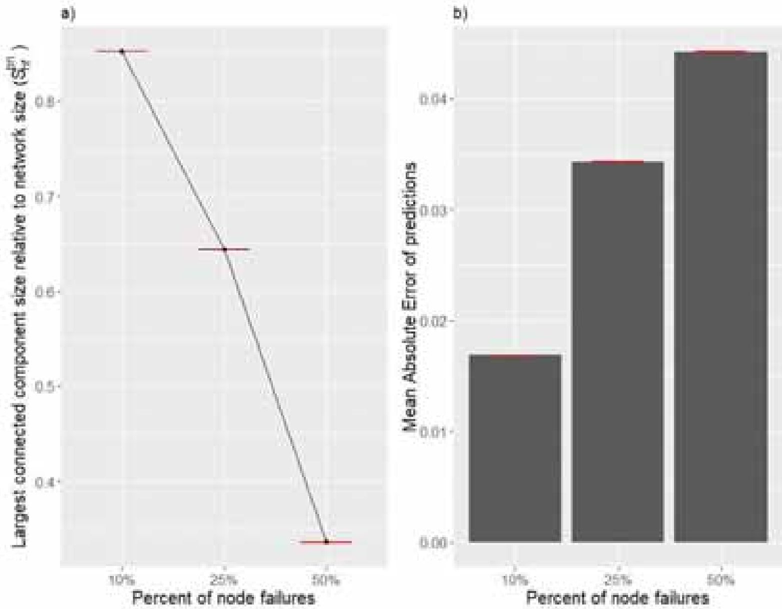

Figure 2: (a) The mean size of the relative largest connected component (S_{hf}^{pn}) for each percentage of node failures and (b) the mean MAE of the predictions of the holdout analysis. For both (a) and (b) the 95% confidence intervals are shown in red.

Figure 3 shows the results of the covariates that are significant at $\alpha = 0.05$ for the beta regression models. The first panel shows the results for the 10% level of node removals, the second the results at the 25% level of node removals and third panel the results at the 50% level of node removals. The bars show the $\hat{\beta}$ value for each statistically significant covariate and the error bars are the 95% confidence interval for the covariate coefficient. We find that seven variables are statistically significant across all levels of node removals: mean nodal degree (k, mean), mean clustering coefficient (C, mean), maximum path length (L, max), path length standard deviation (L, std dev), the distance from the hazard epicenter to the center of the network (Distance) and the covariance of the hazard field (Covariance), and were almost always so in the training data. Across all levels of node removals mean nodal degree, mean clustering coefficient, maximum path length, path length standard deviation, distance from hazard epicenter to graph center and covariance of the hazard field have a positive influence on network robustness. Clustering coefficient standard deviation had a negative influence for all levels of node removals. For 10% and 25% of node removals, mean and maximum betweenness centrality (Cb, mean and Cb, max) were also significant with the mean having a negative influence and the maximum a positive influence.

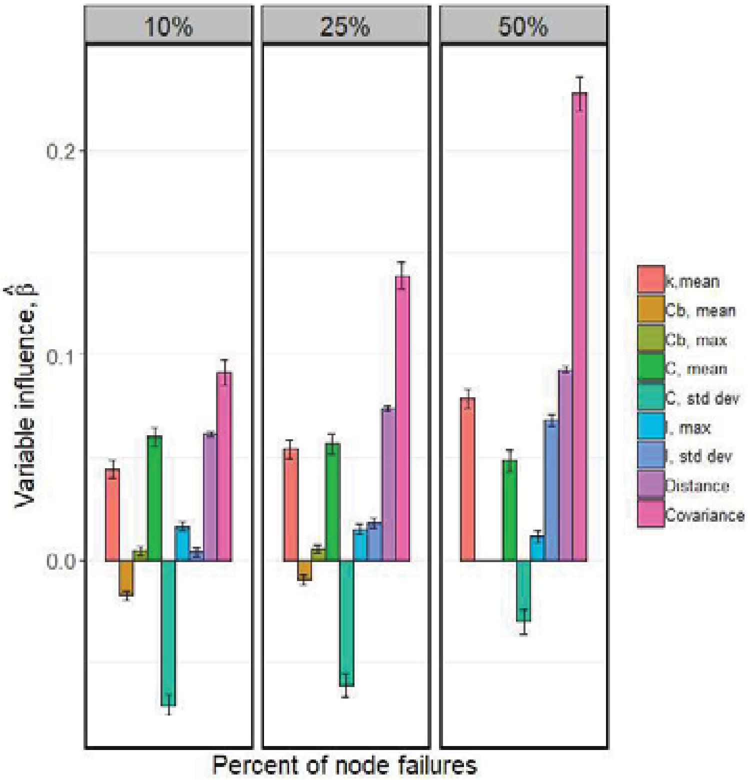

Figure 3: The influence of the significant topology measures on the robustness of the networks for 10%, 25% and 50% of node failures. The influence is given by the $\hat{\beta}$ value from the regression model.

From Figure 3, we can see that the most influential variable is the hazard field covariance, which has a positive influence on network robustness. This indicates that the greater the value of the hazard field covariance, the greater the size of the largest connected subgraph after node removals. Two hazard field scenarios are plotted in Figure 4 to provide a visual aid to explain why this is the case. Figure 4a and b show two of the 50 hazard field scenarios plotted atop one of our 2,000 simulated networks. The hazards' epicenters are represented as crosses, ×, and the location of the nodes are shown as circles, ○. The size of the network that is shown is 100 nodes. For the simplicity of this illustration, the edges are not shown. Figure 4a has a larger covariance than that of Figure 4b, with the values of 0.885 and 0.3044 respectively.

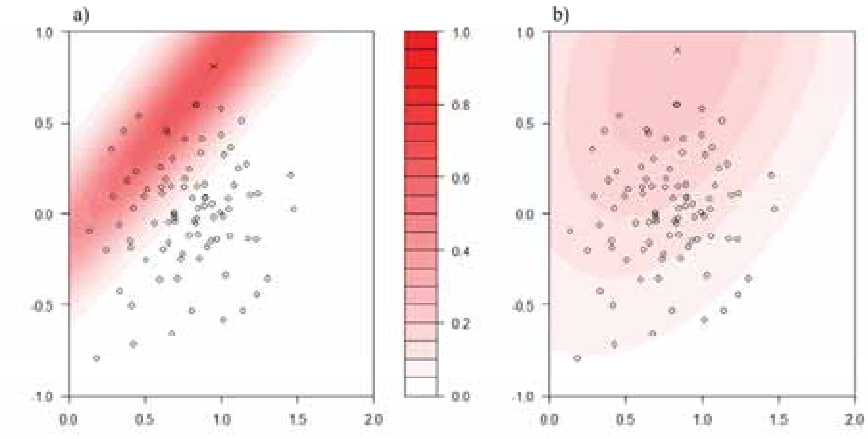

Figure 4: A network of size 100 with the hazard field distribution for (a) a hazard field with μ = (0.9484, 0.8103) and covariance of 0.885 and (b) a hazard field with μ = (0.8399, 0.9017) and covariance of 0.3044. Note that the network is identical in both (a) and (b). The nodes of the network are represented by circles and the hazards' epicentres are denoted with a cross.

We can see from Figure 4a that when the covariance of the hazard field is closer to 1, the hazard is more concentrated. The probability of failure is higher close to the epicenter and decreases rapidly as the distance from the epicenter increases. Therefore, the nodes closer to the epicenter have a much greater probability of failure than those further from the epicenter. The hazard field in Figure 4b shows that when the covariance of the network is closer to 0, the probability of failure is more uniform. The probability of nodes that are close to the epicenter failing are not significantly greater than the probability those further from the epicenter. Therefore, the greater the covariance of the hazard field, the more likely nodes closer to the epicenter fail. This, in turn, means that node failures are more likely to be in close proximity to each other and thus the propagation of the disruption through the network after the initial node removals is smaller. Therefore, higher covariance suggests larger connected components after failure.

The distance from the epicenter of the hazard and the center of the network similarly has a positive influence on the relative size of the largest connected subgraph. The center of the network is calculated as the average of the (x, y) coordinates of the nodes within the network. The network layout is determined such that the number of edge intersections is minimized, which results in nodes with higher nodal degree more likely to be toward the center of the network. The further the epicenter of the hazard is from the network center, the less likely the nodes with high nodal degrees are to fail, minimizing the propagation the effects of the disruption through the network.

Mean nodal degree and mean clustering coefficient are the two most influential network topology measures for characterizing the relative size of the largest connected subgraph, both with a positive influence. Both measures provide an indication of the redundancy of the network. The mean nodal degree gives a measure of the general redundancy within the network, as the more edges the network has, the more pathways that are available between each pair of nodes in the network. The mean clustering coefficient indicates the level of local redundancy within the network, with a higher clustering coefficient indicating more edges within neighborhoods (or clusters) of the network.

For the 10% level of node removals, the mean clustering coefficient has a slightly greater influence on the size of the largest connected subgraph than the mean nodal degree. This suggests for lower node removals when spatially-correlated hazards occur, local redundancy is important. At the 25% level of node removals, the influence of the two topology measures is similar. For the 50% level of node removals, the mean nodal degree has a greater influence on the size of the largest connected subgraph than the mean clustering coefficient. This suggests that when a large percentage of nodes fail as a result of spatially-correlated hazards, the local redundancy is less important than the overall redundancy of the network. When a large percentage of nodes are removed due to spatially-correlated failures, they are more likely to be nodes within close proximity of each other. Thus, it is more likely for nodes within a same neighborhood to be removed, decreasing the influence of the clustering coefficient.

The clustering coefficient standard deviation has a negative effect on the size of the largest connected component for all levels of node removals. This is likely due to a combination of the clustering coefficient distribution being asymmetric and is positively skewed and the relationship between the clustering coefficient and the largest connected component being non-linear. The minimum value of the clustering coefficient is always zero, as seen in Table 2. Therefore, when the standard deviation increases, it is due to an increase in the larger clustering coefficient values rather than a decrease in the lower clustering coefficient values. When a node is removed, it is more likely to be a node with a low clustering coefficient value, i.e. a node with a low level of regional redundancy. This in turn leads to many small clusters of the network remaining and thus less nodes in the largest connected component. The influence of clustering coefficient standard deviation decreases as the percentage of initial failures increased. This, as with the decreasing influence of the mean clustering coefficient, may be due to the nature of the hazard being spatially-correlated, which increases the likelihood of nodes in a neighbor being removed due to the hazard when a greater number of nodes are initially affected. The removal of nodes from the same neighborhood decreases the importance of local redundancy, thus decreasing the importance of the clustering coefficient parameters.

Both the maximum and standard deviation of the path length have a positive influence on the size of the largest connected subgraph. The longer the maximum path length, the more likely that alternate paths are available. Thus, if part of a route is removed, there is more likely to be alternative paths of the same length still available. The influence of the maximum path length is small and decreases as the level of node removal increases. This decrease may be due to more node removals, meaning more alternative path lengths between nodal pairs are affected. Path length standard deviation has the opposite trend, with an increasing influence as the level of node removals increase. One potential explanation that could be further investigated is that the more variability there is in path length, the more variety of nodes are traversed leading to more redundancy in paths between nodes.

Mean betweenness centrality has a negative influence on the size of the largest connected subgraph at the 10% and 25% levels of node removals, but is no longer significantly significant at the 50% level of node removals. The maximum betweenness centrality is similarly only significant at the 10% and 25% levels of node removals, but with a positive influence on the size of the largest connected subgraph. Betweenness centrality is a measure of how critical (or "central") nodes are in terms of shortest path length. As the percentage of node removals increases, it becomes more likely that the connection between nodal pairs is no longer through the shortest path, which may explain why the mean and maximum betweenness centrality is no longer statistically significant at the 50% level of node removals.

The greater the mean betweenness centrality, the more likely it is that there are fewer alternative shortest paths between nodal pairs. This thus decreases network redundancy and implies a negative relationship between mean betweenness centrality and relative network connectivity. The maximum shortest path has positive influence on relative network size. This seems counterintuitive as the greater the maximum betweenness centrality value, the more likely the network is to fragment if the node with the maximum betweenness centrality is removed. However, the maximum betweenness centrality of the network also provides information on the number of shortest paths in the network, and so a network with a higher betweenness centrality could indicate a greater number of alternate shortest paths.

4.2. Comparison to random failure scenarios

Our results of the significant topology measures for characterizing network robustness with regards to spatially-correlated failures can be compared to those of LaRocca and Guikema[2] characterizing the robustness of networks for random failure scenarios. The statistically significant topology measures for the two different failure scenarios (random and spatially-correlated) are the same, except for maximum betweenness centrality. It is significant when considering spatially-correlated failures, but not when considering random failures. Betweenness centrality provides a measure of the importance of a given node to shortest paths in the network. In a spatially correlated failure event, nodes near each other are more likely to fail together, potentially impacting more of the shortest paths, leading betweenness centrality to be a more important measure of network fragmentation in the spatially correlated failure case. Maximum path length differs in the direction of the influence on the robustness of the network, likely due to the more compact nature of the failures in the spatially correlated failure case.

In the results presented by LaRocca and Guikema[2] both the mean nodal degree and mean clustering coefficient have a steadily increasing positive influence on the size of the largest connected subgraph for increased levels of node removals. The increase of the mean nodal degree in our results is not seen to the same extent, and the influence of the mean clustering coefficient slightly decreased with increased level of node removals. We hypothesize that this is because of the more compact nature of the spatially correlated failures with clustering being less important at increased node removal levels in the spatially correlated case because more concentrated clusters of nodes have already failed at the higher levels.

Other differences in the results of random and spatially-correlated failures are seen in relation to the topology measures associated with path length. The first is the difference of when the maximum path length is statistically significant. For random failure scenarios, maximum path length is only statistically significant at the 75% level of node removals, but for spatially-correlated failures, it is significant for all (10%, 25% and 50%) levels of node removals. The influence of the maximum path length also differs for the two results, having a positive influence under spatially-correlated failure scenarios and a negative influence, when significant, for random failure scenarios. We hypothesize that this occurs because longer shortest paths suggest a network in which there are more intermediate nodes in the path between any given set of nodes. Spatially correlated failures are more likely to lead to tighter clustering of node failures for a given fraction of nodes failed. If the shortest paths are longer, there would more likely be sub-paths of these paths still connected than if there were fewer edges in the path between a set of nodes, leading to a larger connected subgraph. This is a hypothesis that subsequent work could focus on more.

The second difference regards the path length standard deviation. Although it has a positive influence for both random and spatially-correlated failures, the influence of the path length standard deviation increases more rapidly with the level of node removals in spatially-correlated failure scenarios than random failure scenarios. We hypothesize that the reason for this is similar to the reason for the change in the influence of path length – more diversity in path lengths leads to larger connected subgraphs after a spatially correlated failure event.

Comparing Figure 2a to Figure 1b of LaRocca and Guikema[2] it can be seen that mean size of the largest connected subgraph for both spatially-correlated and random failures is similar across all levels of node removals. This suggests that there is a limit to the effects of removing a percentage of nodes within a network, no matter the method of node removal. Figure 2b can also be compared with that of Figure 1c in LaRocca and Guikema[2] to see the difference in the MAE values for the holdout regression. For spatially-correlated failures, the MAE value increases with the level of node removals, but does not for random failures. Instead, the MAE values for the 25% and 50% level of node removals are similar, with the 50% level having a slightly smaller value for random failures.

5. Discussion

In the analysis presented, we explore how useful network topology measures and spatial properties of hazards are for characterizing network robustness. These results form the basis for recommendations to infrastructure owners or management to consider when designing new system, or are in the process of updating existing infrastructure.

The most influential variables were those associated with the hazard field: the distance from the epicenter to the network center and the hazard field covariance. When a spatially-correlated failure occurs, the location and covariance are dictated by the nature of the hazard and is not something that infrastructure owners/management can control. However, for some hazards, such as earthquakes, there is an understanding of the phenomena and reliable knowledge on the location of where faults are situated, indicating areas that earthquakes can occur. Our results suggest that when constructing new infrastructure, the center of the network should be placed as far from these known hazard areas as possible.

If the position of the infrastructure cannot be changed, the results could also be used, in conjunction with a flow model to take preemptive action in systems such as water systems, where parts of the network can be shut down to reduce the occurrence of negative pressures in the system. This can be done for events that can have some warning, such as tropical storms or earthquakes. When an estimation of the location and strength of the hazard is available before the event, it can be used to construct an estimate of the hazard field and identify areas of the infrastructure are more likely to be affected by the event.

For some hazards, such as tornados, it is impossible to identify the epicenter or the intensity before the event. Instead, infrastructure managers and owners can, to some extent, influence the topology when designing new infrastructure or improving existing infrastructure. The results of our analysis, alongside those from LaRocca and Guikema[2], highlight the most important factors to consider. The mean nodal degree and mean clustering coefficient are the most influential topology measures regardless of failure scenario (i.e., random or spatially-correlated). Both these topology measures give an indication of the level of redundancy the network has and suggest these are important measures to consider when improving existing infrastructure or designing a new system. These results emphasize the importance of redundancy within a network, regardless of the type of failure.

The method could also be used by infrastructure management to estimate how a variety of spatially-correlated failures could affect their infrastructure. This analysis highlight areas within the system that are more likely to be affected, and as such, show where improvements should be made to reduce the effects of spatially-correlated failure events on the system.

The networks used in this research are simplified representations of real infrastructure. Using the largest connected component as a measure of network robustness means that the method is quick to implement, but this method could be extended to include sink and source nodes to better model the flow present in a real infrastructure system. For specific infrastructures, the commodity flow, (e.g., the flow of electricity in a power network), could be included to increase the accuracy of the results.

6. Conclusion

The relationship between the topological properties and the robustness of the networks is explored by simulating the effects that spatially-correlated failure fields have on power-law networks. Because topological properties are fast to calculate, the method discussed in this work can assist in quickly estimating network robustness without excessive computational and data requirements. Further, by simulating spatially-correlated failures, this method provides a more realistic representation of spatial failures than previous methods that simulate spatially-localized failures. Rather than all nodes (or edges) in a given area of the network failing, the probability of each component failing is dependent on its position relative to the hazards epicenter and the hazard's spatial variance. To explore the relationship between topological properties of the networks, spatial properties of the hazard and network robustness and Beta regression model is used to identify which properties are significant to the robustness of the networks.

We find that the factors relating to the hazard's position and field covariance are the most influential on the robustness of the network. The further the hazard's epicenter is from the center of network, the more robust the network is. The higher the hazard field covariance, the more concentrated the effects of the hazard are, and thus the less disruption effects the network. For infrastructure management, the important factors to consider are the topology measures that have the greatest influence on the network robustness. These, to some degree, can be influenced or adapted to increase the robustness of the system to failures. These factors are mean nodal degree, mean clustering coefficient, clustering coefficient standard deviation and path length standard deviation. The most influential of these topology measures are the mean nodal degree and mean clustering coefficient, which provide some indication of the global and local redundancy of the network, respectively. Thus, giving attention to these factors could lead to a more robust network to both random and spatially-correlated failures.

Acknowledgement

We would like to thank the three anonymous reviewers for their useful comments and suggestions on earlier versions of the present article.

References

1. Nehamas N and Dahlberg N. FPL spent $3 billion preparing for a storm. So why did Irma knock out the lights? *Miami Herlald*, 2017.
2. LaRocca S and Guikema SD. Characterizing and predicting the robustness of power-law networks. *Reliability Engineering & System Safety* 2015; 133: 157-166. DOI: http://dx.doi.org/10.1016/j.ress.2014.07.023.
3. Watts DJ and Strogatz SH. Collective dynamics of 'small-world' networks. *Nature* 1998; 393: 440-442.
4. Barabási A-L and Albert R. Emergence of scaling in random networks. *Science* 1999; 286: 509-512.
5. Amaral LAN, Scala A, Barthelemy M, et al. Classes of small-world networks. *Proceedings of the national academy of sciences* 2000; 97: 11149-11152.
6. Albert R and Barabási A-L. Statistical mechanics of complex networks. *Reviews of modern physics* 2002; 74: 47.
7. Patterson SA and Apostolakis GE. Identification of critical locations across multiple infrastructures for terrorist actions. *Reliability Engineering & System Safety* 2007; 92: 1183-1203. DOI: https://doi.org/10.1016/j.ress.2006.08.004.
8. Jenelius E and Mattsson L-G. The vulnerability of road networks under area-covering disruptions. In: *INFORMS annual meeting, Washington DC, USA* 2008, pp.12-15.
9. Johansson J and Hassel H. An approach for modellng interdependent infrastructures in the context of vulnerability analysis. *Reliability Engineering and System Safety* 2010; 95: 1335-1344.
10. Berezin Y, Bashan A, Danziger MM, et al. Localized attacks on spatially embedded networks with dependencies. *Scientific Reports* 2015; 5: 8934. Article. DOI: 10.1038/srep08934

https://www.nature.com/articles/srep08934#supplementary-information.
11. Shao S, Huang X, Stanley HE, et al. Percolation of localized attack on complex networks. *New Journal of Physics* 2015; 17: 023049. DOI: 10.1088/1367-2630/17/2/023049.

12. Yuan X, Shao S, Stanley HE, et al. How breadth of degree distribution influences network robustness: Comparing localized and random attacks. *Physical Review E* 2015; 92: 032122. DOI: 10.1103/PhysRevE.92.032122.
13. Hu F, Yeung CH, Yang S, et al. Recovery of infrastructure networks after localised attacks. *Scientific Reports* 2016; 6: 24522. Article. DOI: 10.1038/srep24522

https://www.nature.com/articles/srep24522#supplementary-information.
14. Ouyang M. Critical location identification and vulnerability analysis of interdependent infrastructure systems under spatially localized attacks. *Reliability Engineering & System Safety* 2016; 154: 106-116. DOI: https://doi.org/10.1016/j.ress.2016.05.007.
15. Broido AD and Clauset A. Scale-free networks are rare. *arXiv preprint arXiv:180103400* 2018.
16. Ouyang M, Tian H, Wang Z, et al. Critical Infrastructure Vulnerability to Spatially Localized Failures with Applications to Chinese Railway System. *Risk Analysis* 2019; 39: 180-194. DOI: doi:10.1111/risa.12708.
17. Daqing L, Yinan J, Rui K, et al. Spatial correlation analysis of cascading failures: congestions and blackouts. *Scientific reports* 2014; 4: 5381.
18. Motter AE. Cascade Control and Defense in Complex Networks. *Physical Review Letters* 2004; 93: 098701. DOI: 10.1103/PhysRevLett.93.098701.
19. Simonsen I, Buzna L, Peters K, et al. Transient dynamics increasing network vulnerability to cascading failures. *Physical Review Letters* 2008; 100: 218701.
20. Wilkinson SM, Dunn S and Ma SJNH. The vulnerability of the European air traffic network to spatial hazards. 2012; 60: 1027-1036. journal article. DOI: 10.1007/s11069-011-9885-6.
21. Guikema S and Gardoni P. Reliability estimation for networks of reinforced concrete bridges. *Journal of Infrastructure Systems* 2009; 15: 61-69.
22. Rezaei P, Hines PDH and Eppstein M. Estimating cascading failure risk: Comparing Monte Carlo sampling and Random Chemistry. In: *2014 IEEE PES General Meeting | Conference & Exposition* 27-31 July 2014 2014, pp.1-5.
23. LaRocca S, Johansson J, Hassel H, et al. Topological Performance Measures as Surrogates for Physical Flow Models for Risk and Vulnerability Analysis for Electric Power Systems. *Risk Analysis* 2015; 35: 608-623. DOI: 10.1111/risa.12281.
24. Jia Y, Xu Z, Lai LL, et al. Risk-Based Power System Security Analysis Considering Cascading Outages. *IEEE Transactions on Industrial Informatics* 2016; 12: 872-882. DOI: 10.1109/TII.2015.2499718.
25. Guo J, Liu F, Wang J, et al. Toward Efficient Cascading Outage Simulation and Probability Analysis in Power Systems. *IEEE Transactions on Power Systems* 2018; 33: 2370-2382. DOI: 10.1109/TPWRS.2017.2747403.
26. Haghighi N, Fayyaz SK, Liu XC, et al. A Multi-Scenario Probabilistic Simulation Approach for Critical Transportation Network Risk Assessment. 2018; 18: 181-203. journal article. DOI: 10.1007/s11067-018-9392-3.
27. Winkler J, Dueñas-Osorio L, Stein R, et al. Performance assessment of topologically diverse power systems subjected to hurricane events. *Reliability Engineering & System Safety* 2010; 95: 323-336. DOI: https://doi.org/10.1016/j.ress.2009.11.002.
28. Adachi T and Ellingwood BR. Serviceability assessment of a municipal water system under spatially correlated seismic intensities. *Computer-Aided Civil and Infrastructure Engineering* 2009; 24: 237-248.
29. Hines P, Cotilla-Sanchez E and Blumsack S. Do topological models provide good information about electricity infrastructure vulnerability? *Chaos: An Interdisciplinary Journal of Nonlinear Science* 2010; 20: 033122.
30. Albert R, Albert I and Nakarado GL. Structural vulnerability of the North American power grid. *Physical Review E* 2004; 69: 025103.
31. Wang J-W and Rong L-L. Cascade-based attack vulnerability on the US power grid. *Safety Science* 2009; 47: 1332-1336.
32. Barabási A-L, Albert R and Jeng H. Mean-field theory for scale-free random networks. *Physica A* 1999; 272: 173-187.

33. Newman MEJ. Scientific collaboration networks. I. Network construction and fundamental results. *Physical Review E* 2001; 64: 016131. DOI: 10.1103/PhysRevE.64.016131.
34. Jeong H, Tombor B, Albert R, et al. The large-scale organization of metabolic networks. *Nature* 2000; 407: 651. DOI: 10.1038/35036627

https://www.nature.com/articles/35036627#supplementary-information.
35. The Sage Developers. SageMath, the Sage Mathematics Software System. 8.2.0 ed.: Sage Development Team, 2018.
36. Albert R, Jeong H and Barabási A-L. Error and attack tolerance of complex networks. *Nature* 2000; 406: 378.
37. Ferrari S and Cribari-Neto F. Beta regression for modelling rates and proportions. *Journal of Applied Statistics* 2004; 31: 799-815.
38. Cribari-Neto F and Zeileis A. Beta Regression in R. *2010* 2010; 34: Journal of Statistical Software. 2010-04-05. DOI: 10.18637/jss.v034.i02.
39. R Core Team. R: A language and environment for statistial computing.: R Foundation for Statistical Computing, 2016.

Paper IV

Dependent infrastructure system modeling: A case study of real-world power and water distribution systems.

Authors: Kaia Stødle, Caroline A Johnson, Logan G Brunner, Julian N Saliani, Roger Flage and Seth D Guikema

Revised and resubmitted for possible publication in *Reliability Engineering & System Safety*.

Dependent infrastructure system modeling: A case study of the St. Kitts power and water distribution systems

Kaia Stødle[1], Caroline A. Johnson[1], Logan G. Brunner[2], Julian N. Saliani[2], Roger Flage[1] & Seth D. Guikema[3]
[1] *University of Stavanger, Norway*
[2] *Johns Hopkins University, USA*
[3] *University of Michigan, USA*

Abstract

Critical infrastructure systems underlie the economy, national security, and health of modern society. These infrastructures have become increasingly dependent on each other, which poses challenges when modeling these systems. Although a number of methods have been developed for this problem, few case studies that model real-world dependent infrastructures have been conducted. In this paper, we aim to provide another example of such a case study by modeling a real-world water distribution system dependent on a power system. Unlike in the limited previous case studies, our case study is in a developing nation context. This makes the availability of data about the infrastructure systems in this case study very limited, which is a common characteristic of real-world studies in many settings. Thus, a main contribution of the paper is to show how one can still develop representative, useful models for systems in the context of limited data. To demonstrate the utility of these types of models, two examples of different analyses are performed, where the results provide information about the most vulnerable parts of the infrastructures and critical linkages between the power and water distribution systems.

Key words: Critical infrastructures, dependencies, modeling, case study

1 Introduction

Critical infrastructures provide essential services to modern societies, and the functionality of these infrastructures are important. There has been an increase in dependencies of a given infrastructure on one or more other infrastructure systems, particularly dependencies on the power system. These dependencies are often poorly understood in practice, despite assumptions to the contrary made by academic modelers. Even when they are understood, modeling the cascading effects of failures from one system onto other systems is challenging. Many methods for modeling dependent infrastructures using network models have been developed and suggested in existing literature (e.g., Buldyrev et al., 2010, Parshani et al., 2011, Fu et al., 2014). Many of these papers adopt a network theoretic perspective (e.g, Gao et al., 2016, Johnson et al. 2019, Diu et al. 2020). That is, they conceptualize a set of infrastructure networks as graphs of vertices and edges and approximate performance with one of a number of topological or connectivity-based approaches. However, LaRocca et al. (2015) showed that these network theory-based approaches, while useful for generic networks, provide poor approximations of the performance of actual infrastructure systems. Despite this, relatively few detailed case studies of the modeling of real-world dependent infrastructures are published in the scientific literature (e.g. Chai et al., 2016; Dueñas-Osorio, Craig and Goodno, 2007; Johansson and Hassel, 2010; Johansson, Hassel and Cedergren, 2011; Poljanšek, Bono and Gutiérrez, 2012; Thacker et al., 2017; Ouyang and Wang, 2015). Nearly all of these are done in unique data-rich environments that are not representative of the situation faced by many infrastructure managers. Many infrastructure managers, even in developed countries, face significant data limitations, especially about dependencies on other infrastructures. In many cases, performance models (e.g., hydraulic models for drinking water systems) are out of date or have not been calibrated in many years. The main contribution of this paper is to show how real infrastructure systems involving dependencies can be modeled in low-data environments in a way that provides useful information on the performance of these systems during natural hazards.

This paper differs substantially from previous case studies in relatively data-rich areas such as the United States and Europe. We present a case study where we analyze the effect of hurricane disruptions on the performance of the power and water distribution systems of the Caribbean island of St. Kitts. The available information about these infrastructure systems is highly limited, thus, the objective of this paper is to develop a representative model for these systems despite significant data limitations. It should be mentioned that the issue of limited data availability might be present for data-rich areas too. Although the requisite data to develop models exist it can be unavailable due to confidentiality reasons. This adds an additional motivation for this paper.

This paper is organized as follows: In the next section (Section 2), background information about St. Kitts and its power and water distribution systems are given along with a description of the threat that hurricanes pose to the island. Section 3 contains a description of the simulation model developed for this case study. In order to demonstrate how this model can be used and what types of modeling results that can be obtained, Section 4 presents the results of analyses aimed at identifying critical components in the systems. Section 5 shows how the model can be used to simulate failures of recent or forecasted hurricanes. Section 6 includes a discussion of the results as well as of the challenges associated with modeling real-world infrastructure systems and the differences between modeling real-world systems and fictional systems. Finally, Section 7 presents the conclusions.

2 Background for the case study

St. Kitts is one of the twin islands of the Federation of St. Kitts and Nevis, which is located in the eastern Caribbean Sea. The nation has an estimated population of about 56,000, with most of the population living on the island of St. Kitts (World Population Review, n.d.). St. Kitts is a small and elongated island with an area of 69 square miles (The Official Website of St. Kitts and Nevis, n.d.). The island is of volcanic origin and has a group of volcanic peaks in the middle of the island. Due to these steep mountains, the majority of the population reside by the coastline around the island. The highest populated area is in and around the capital of Basseterre, which is located in the south of the island between the mountains and a peninsula (see the map in Figure 1).

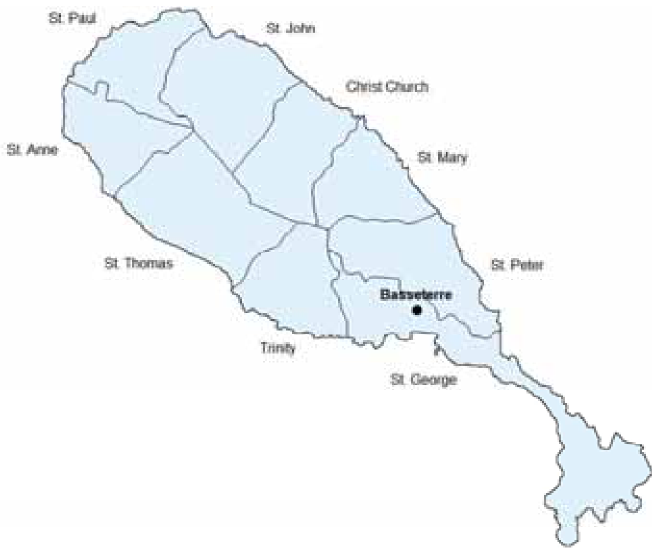

Figure 1: Map of St. Kitts with parish labels

The power system is operated by St. Kitts Electricity Company Limited (SKELEC), who provide power from 10 diesel generators located at the power station near Basseterre. The power is distributed to the community through 12 lines (11 kV), of which nine are located in and around Basseterre. The remaining three lines stretch along the entire coastline around the island, where one goes along the peninsula to the southernmost point of the island and the other two go up to the north following opposite sides of the island (see the schematic of the main trunk lines in Figure 2).

St. Kitts is self-sufficient for fresh water. The water distribution system has a production capacity of up to 7 million gallons per day (MGD), which meets the average demand of 5.5 MGD. The different types of water sources come in the form of 30 groundwater wells, 30 surface storage tanks, and 6 river reservoirs. Thus, there is a mixture of groundwater and surface water sources with, on average, 67% of water provided from groundwater sources and 33% from surface water sources. The system is mainly gravity fed. The exception is the wells that require electricity to pump water into the distribution system. A visit to the site found that there were no back-up generators at the groundwater wells. Thus, the water distribution system is dependent on the power system for water production (see the schematic of the modeled water system in Figure 3).

Due to the location of St. Kitts, hurricanes pose a significant threat to the functionality of the island's critical infrastructure. The power system is particularly vulnerable to hurricanes due to its wooden power poles that can fail during strong winds. In addition, the power system in St. Kitts is radial, at least at the time of this case study. That is, there is no redundancy between the lines, particularly between the three lines that provide power to most of the island, discussed further below. When a power outage occurs in an area, the water wells in this area lose their power supply and stop functioning, which puts the water distribution system at risk of negative pressures and insufficient delivery of water. Therefore, in this case study, hurricanes are simulated and used as a natural cause of disruption to the power and water distribution systems. St. Kitts has experienced many strong hurricanes that have caused disruptions to infrastructure systems. Most notably was Hurricane Georges that made landfall on the island in 1998, resulting in severe damage to the infrastructure across all parts of the island. Over 80 percent of all homes were damaged, with some completely destroyed. Severe damages were also seen to other buildings, including the airport, the seaport, the main hospital, schools, businesses, hotels, and emergency shelters. Hurricane Georges resulted in five fatalities and left many people without homes and work, with repair costs reaching approximately $445 million USD (Douglas, 1998; IFRC, 2002).

3 The simulation model

This section describes how the infrastructure systems and the hurricanes are modeled and how the overall simulation process is performed. This process includes a description of how the power and water system models are coupled together.

3.1 *The modeled power system*

Very limited information is available about the power system of St. Kitts. The data we do have is from the SKELEC (St. Kitts Electric Company Limited) website (SKELEC, n.d.) and from a visit by one of the authors to the island. Based on this information, the system is modeled as consisting of three main power lines with their center located at the generators near Basseterre. Figure 2 presents a schematic of the modeled power system. Each line mimics one of the three main trunk lines that surrounds the entire island. In the remainder of this paper, these modeled lines are referred to as the Southern, Western, and Northern power lines. The Southern power line (represented by dots in Figure 2) supplies Basseterre as well as the peninsula, the Western power line (triangles) supplies the western coast up to the parish of St. Anne, and the Northern power line (squares) supplies the eastern and northern coast to the point where the Western power line stops. Due to limited information about the power network, the nine smaller trunk lines that are located in and around Basseterre are not included. The exclusion of these trunk lines makes the modeled power system in the Basseterre area a very simplified version of the real system. This causes all the wells in Basseterre to be connected to the Southern power line in the model, instead of potentially being connected to different smaller trunk lines. Without access to more detailed power system data as well as data of exact locations of connection between water wells and the power system, it is difficult to evaluate the severity of this simplification.

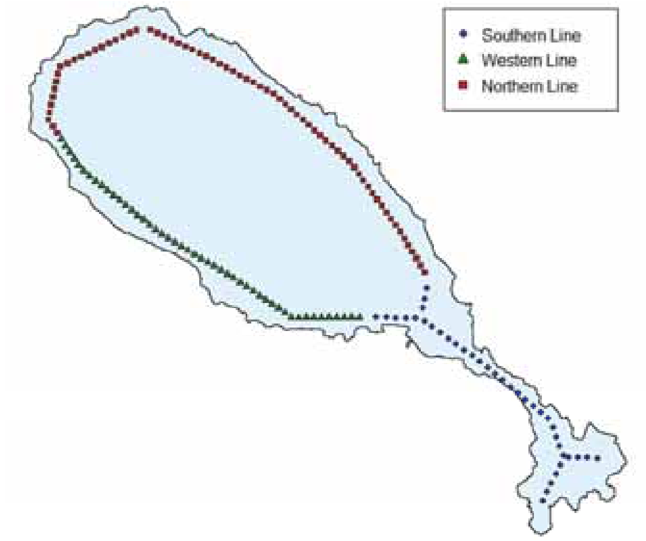

Figure 2: Schematic of the modeled power system.

A network-based approach is used to model the power system, where the power poles are modeled as nodes and the power lines as the links between the nodes. There are a total of 157 poles in the modeled system, with pole spacing selected to give span lengths (between pole distances) typical of lower-voltage power systems. The ability of the system to provide power at each pole location depends on the status of all preceding poles. If one pole fails due to wind along any of the three lines, all the downstream nodes switch to non-active status and are be unable to provide power. That is, there is no redundancy in the system. Because of this lack of redundancy, the failure is assumed to be instantaneous. Note that this is an approximation to the actual power flow. LaRocca et al. (2015) showed that such a connectivity-based approach is a poor approximate to actual power flow for high voltage transmission systems. However, for purely radial, lower voltage distribution systems such as the one in our case study, the connectivity-based approach is a much better first order approximation.

3.2 *The modeled water system*

The water distribution system is modeled using the publicly available widely used software package EPANET 2.0 (Rossman, 2000). EPANET models the hydraulics of water flow in pressurized pipe. We used a demand-driven simulation mode (as opposed to pressure-driven) and assumed there were no pipe breaks in the system. EPANET is widely used in infrastructure modeling in both practice and research, and additional details are available in Rossman (2000). Our EPANET model includes the distribution system pipes along with supply sources and demand nodes. A network schematic of the modeled water system is presented in Figure 3. The network schematic, supply capacities, and demand values have been provided and approximated based on information from the St. Kitts Water Department. The department provided information on 24 of the 30 wells in terms of both their safe yield and their respective elevations. Because water consumption data are not readily available, the total 5.5 MDG average water demand is partitioned per parish based on its population.

Figure 3 shows the network flow model of the water system as modeled in EPANET. The red dots represent the wells within the water system and are located around the perimeter of the island. The green dots represent the demand nodes within the model. The water wells and demand nodes are collectively referred to as the water nodes within the model. The reservoirs are represented as black squares and mainly located towards the center of the island, which is the mountainous region. The storage tanks are shown as black dots. Using EPANET allows the movement of water within the system as well as the pressures at each node to be modeled during a simulation of a specified duration.

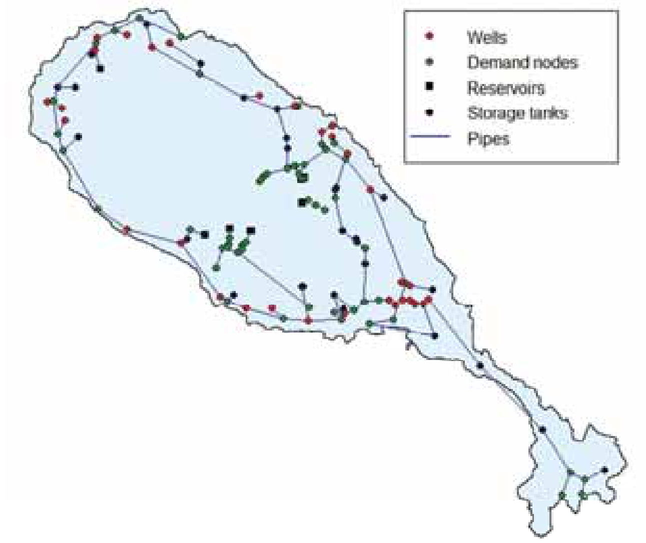

Figure 3: Schematic of the modeled water system.

When the system was first fully mapped to replicate the St. Kitts water system based on the limited information available, there were a significant number of nodes that produced low and negative pressures under normal conditions. Low pressures are in this paper defined as pressures below 20 psi. This pressure limit is chosen because a minimum pressure of 20 psi in water distribution systems is used as a standard in several U.S. states based on pressures needed for fire-fighting activities (GLUMR Board, 2012). Some of the water nodes generate negative pressures that are very close to zero. Therefore, a classification "rule" is made in this study saying that negative pressures are pressures below -1 psi. EPANET was unable to handle the water demand magnitude of each parish effectively, likely because these large demands for each parish are placed at only a few nodes instead of spreading the demand out to replicate the true housing community. The details of these connections to the system were not available, and even in the U.S., demand aggregation to a smaller number of representative nodes is common in developing an approximate hydraulic model for a city. One of the wells in the parish of St. Anne is divided into two wells in the model in order to keep the pressure within the parish from reaching below 0 pounds per square inch [psi]. In order to further mitigate this limitation driven by the available data, the magnitudes of the demands and inflows of water are reduced but kept at the same ratio in order to accurately replicate the overall functionality of the distribution system.

3.3 *The hurricane model*

Because hurricanes are one of the more frequent causes of disruption to the power and water systems of St. Kitts, we focused on hurricane-induced damage to the power and water systems. Because of the topography of the island and where the population is located, most of the power and water system components that could be sensitive to flooding are either on poles or are at elevations higher than those impacted by coastal flooding. We consequently focus on only wind-induced damage. To estimate wind speeds, we use a parametric wind field model, the same model used in previous work (e.g., Han et al., 2009 and Guikema et al., 2014). This model estimates gust wind speed at the location of each well by assuming a parametric decrease in wind speed with distance from the center of the storm. The hurricane track and intensity (central pressure) are input, and the storm is then translated along the track and rotated on its axis to produce the wind speed estimates. The model has been validated against actual time-varying wind speeds in the Gulf Coast region by comparing the wind field estimates with the actual wind fields for hurricanes making landfall in the Gulf Coast region in previous research (e.g., Han et al. 2009) and has been widely used. Additional details are available in Han et al. (2009). An open source version of the model is available for the R statistical language (CRAN, 2020).

This model estimates the maximum wind speed during a hurricane at predefined locations on the island. St. Kitts is divided into nine parishes, each of which is represented by one location in the wind field model. The only exception is for the southernmost parish of St. George which is given three locations because it encompasses the long peninsula and therefore yields different wind speeds depending on where the track is located. Thus, in total 11 locations at St. Kitts are used in this case study in the wind field model. The model does not take into account the elevation of the mountainous landscape of St. Kitts. This is likely not particularly limiting for this case study as the power lines are located on the outskirts of the island, which is only slightly above sea level. There may be some reduction in wind speeds on the side of the island sheltered behind the hills in the middle of the island for hurricanes that are close to the island. However, the computational complexity of including these terrain effects would be substantial, and the effects are generally not that large given the small size of the island relative to the size of a strong hurricane.

Based on the resulting maximum wind speeds, the probability of damage to the power poles is computed from the fragility curve presented in Figure 4. As the maximum wind speeds are simulated on a parish level, also the resulting power pole failure probabilities are given on a parish level. For the case study, this means that all power poles within each parish are given the same probability of failure during a hurricane. The fragility curve was developed through expert judgement (co-author Guikema) based on (1) damage reports of the impacts of previous hurricanes in St. Kitts, (2) previous research on fragility functions for hurricane-induced failures (e.g., Han et al. 2014), (3) and informal observations of pole conditions during a visit to the island. The damage reports for the Hurricanes Lenny[1], Earl[2], Georges (IFRC, 2002), Jose[3], Hugo[4], and Luis[5] are publicly available. However, the reports are not consistent in the information related to damages caused. Some only give information relaying which main island structures were damaged, while others provided specific damage percentages pertaining to the island's power system. The maximum wind speed of Hurricane Georges is used to determine the on-island wind speed that caused the failure of approximately 50% of the poles on the island. The distribution of the fragility curve is based off the reports for Hurricanes Luis, Hugo, Lenny, and Jose using the framework presented by Shafieezadeh et al. (2014). This resulted in a fragility curve with the 50% failure probability associated with 117 mph or 102 kts on-island wind speed.

[1] https://reliefweb.int/report/anguilla/hurricane-lenny-ocha-situation-report-no-7
[2] https://reliefweb.int/report/antigua-and-barbuda/cdema-situation-report-3-hurricane-earl
[3] https://reliefweb.int/report/anguilla/hurricane-jose-post-impact-situation-report-2
[4] https://reliefweb.int/report/anguilla/hurricane-jose-post-impact-situation-report-2
[5] https://reliefweb.int/report/antigua-and-barbuda/caribbean-hurricane-luis-sep-1995-un-dha-situation-reports-1-10

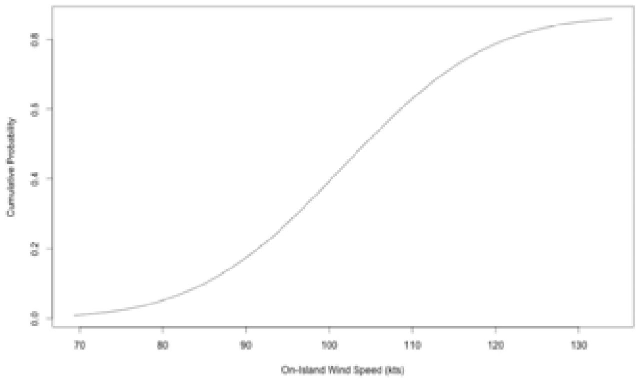

Figure 4: Estimated fragility curve of the power poles in the St. Kitts power system.

3.4 *System dependencies*

Since the wells within the water network rely on the input of electricity from the power network to function, the dependencies in the model are formed between all 30 wells within the water network and the power node which they are closest to, allowing multiple wells to depend on the same power node. The electricity within the power network is generated by diesel generators (SKELEC, n.d.) and thus does not rely on input from the water network. Figure 5 shows the position of the wells in relation to the power nodes and which power nodes each well depends on. The networks within the island are self-contained, and are fairly small in terms of size, making the network relatively simple to model. This allows the electric power and water system of St. Kitts to make a good case study of a real-world dependent infrastructure system.

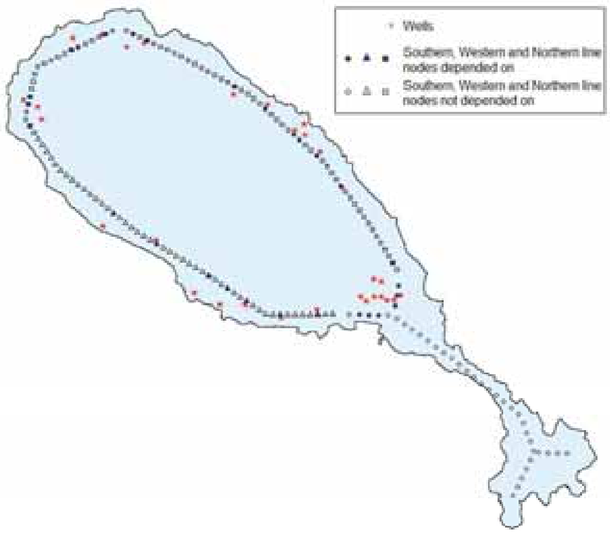

Figure 5: Schematic illustrating the dependencies within the model.

3.5 *The simulation procedure*

The process of simulating hurricanes and their corresponding damages to the power and water systems of St. Kitts is a two-stage process. In the first stage, the hurricane of interest is simulated through the hurricane model. As mentioned above, the hurricane model first simulates the maximum on-land wind speeds for each parish before it computes the corresponding failure probability of the power poles.

In the second stage, a Monte-Carlo simulation model is used to couple the power and water system models. First, the power system model simulates which power nodes break based on the power pole failure probabilities. This is done by first assigning each power pole a random value between 0 and 1. The random value is then compared to the respective node's probability of power pole failure. If a node's failure probability is higher than the randomly generated value, the node is set to be failed. This process generates a set of power node failures. We then use a connectivity-based model for the power system. That is, a given node in the system functions (provides power) if (1) there is a path from that node to the generator for which there are no failed nodes and (2) that node itself has not failed. Thus, the power system failure state is generated by setting all power nodes downstream of the initially broken nodes to non-functional.

Next, the state of the water system is computed based on the power system failure state. The power and water distribution systems are coupled through the water wells' dependency on the power system. This dependency is modeled by linking each water well to the power node closest to it, which means that if a power node linked to a well is set to be non-functional, then the well also becomes non-functional. The well states are updated based on the state of the power system, and then the water system is modeled through EPANET for a chosen simulation period (length of time simulated). The simulation period represents the duration of the power outage. This duration can be chosen either based on actual reported power outage durations or estimated based on a best guess of the time it will take the repair crews to arrive at the location, replace damaged equipment, and restore the power. During the simulation, EPANET records the minimum pressures obtained for every node in the water system. This process is repeated for a chosen number of iterations, N, which in this case study is set to 6,000 based on a convergence analysis focused on convergence of the mean. A graphic illustration of the entire simulation process is presented in Figure 6.

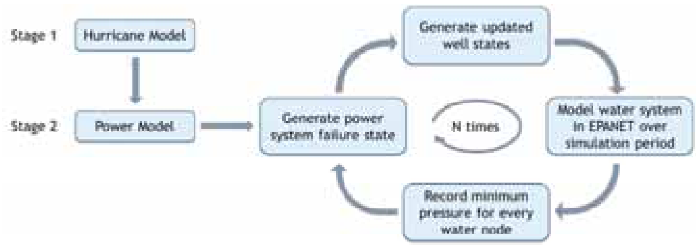

Figure 6: Graphic illustration of the simulation process.

A limitation of this modeling approach is that the functionality states of the nodes in the power and water systems are constant during the simulations in EPANET. This means that if a power outage is simulated to last for 24 hours, the model does not allow for any of the power nodes to be repaired and added back as a functional node during the simulations. In other words, all non-functional power and water nodes remain non-functional throughout the simulation. This could be changed if information were available on pole-level restoration times. However, this was not available for past storms for St. Kitts.

4 Analysis and results

We demonstrate the usefulness of a model such as this by performing two different analyses. The first analysis is a vulnerability assessment that aims to identify critical components in the power system. The second analysis focuses on the linkages between the power and water systems, focusing particularly on how to identify critical wells that would be good candidates for the installation of back-up power.

4.1 *Identifying critical components in the power system*

To identify the most critical components of the power system in terms of the cascading effects to the water system, simulations of individual power pole failures are performed. In the simulations, one power node at a time is set to fail, causing all down-stream power nodes to stop functioning. The resulting disruption on the water system is estimated for power outage durations of both 12 and 24 hours. Although failures to the power system can be repaired relatively quickly during normal conditions, the restoration time during hurricanes can be much longer due to weather conditions and difficulties for the repair crew of getting to the damage locations. By analyzing two different outage durations (12 hours vs. 24 hours), we can study the effect on the water system of different power restoration times. The simulated disruptions are measured in the form of the average number of water nodes generating negative (< 0 psi), low (0-20 psi) and high (> 20 psi) pressures during the simulation over all 6,000 iterations.

The result of the 24-hour simulations is presented in Figure 7, where the color of each of the power nodes represents the percentage of water nodes experiencing negative pressure when the given power node is the one node that initially failed. Recall that when one power node fails, all downstream nodes along the given power line also stops functioning. The percentage of water nodes experiencing negative pressures is given by a color scale ranging from white to red, where white means that no water nodes obtained negative pressure and red means that 3.2% of the water nodes obtained negative pressures. The greatest disruption to the water system of 3.2% is obtained when any of the first four nodes along the Southern power line initially failed. When one of these nodes breaks and all downstream nodes fail, several of the water wells in the capital of Basseterre become non-functional. Basseterre and the surrounding area have the highest water demand on the island. Thus, when the wells in this area stop pumping water into the distribution system over a time period of 24 hours, the water system is unable to maintain a sufficiently high pressure throughout this period.

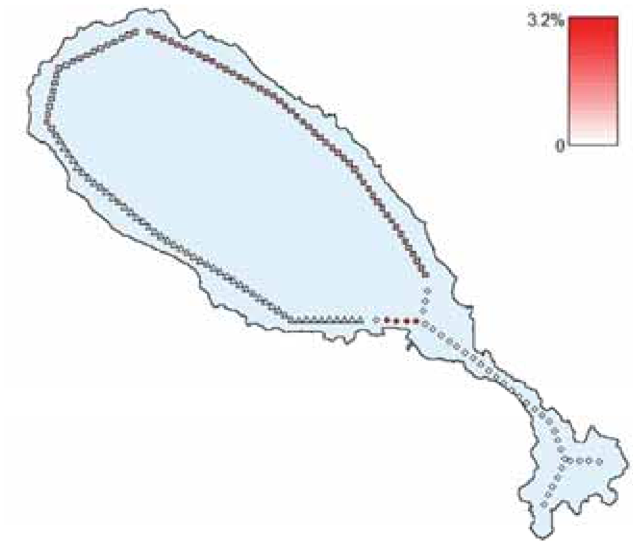

Figure 7: The percentage of all water nodes having negative pressure during a 24-hour simulation for each single-pole failure simulation. That is, the color of each power node gives the average percentage of water nodes with negative pressures if that power node fails by itself.

Negative pressures also appeared when failing any of the nodes along the Northern line. Even failing the very last node along that line causes disruptions to the water system. The reason for this is that this node provides electricity to the well with the highest water production capacity in the water system. This well has a capacity that is almost three times as high as the average capacity across all the wells. As this well is connected to the last power node along the Northern line, the well is affected by power outage when any of the power nodes along the line breaks. In addition to this well, the Northern line also supplies 15 other wells, which correspond to half of the wells in the water system. Thus, failures to this power line cause a reduction in the inflow of water to the distribution system that the water system is unable to cope with over a period of 24 hours. In comparison, no disruptions to the water system are seen by disrupting any of the nodes along the Western line, not even the first node that causes the entire line to fail. These results indicate that the power nodes along the Northern line as well as some of the central nodes in Basseterre are the most vulnerable components of the system.

Figure 8 presents the results when the simulation duration is reduced to 12 hours. In this figure, we observe that single-node failures have the same effect on the water system as during the 24-hour simulations for most of the power nodes. The only exception is for the four power nodes in Basseterre that induced the greatest disruption to the water system during the 24-hour simulations. Failing any of these nodes do not cause any disruption to the water system during a 12-hour simulation. These results indicate that the water system is able to cope without the contribution from most of the wells supplied by the Southern line for a short period of time due to within-system storage, but not for a longer time. Breaking any of the nodes along the Northern power line, on the other hand, caused negative pressures to occur in the water system also for this shorter simulation duration.

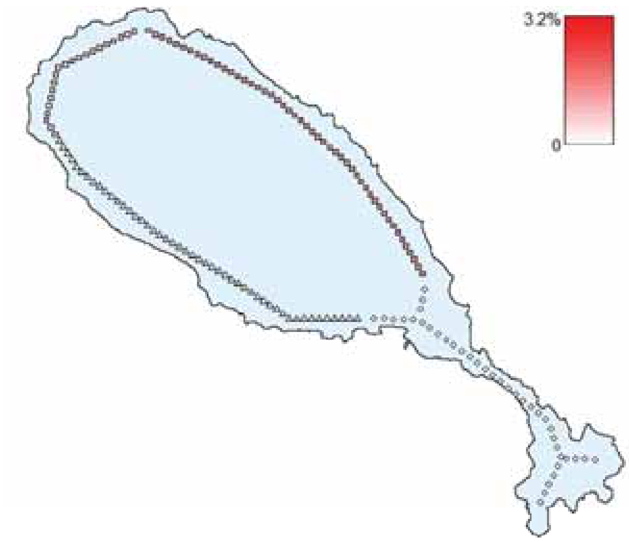

Figure 8: The percentage of water nodes obtaining negative pressure during a 12-hour simulation.

4.2 *Analyzing linkages between the power and water systems*

To identify the critical linkages between the power and water systems, simulations are performed where the wells' dependencies to the power system are removed one well at the time. In real life, this can be done by, for instance, installing a back-up power generator at the site of a well, which will allow the well to function even though there is a power outage in the area. The hurricane used in this analysis is a hurricane that is constructed to make landfall on the island. The hurricane is constructed to move according to typical Caribbean hurricanes that move westwards before bending toward the north. Figure 9a presents a map of the hurricane track. Different wind speeds ranging from 20 to 120 knots are simulated and the resulting power outage is set to last for 72 hours. Under normal conditions, this is a relatively long restoration time for the power system. However, in the scenario of a hurricane making landfall on the island, it is not unreasonable to assume that it would take at least 72 hours to get the power system back to normal operation. In Figure 9b, the resulting average number of negative water node pressures obtained over the 6,000 iterations are plotted against the simulated wind speeds. At wind speeds of 100 knots or higher, the hurricane caused the entire power system to fail, which means that none of the wells are functioning. This situation is referred to as the worst-case scenario for the remainder of this paper. In Figure 9b, we observe that the average number of negative pressures reaches a plateau at 39 (out of a total of 123 nodes in the system) when the hurricane causes this worst-case scenario.

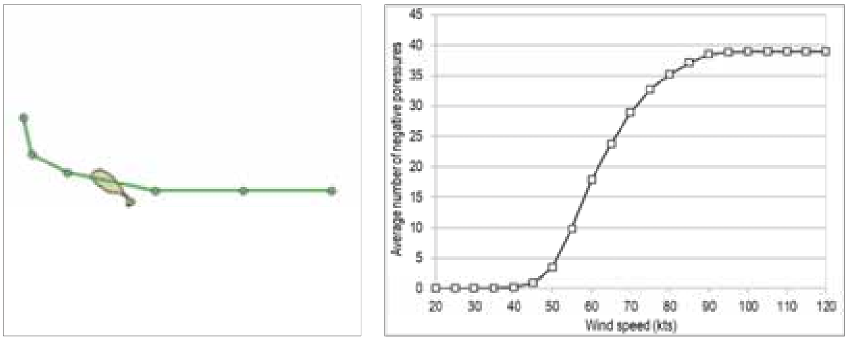

(a) (b)

Figure 9: A map of the constructed hurricane track (a) and the resulting average number of water nodes that obtained negative pressure during 72-hour power outage simulations caused the hurricane for winds speeds ranging from 20 to 120 knots (b).

Figure 10 presents the minimum pressures obtained at each water node when simulating the worst-case scenario in EPANET over a time period of 72 hours, where dark red points represent nodes experiencing negative pressure, light red points represent low pressure (0-20 psi), and white points represent pressures above 20 psi. We can see that negative pressures are appearing throughout the entire distribution system.

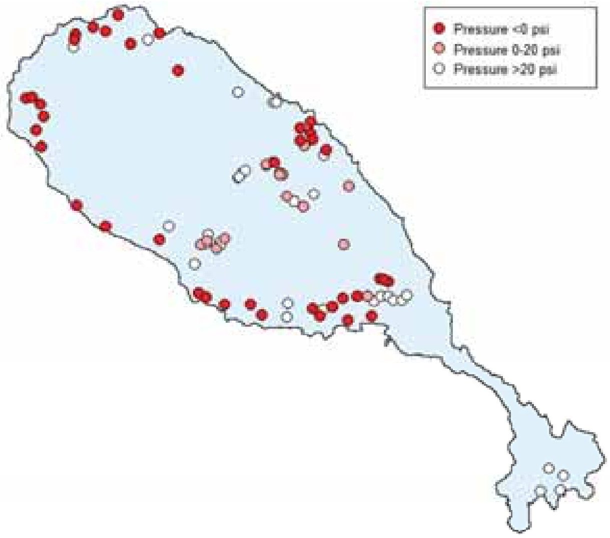

Figure 10: Minimum water node pressures simulated when no wells are functioning over a period of 72 hours.

The results of the simulations where one well at a time has its dependency on the power system removed are compared to the result of the worst-case scenario. By doing this, we can study how much each of the wells is able to improve the worst-case results. The resulting percentage reductions in the number of negative water node pressures obtained for each of the wells are presented in Figure 11. The results are given by a color scale ranging from white to green, where white means that there is no reduction in the average number of negative pressures appearing in the water system compared to the worst-case simulation and green means that a reduction of 31% in negative pressures is obtained.

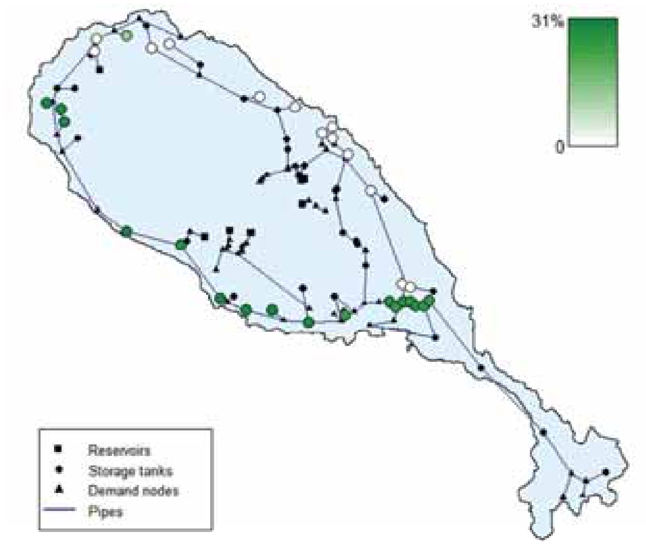

Figure 11: The percentage reduction in the number of negative water node pressures compared to the worst case where no wells are functioning.

The maximum reduction of negative pressures of 31% is observed when any of the wells along the southwestern coastline has its dependency on the power system removed. In comparison, no wells on the opposite side of the island, except one at the northernmost point of the island, gave any improvements compared to the worst-case simulation. The reason for that northern well showing some improvements is that this well is the second highest water producing well in the system, with a capacity that is 2.5 times as high as the average capacity across all wells. Recall that the well with the highest capacity is one of the three dark green wells located at the westernmost point. Thus, the water production capacity of the wells has some effect on the results. But we can clearly see that the location of the wells seems to have a higher effect, as the wells on the southwestern side of the island show such a high potential of reduced disruptions to the water system while most of the wells on the other side does not show any potential to reduce the disruptions.

An explanation for these results is that the northeastern side of the island has a higher number of reservoirs and storage tanks, i.e., water sources that are unaffected by power outages, than in the southwestern side. In Figure 11, the reservoirs and storage tanks are illustrated by black squares and dots, respectively. The area in and around Basseterre has the highest water demand. Due to the pressure drop that will be created as a result of the high demand, we believe that the water from both the western and eastern side of the island is flowing towards Basseterre. Since the western side of the island has a fewer number of reservoirs and storage tanks, this part of the distribution system will struggle more to maintain a positive pressure without any contribution from the wells. Thus, the contribution from allowing only one well to function on backup power is higher when this one well is located along the western side of the island compared to on the northeastern side.

5 Model validation

In order to validate the developed model for the power and water system at St. Kitts, a real hurricane is simulated in the model with the aim of comparing the simulated disruptions to the infrastructure systems with the actual disruptions caused by the hurricane. The hurricane used in this validation process is Hurricane Maria, which moved over the Eastern Caribbean Sea in September 2017. When passing St. Kitts on the 19th of September, Hurricane Maria was a category 5 hurricane with its center located approximately 90 miles southwest of the island (Burke, 2017). Data about the hurricane track and wind speeds are obtained from the National Oceanic and Atmospheric Administration National Centers for Environmental Prediction FTP site (NOAA, 2017).

The track and wind speed data obtained for Hurricane Maria is first used as input to Stage 1 of the simulation process (as shown in Figure 6) to estimate the on-island wind speeds. The on-island wind speed estimates are then used as input to Stage 2 of the simulation process and the probability of power pole damage for each parish is obtained. 6,000 iterations of the simulation are then run to simulate the effects of the hurricane on St. Kitts' power and water systems. For each iteration, a power outage duration of 60 hours is simulated. A press release from SKELEC (SKELEC, 2017) states that repair crews began assessing the damage of Hurricane Maria on the 20th of September, 2 days after the power system was first affected by the storm. For power restoration after a hurricane, there is typically another 1-2 days to fully mobilize repair resources, especially on an isolated island. Therefore, we estimate that repair work began 60 hours after the power outage began.

The results first focus on the simulated effect of the hurricane on the power system. Figure 12 shows the frequency over the 6,000 simulations with which each pole is broken due to the hurricane wind. The nodes along the south-western side of the island have the greatest probability of breaking due to Hurricane Maria. This is the side of the island that the hurricane passed closest to and, therefore, experienced stronger wind speeds during the hurricane. It is worth noting that the greatest frequency of pole damage due to the winds within the model is low, at just above 2% at 2.15%.

Figure 12: Frequency of power node breaks during the simulation of Hurricane Maria.

For each iteration, the cascading effects of the pole damage on downstream power nodes are recorded, allowing analysis of the frequency of each power node not functioning. Figure 13 shows the frequency that each power pole is non-functional during the simulation of Hurricane Maria. The nodes towards the end of each power line have the greatest frequency of being non-functional. This is as expected, as when a node in a power line breaks, all downstream nodes are set to be non-functioning, and so the nodes towards the end of each power line have a greater probability of being non-functional than those towards the beginning of the line. The greatest frequency of a node being non-functional is 54% of the iterations.

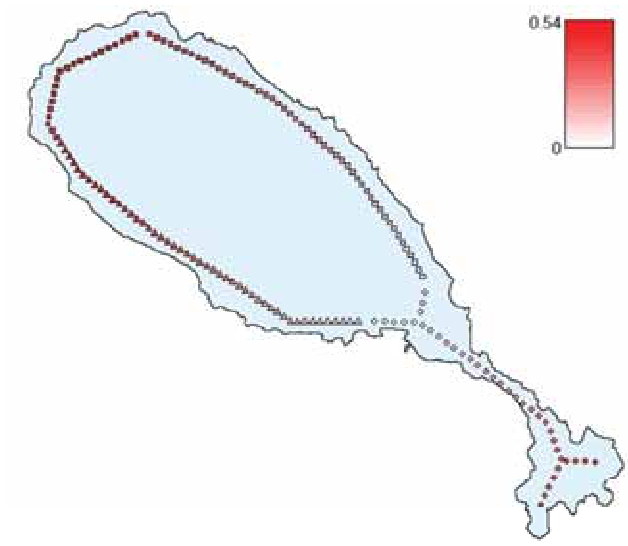

Figure 13: Frequency of power nodes being in a non-functional state during the simulation of Hurricane Maria.

The effects the simulated power outages have on the water distribution is also investigated. First, the frequency with which each well is without power can be shown. Figure 14 shows that the wells with the greatest frequency of power disruptions follow the same pattern as the frequency of non-functioning power nodes. The frequency is low for those towards the southeast of the island and increases over towards the north-western area of the island, where the ends of both the Western and Northern power lines are located.

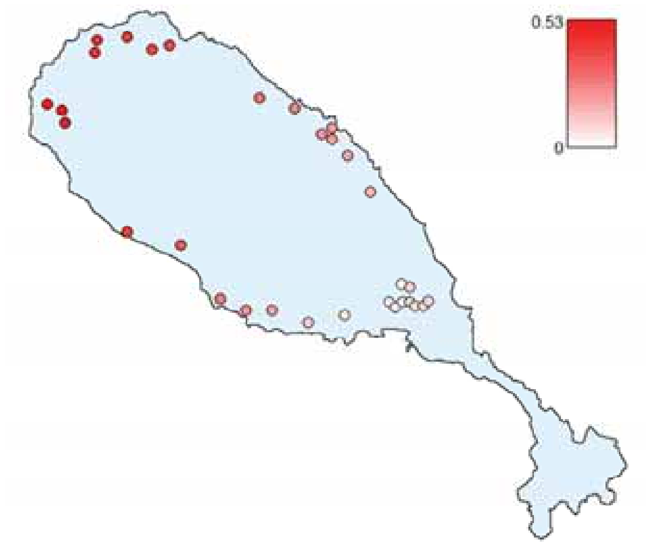

Figure 14: The frequency of which water wells lost power during the simulation of Hurricane Maria.

The effects of the loss of power at the wells on the water system can be seen in Figure 15, which shows the water nodes that experienced negative pressures during the simulation. All water nodes that experience negative pressures during the simulation are located in the northern part of the island, situated towards the end of the Northern and Western power lines. These areas are more likely to experience power outages to the wells, increasing the likelihood that the closer water nodes will experience negative pressures. However, the water nodes in the middle and south of the island are not affected in the simulation.

This analysis can suggest to the water system operator which areas of the system require attention. This could be in the form of introducing redundancy, such as back-up generators for the wells that experience the greatest frequency of power outages during the simulation or in the form of adding storage reservoirs in that portion of the system to increase the ability of the system to withstand short power outages.

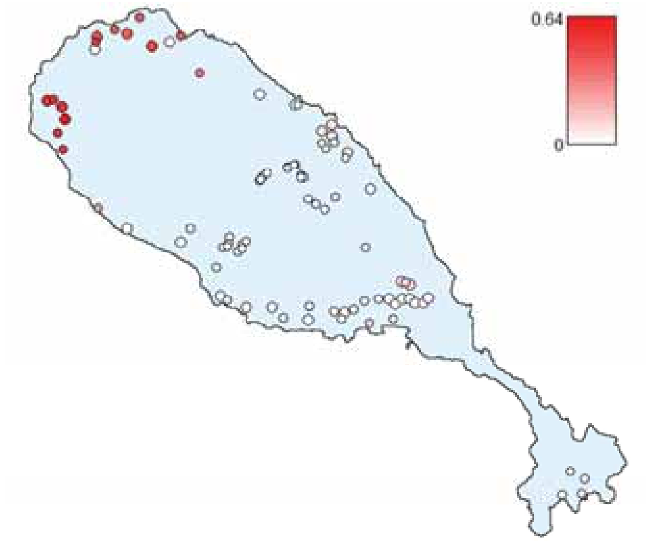

Figure 15: The frequency of which water nodes experience negative pressures during the simulation of Hurricane Maria.

The aim of using our model to simulate the effects of Hurricane Maria on the power and water systems is to compare the results to the actual outages that occurred on St. Kitts. Unfortunately, the publicly available information about the actual disruptions to the power and water systems is very limited. This is typical, even in the U.S. The best information about disruptions to the power system is found in a press release at the SKELEC webpage (SKELEC, 2017), which stated that "Most of our feeders remained intact and online during the passage of the storm. Some like the Canada feeder which services Conaree, Halfmoon and Canada Estates came offline, also Basseterre North Buckley's to Trinity also is fully offline". For the water system, on the other hand, we are unable to find any information about the disruptions caused by Hurricane Maria.

From the limited information found on the effects of Hurricane Maria to the power system of St. Kitts, a crude comparison can be made to the results of our simulations. Figure 16 shows the areas that SKELEC stated in the press release were offline due to Hurricane Maria and the results of our simulations. As the press release from SKELEC only named areas that were without power, the outline of these areas encompasses the entire residential areas mentioned in the press release and, thus, do not represent the actual outages due to Hurricane Maria.

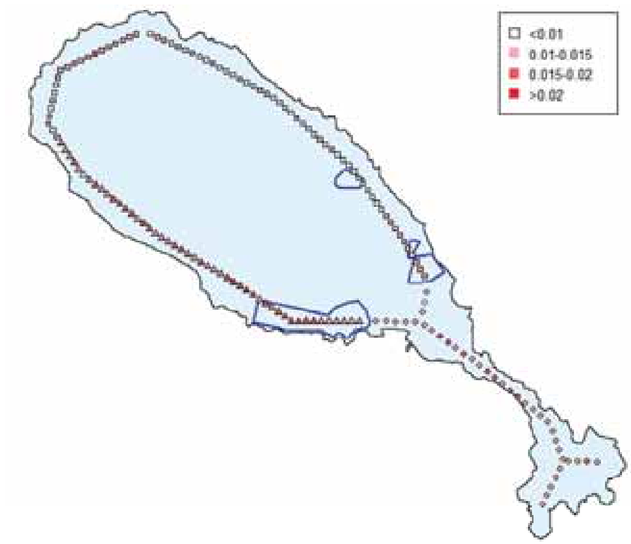

Figure 16: Comparison of the simulated frequency of power node breaks to the areas of St. Kitts that were reported to lose power due to Hurricane Maria.

The areas that were said to be affected in the SKELEC press release are all located close to the start of either the Northern or Western lines, while areas further downstream of all truck lines were not reported to lose power. This suggests that the outages that occurred due to Hurricane Maria were due to disruptions in the smaller distribution lines that are not included in the power model. Comparing the areas affected due to the hurricane with the initial outages seen in the model, the affected area of Basseterre North Buckley's to Trinity (on the south-western side of the island), somewhat matches with power nodes that have a high frequency of breaking during the simulation.

The Canada area of St. Kitts is the smallest area outlined in Figure 16 (the northernmost outline shown). The press release states that all outages on the eastern side of the island were due to the feeder at Canada being offline. Therefore, the power outages on the eastern side of the island are not due to disruptions to the main trunk lines and thus cannot be compared to the results of our simulations.

No data of the disruption caused to the water system was made publicly available. The only reference to damage within the water system was in the Prime Minister's post Hurricane Maria address stating "Some critical infrastructure such as our electricity and water services… sustained serious damage" (Organisation of Eastern Caribbean States, 2017). Unfortunately, the lack of information publicly available to the effects of Hurricane Maria on both the power and water systems make validation of the model difficult. However, this is not unusual and points to a research need. We as a research community need to do a better job of collecting and archiving spatially detailed data about the performance of infrastructure systems after natural hazards.

6 Discussion

A model for the dependent power and water systems at St. Kitts has been developed and the area of application for this model has been exemplified by performing two analyses: one that aimed at identifying critical components in the power system and another that analyzed the linkages between the power and water systems. In this section, we will first discuss how results obtained with our model can be used by providing examples of how the results can support decisions regarding system upgrades and emergency preparedness plans. Afterward, we will discuss the challenges faced when modeling real-world dependent infrastructure systems in relatively data-poor environments, as well as the differences between modeling these systems and fictional systems.

6.1 *Decision support*

Many emerging and developing countries do not have access to the resources needed to quickly repair infrastructure failures, which make them significantly more vulnerable to infrastructure damage and water shortages. The power and water systems on St. Kitts fall into this category. The power and water systems are spread across the entire island, but the operators may not have the resources to immediately fix large-scale blackouts or blackouts located away from the population centers. Therefore, the result of analyses like the ones performed in this paper can be used to support decisions about system upgrades that can help the operators avoid disruptions. The results can also help the operators and society in general to support decisions about emergency preparedness plans. For instance, information about the most critical components of the power system can be used to support decisions about which parts of the power system should be strengthened to better withstand strong winds. Repair crews and spare equipment are scarce resources. Thus, when a hurricane is forecasted and severe disruptions are predicted, the utility operators can benefit from knowing which parts of the system are most critical and therefore which parts of the system should be prioritized to be repaired and where to store back-up equipment required to perform repairs.

The results of comparing the simulated disruptions to the water system during different power outage durations illustrate the importance of getting water wells back in normal operation as fast as possible during downtimes. The results indicate that the water system can cope with power outages in the area of Basseterre for 12 hours, but not for 24 hours. Thus, if the power utility operators are not able to restore the power supply to the water system quickly, the water utility operators should consider other alternatives to avoid loss of service. One possibility is to manually shut down some parts of the system to reduce the pressure drop in the critical areas. Another solution is to supply the critical wells with electricity from a different source such as a back-up power generator. The result of the analysis where the linkages between the power and water systems, i.e., the wells, were analyzed can help support decisions about whether or not to invest in back-up power generators, and if so, where these generators should be installed. The analysis in this paper only simulated the situation where one well at a time had access to a back-up generator. The results indicate that a power generator should be installed to supply any of the wells along the southwestern side of the island. We would like to emphasize that this is not a final recommendation. This analysis is only studying the effect of removing a well's dependency on the power system during a worst-case scenario where the entire island is affected by a power outage. For less severe hurricanes, only parts of the power system will fail, which will cause only a portion of the wells to stop functioning. Such scenarios are not analyzed in this paper. In addition, in this analysis we are only looking at the possibility of removing the dependency between the wells and the power system one well at a time. What if the back-up power generator can supply more than one well at a time? What if two or more back-up power generators can be installed at different locations of the island? These questions cannot be answered from the analysis performed here, and further analysis is required before any conclusions can be made. However, this analysis provides a good example of an area of application for the model.

6.2 *Challenges when modeling real infrastructure systems in data-poor areas*

From an academic perspective, there are many potential challenges that can arise when modeling real infrastructure systems, especially when dependencies between the systems have to be accounted for. We discuss some of these challenges in this section, focusing specifically on doing this type of modeling in relatively data-poor areas.

The largest challenge is to get access to the requisite data to develop a model. The available data is often limited, which makes the task of developing models that accurately represent the infrastructure systems challenging. The required data includes data about infrastructure topology, i.e., data about how the systems are structured and how they are connected to each other, data about the infrastructure states both during normal operation and during emergencies, and other relevant data that influence operations, like government and corporate policies (Rinaldi, 2004). The private sector is often the owners of the infrastructures, and thus, the owner of the data. Therefore, regardless of the system being in a data-poor or data-rich area, the data is usually considered sensitive and is therefore kept confidential. Getting access to the data requires approval from stakeholders, which can be hard to achieve (Johansson and Hassel, 2010). Limited availability of relevant data was a significant challenge for the case study in this paper. As previously mentioned, the only relevant data found about the power system is the publicly available data obtained through the SKELEC webpage. The available data about the water system, on the other hand, is much better as relevant information was provided from the St. Kitts Water Department.

Another problem related to getting access to requisite data is that the available data is not detailed enough or the data might not even exist, which can be the case for operational data. Advances in technology in recent decades have resulted in increased use of sensors and real-time monitoring of infrastructures, which provides large amounts of operational data during both normal operations and crises. However, not all infrastructures utilize these new technologies, particularly in resource-constrained systems. For these infrastructures, the quality of the available operational data is dependent on the routines of documenting abnormalities and accidents during operations. However, even if infrastructure do have up-to-date technology and are capable of recording data related to operations, the issue of the sensitivity of the data again comes into play. Many companies do not want to advertise how much their operations have been impacted when hazards occur. Another worry for companies is how the release of outage data may affect their customers' perception of their ability to operate and their public reputation.

Even if an infrastructure company agrees to share information about their system to be used to develop a model, the data needs to be reviewed regularly to assess how relevant it is compared to the infrastructure. Infrastructures are not static, but instead are constantly being updated either to be better prepared for disruptions or sometimes re-built after a disruption occurs. To ensure that the model is representative of the current system, the model developers need information about such updates from the infrastructure management. When modeling dependencies between infrastructures, the dependencies can also change over time and must be considered when assessing if the model is representative of the current systems and their dependencies.

Once the relevant data is available to develop a model, there are always assumptions made in order to go from a complex real-world system to a simpler representation that can be modeled. The more detail included in the model, the more computational power is needed to produce a viable simulation. There is a trade-off process of including enough information within the model that it relates to the real-world system, and not including too much information that the model is slow to run simulations. For dependent infrastructure models, this again extends to the dependencies modelled between the systems. They must represent accurately the interactions between the systems, but not be so complex that the model is difficult to construct.

For the model presented, due to the size and population of St. Kitts, the water and power systems are relatively small compared to systems seen in other parts of the world. Despite being relatively small systems, assumptions were made in order to be able to develop the models. The Water Department of St. Kitts agreed to share the data they had available to them, which included information on 24 of the 30 wells and the demand at the parish level, rather than household level. This affected the water model developed in EPANET which struggled to handle the magnitude of demand and inflow of each parish effectively. In order to combat this issue, the magnitude of the demand and inflow of water was reduced but kept at the same ratio to allow the model to be an accurate representation of the water distribution within the system.

Unfortunately, very limited information on the power system is publicly available, and thus more assumptions were made when developing the power model than the water model. Only three of the main truck lines were included in the model. The information used to develop the model came from information found on the company website, and observations made by members of the Guikema Research Group on the spacing of the power poles of the 3 trunk lines. The smaller distribution lines could not be included in the model due to lack of available information.

The hurricane model used is a model developed previously (Han et al. 2009). A limitation of the wind field model is that it currently does not take the elevation of St. Kitts into account. The mountainous area in the center of the island will have some effect on the on-island wind speeds which is not accounted for in the model. The simulation also only accounts for damage to the power and water systems due to the strong winds experienced during hurricanes and no other events that can also occur such as flooding due to storm surge.

After developing a model, there can be great challenges involved in validating the model, as was experienced in this case study. When collecting data about a disruptive event and its consequences to the infrastructure systems, the same problems as the one faced when collecting system specific and operational data prior to the model development appears. In our case study, we were unable to find public information that in detail described the damages to the systems caused by Hurricane Maria and the duration of the resulting disruptions. An attempt was made to collect data about damages and disruptions caused by other hurricanes too, but even less data was found then. Without access to more data it is impossible to perform a complete validation of the model.

6.3 *Why study real systems rather than just fictitious systems?*

There have been many studies of infrastructure that have used fictitious systems to study interdependencies. However, relatively few studies have been conducted with real-world examples (e.g., Johansson and Hassel, 2010). The available studies have all been done in wealthy countries with considerably higher capacity for collecting and maintaining data on infrastructure systems than our case study.

Real-world studies are undeniably more challenging to perform for academic researchers. The needed data must be gathered if it is even available, and real-world systems are much more complicated than fictitious systems. Why study real systems? One of the main reasons is to better understand if the findings from studies of fictitious systems still hold if more of the complexities of real-world systems are accounted for. Does leaving out the messy, real-world details fundamentally change the insights? In our study, we see that accounting for the actual engineering performance of the water system reveals key insights into where to strengthen it that likely would not be revealed by a more typical network theoretic based approach that does not account for the distribution of demand and the physics of pipe flow. A second key reason for studying real systems is to demonstrate *how* existing methods can be adapted and used given real-world data and, in many cases, the lack of full data about the systems. This is critical for moving these types of analysis tools from academic studies to real-world use.

7 Conclusions

The dependent power and water systems of St. Kitts have been modeled, providing a real-world example of a dependent infrastructure model. Although the data available to develop the model was suboptimal, a simple representation of the island's power and water systems was created. We have seen that dependencies between infrastructures can cause substantial performance degradations, even in relatively simple systems with limited interactions between them. Thus, dependencies, even in simple systems, need to be taken into consideration. We have also shown how improvements within the water system could be made to reduce the impacts of disruptions within the power system. Even with the challenges associated with developing real-world case studies, we have shown that it is possible in a low-data setting to produce a simple model of a real-world case study in a way that could support risk management decision making.

Acknowledgement

This work was partially funded by the U.S. National Science Foundation through grant numbers NSF-1621116 and NSF-0968711. The opinions are those of the authors and do not necessarily represent the opinions of the U.S. National Science Foundation. The work was also partially funded by the Norwegian Ministry of Education and Research.

References

Buldyrev, S. V., Parshani, R., Paul, G., Stanley, H. E., & Havlin, S. (2010). Catastrophic cascade of failures in interdependent networks. *Nature*, *464*(7291), 1025. doi:10.1038/nature08932.

Burke, E. (2017). Hurricane Maria remains powerful, dangerous hurricane [News Update], *St. Kitts & Nevis Observer*, Retrieved from http://www.thestkittsnevisobserver.com/breaking-news/hurricane-maria-remains-powerful-dangerous-hurricane-news-update/ [Accessed on 05 February 2019].

Chai, W. K., Kyritsis, V., Katsaros, K. V., & Pavlou, G. (2016). Resilience of interdependent communication and power distribution networks against cascading failures. In 2016 *IFIP Networking Conference (IFIP Networking) and Workshops*, 37-45. IEEE. doi:10.1109/IFIPNetworking.2016.7497224.

CRAN (2020). Details of the stormwind package. http://cran.seoul.go.kr/web/packages/stormwindmodel/vignettes/Details.html, [Accessed on 9 April 2020].

Douglas, D. L. (1998). Dear Mr. Camdessus [Open letter]. Retrieved from https://www.imf.org/external/np/loi/121098.htm [Accessed on 14 January 2019].

Dueñas-Osorio, L., Craig, J. I., & Goodno, B. J. (2007). Seismic response of critical interdependent networks. *Earthquake engineering & structural dynamics*, *36*(2), 285-306. doi:10.1002/eqe.626.

Dui, H., Meng, X., Xiao, H., & Guo, J. (2020). Analysis of the cascading failure for scale-free networks based on a multi-strategy evolutionary game. *Reliability Engineering & System Safety*, 106919. doi: 10.1016/j.ress.2020.106919.

Fu, G., Dawson, R., Khoury, M., & Bullock, S. (2014). Interdependent networks: vulnerability analysis and strategies to limit cascading failure. *The European Physical Journal B*, *87*(7), 148. doi:10.1140/epjb/e2014-40876-y.

GLUMR Board (2012). Recommended standards for water works: Great Lakes--Upper Mississippi River Board of State Public Health Environmental Managers. Water Supply Committee. Retrieved from https://www.broward.org/WaterServices/Documents/states_standards_water.pdf [Accessed April 2019].

Gao, J., Barzel, B., & Barabási, A. L. (2016). Universal resilience patterns in complex networks. *Nature*, *530*(7590), 307. doi: 10.1038/nature16948.

Guikema, S. D., Nateghi, R., Quiring, S. M., Staid, A., Reilly, A. C., & Gao, M. (2014). Predicting hurricane power outages to support storm response planning. *IEEE Access*, *2*, 1364-1373. doi:10.1016/j.ress.2008.02.018.

Han, S. R., Guikema, S. D., Quiring, S. M., Lee, K. H., Rosowsky, D., & Davidson, R. A. (2009). Estimating the spatial distribution of power outages during hurricanes in the Gulf coast region. *Reliability Engineering & System Safety*, *94*(2), 199-210. doi:10.1016/j.ress.2008.02.018.

Han, S. R., Rosowsky, D., & Guikema, S. (2014). Integrating models and data to estimate the structural reliability of utility poles during hurricanes. *Risk analysis*, *34*(6), 1079-1094. doi: 10.1111/risa.12102.

IFRC. (2002). Caribbean - Hurricane Georges Appeal No. 29/1998 Final Report. Retrieved from https://reliefweb.int/report/antigua-and-barbuda/caribbean-hurricane-georges-appeal-no-291998-final-report [Accessed on 14 January 2019].

Johansson, J., & Hassel, H. (2010). An approach for modelling interdependent infrastructures in the context of vulnerability analysis. *Reliability Engineering & System Safety*, *95*(12), 1335-1344. doi:10.1016/j.ress.2010.06.010.

Johansson, J., Hassel, H., & Cedergren, A. (2011). Vulnerability analysis of interdependent critical infrastructures: case study of the Swedish railway system. International journal of critical infrastructures, 7(4), 289-316. doi:10.1504/IJCIS.2011.045065.

Johnson, Caroline A., Roger Flage, and Seth D. Guikema. (2019) "Characterising the robustness of coupled power-law networks." *Reliability Engineering & System Safety* 191: 106560. doi: 10.1016/j.ress.2019.106560.

LaRocca, S., Johansson, J., Hassel, H., & Guikema, S. (2015). Topological performance measures as surrogates for physical flow models for risk and vulnerability analysis for electric power systems. *Risk Analysis*, *35*(4), 608-623. doi: 10.1111/risa.12281.

NOAA. 2017. Retrieved from National Centers for Environmental Prediction FTP site: https://ftp.emc.ncep.noaa.gov/wd20vxt/hwrf-init/decks/bal152017.dat [Accessed on 24 April 2019].

Organisation of Eastern Caribbean States. (2017). *Prime Minister Dr. the Hon. Timothy Harris' Post-Hurricane Maria Address*. [ONLINE] Available at: https://pressroom.oecs.org/prime-minister-dr-the-hon-timothy-harris-post-hurricane-maria-address. [Accessed on 27 February 2019].

Ouyang, M., & Wang, Z. (2015). Resilience assessment of interdependent infrastructure systems: With a focus on joint restoration modeling and analysis. Reliability Engineering & System Safety, 141, 74-82. doi: 10.1016/j.ress.2015.03.011.

Parshani, R., Rozenblat, C., Ietri, D., Ducruet, C., & Havlin, S. (2011). Inter-similarity between coupled networks. *EPL (Europhysics Letters)*, *92*(6), 68002. doi:10.1209/0295-5075/92/68002.

Poljanšek, K., Bono, F., & Gutiérrez, E. (2012). Seismic risk assessment of interdependent critical infrastructure systems: The case of European gas and electricity networks. Earthquake Engineering & Structural Dynamics, 41(1), 61-79. doi: 10.1002/eqe.1118.

Rinaldi, S. M. (2004). Modeling and simulating critical infrastructures and their interdependencies. *Proceedings of the 37th annual Hawaii international conference on System Sciences*. IEEE. doi:10.1109/HICSS.2004.1265180.

Rossman, L. A. (2000). EPANET 2.0 Users Manual. In *N. R. M. R. Laboratory (Ed.): United States Environmental Protection Agency*.

Shafieezadeh, A., Onyewuchi, U.P., Begovic M. M. & DesRoches, R. Age-dependent fragility models of utility wood poles in power distribution networks against extreme wind hazards. *IEEE Transactions on Power Delivery*, *29* (1), 131-139. doi:10.1109/TPWRD.2013.2281265.

SKELEC. (n.d.) System Overview. Retrieved from https://www.skelec.kn/system-overview/. [Accessed on 14 February 2019].

SKELEC. (2017). [Online] Hurricane Maria Restoration Update. Retrieved from http://www.skelec.kn/hurricane-maria-restoration-update-wednesday-september-20-2017/ [Accessed on 05 February 2019].

Thacker, S., Barr, S., Pant, R., Hall, J. W., & Alderson, D. (2017). Geographic hotspots of critical national infrastructure. Risk Analysis, 37(12), 2490-2505. doi:10.1111/risa.12840.

The Official Website of St. Kitts and Nevis. (n.d.) About St. Kitts and Nevis. Retrieved from https://www.gov.kn/ [Accessed on 09 January 2019].

World Population Review. (n.d.) Saint Kitts and Nevis Population 2018. Retrieved from http://worldpopulationreview.com/countries/saint-kitts-and-nevis-population/ [Accessed on 09 January 2019].

Paper V

Feasibility study of PRA for critical infrastructure.

Authors: Caroline A Johnson, Roger Flage and Seth D Guikema

Under revision to be resubmitted for possible publication in *Reliability Engineering & System Safety*.

Feasibility study of PRA for critical infrastructure risk analysis

Caroline A. Johnson[a,*], Roger Flage[a] & Seth D. Guikema[b]

[a] University of Stavanger, Norway
[b] University of Michigan, USA
[*] Corresponding author: University of Stavanger, P.O. Box 8600 Forus, 4036 Stavanger, Norway. E-mail: caroline.a.johnson@uis.no.

Abstract:

Probabilistic Risk Analysis (PRA) has been commonly used by NASA and the nuclear power industry to assess risk since the 1970s. However, PRA is not commonly used to assess risk in networked infrastructure systems such as water, sewer and power systems. Other methods such as network-based, statistical and agent-based models are used to analyse the performance of infrastructure when a disruption occurs. Within the electric power industry N-1 analysis is used to demonstrate system operability when any one component within the system is not functional. Such methods have the advantage of being simpler to implement than PRA. Performing a PRA of an infrastructure system would require full knowledge of the system including component failure probabilities, which combinations of component failures results in a disruption, what the magnitude of the disruption would be as well as the probabilities of the different initiating events. This quickly becomes complex, even for small infrastructure systems. This paper explores the feasibility of using PRA for infrastructure systems, before demonstrating the formulation by performing a PRA of a virtual water system. A comparison of methods currently used to assess infrastructure to that of PRA is given before discussing the feasibility of PRA for modern infrastructure systems.

Key words: Probabilistic Risk Analysis; critical infrastructure; feasibility study; network models; statistical learning theory; *N-1* analysis

1 Introduction

The use of Probabilistic Risk Analysis (PRA) as a tool for risk assessment was popularised in the 1970s with the assessment of the risk associated with nuclear power plants. The WASH 1400 report [1] which assessed accident risk of commercial nuclear power plants in the USA is referred to as the first modern PRA [2, 3]. Various terms such as Quantitative Risk Analysis (QRA) [4] and Probabilistic Safety Analysis (PSA) are also used to refer to the process of PRA, and in all three terms the word analysis is sometimes substituted with assessment.

There are two main elements of PRA: first, the severity of the consequences of a scenario and second, the likelihood of the failure scenario that results in the consequences occurring [5, 6]. The important factor is to provide the likelihood of occurrence and not just the consequences, which is often lacking in assessments where methods of analysis other than PRA are used. In an engineering setting, PRA should fully assess the risks associated with a technological system. PRA then includes scenario identification of what can go wrong, what is the associated likelihood of each scenario occurring as well as the associated consequences [7].

For infrastructure systems such as power, communication and water systems PRA is not a tool commonly used to assess the associated risks. Modern infrastructure systems are vast and complex, resulting in, if applied, an equally complex PRA. By formulating a PRA for infrastructure systems and demonstrating how this could be applied to the water system of a virtual city the complexity of the process will be presented. Elements of PRA contained within more popular methods of analysing modern infrastructure systems will also be explored, indicating how well these methods approximate PRA results.

Tools developed for PRA are also used for stand-alone analysis of infrastructure systems, especially when investigating the possibility of a specific scenario occurring that affects the system. One example is fault trees, which are used to estimate a 'top event' probability by modelling the occurrence of that event based on if other events have occurred in the system or not. Both Lindhe et al. [8] and ten Veldhuis et al. [9] analyse water systems using fault trees. Lindhe et al. [8] assess the risk of the system in terms of the quantity and quality of the water reaching the consumers while ten Veldhuis et al. [9] focus on quantifying the probability of flooding, highlighting areas of the water system that can be improved. The use of fault trees allowed both to investigate the probability of failure within the respective water systems, however, both methods could be extended to provide a PRA of the respective systems. Lindhe et al. [8] could be extended to a PRA by including the likelihood of scenarios which resulted in the basic events present in the fault trees. ten Veldhuis et al. [9] did not include the severity of the consequences associated with a flood, which, if included, would extend the analysis to present a PRA of the water system.

Other methods of assessing the performance of infrastructure systems have also been developed. Such methods include network or graph theory or statistical learning theory [10, 11]. Developments of these methods focus on including the interdependencies between modern infrastructure systems and how the cascading effects due to these interdependencies affect infrastructure risk.

When the infrastructure can be represented as a network, one method of identifying critical components of the system is cut set analysis. In terms of graph theory, a cut set is a set of nodes (or edges) that if removed, will disconnect a specified pair of nodes within the network [12]. Cut set analysis is widely used within transportation networks, where the removal of a link leads to the redistribution of the traffic using diversions. This increases both the distance travelled, as well as the volume of traffic on alternative routes. In this scenario, the cut set analysis can be used to see which link removals are critical in terms of these factors.

Erath et al. [13] presents a method that reduces the network to subnetworks, easing the computational expense of cut set analysis, indicating which link removals cause the greatest increase in cost, viewed as either additional time taken or distance travelled, to the users of the system. Sullivan et al. [14] investigated the partial disruption to links in a transportation network, using cut set analysis as a basis. However, rather than removing a link, they decreased the capacity of the link. Using the increased travel time after the link disruption as a measure of the system's robustness, they conclude that the critical links within the system depend on the magnitude of the disruption.

Matisziw and Murray [15] investigated the cut sets of links that caused the most disruption to an internet network between several universities. Using the Abilene Internet2 backbone system, the removal of only 1 up to all 14 links was investigated. For each level of link removal, the cut set that caused the most disruption of connectivity between the universities was presented. Matisziw et al. [16] suggested an optimisation method to identify minimal cut sets of link removals in an infrastructure system containing source and sink nodes to highlight the vulnerable areas. The focus of the research is developing measures to determine which nodes or links are the most critical in infrastructure network systems when commodity flow is included in the analysis.

In the US electricity power industry a popular method to assess the system's functionality is *N-1* analysis. Bulk power systems (meaning a power system containing both the generation and transmission parts of the system) are regulated in the US to ensure that they are able to maintain service if one of the main N components (generators, transformers, transmission lines) are offline [17]. An extension of N-1 analysis is N-k analysis, where the functionality of the system is analysed when k components are offline simultaneously. This is a more extensive assessment of the system than an N-1 analysis, but the increase in failure combinations to consider increases greatly as the number of components simultaneously offline increases.

Chen and McCalley [18] demonstrated a method to simplify the network structure when components are known to be offline for reasons such as maintenance and thus the topology of the system has changed. The aim is to reduce the number of combinations needed to be assessed for an N-k analysis by grouping components to form subnetworks that are functional or non-functional based on the system's topology. Arroyo and Fernández [19] proposed a genetic algorithm that finds the worst combination of failures for each level of the N-k analysis. This allows the worst possible outcome of each level of the analysis to be considered rather than all possible combinations, however this can still be computationally expensive for large systems. Mori and Goto [20] present a similar idea by proposing the use of a Tabu search to identify the worst combinations of failures for N-k analysis as an alternative to an extensive search of all possible failure combinations or the use of a genetic algorithm.

Although N-1 and N-k analysis investigates if the system can function with the loss of k components, no probabilities are assigned to the failure of each component. The events which lead to the failure of k components simultaneously are also not included in the analysis. Therefore, a combination of k failures that results in a larger disruption than another may be given more attention, but the combination resulting in a smaller disruption may be more likely to occur and thus should also be given attention. The addition of these elements into the analysis extend the method towards that of PRA.

In the present paper we explore a formulation of a full PRA for infrastructure systems before applying it to a water system of a virtual city. The formal formulation of a full PRA, along with the example, demonstrates how complex it can be to perform a PRA for modern critical infrastructure. A discussion on the extent that the current methods of assessing infrastructure risk are estimations of a PRA of infrastructure risk, or which elements of a PRA they encompass will also be addressed. Methods considered will included topology-based and flow-based networks [21, 22] and statistical learning theory [10].

Section 2 gives an overview of PRA as a method. This is followed by the formulation of a full PRA for an infrastructure system in Section 3. In Section 4, this formulation is applied to a virtual water system. Section 5 provides a comparison of other methods used in infrastructure risk analysis to PRA. A discussion of the difficulties associated with performing a full PRA for infrastructure systems is given in Section 6 before the conclusions of the paper are presented in Section 7.

2 Probabilistic risk analysis

Kaplan and Garrick [7] outlined a quantitative definition of risk which is now frequently used as a conceptual basis for PRA. They proposed that by answering three questions the risk associated with a system or event can be presented quantitatively. These questions are:

1) What can happen/go wrong?
2) What is the likelihood that is will happen?
3) Given it does happen, what are the consequences?

The quantitative definition of risk, R, that results from answering these three questions is expressed as

$$R = \{\langle s_i, l_i, x_i \rangle\}, \qquad i = 1, 2, \dots, N \tag{1}$$

which defines risk as the set of triplets where each triplet contains a scenario of what can go wrong, s_i, the likelihood that the scenario will occur, l_i, and the consequence associated with the scenario, x_i [23]. The set contains N triplets which is the number of possible scenarios that are identified by the assessor.

The risk is often presented as a risk curve. To generate the risk curve, the scenarios are arranged in increasing order of severity of damage, before calculating the cumulative likelihood of the scenarios. The consequences are then plotted against the cumulative likelihood, resulting in a staircase function. Considering the staircase function as a discrete approximation of a continuous risk curve, a continuous risk curve can be approximated as the smoothed curve fitted to the staircase function. An example plot can be seen in Figure 1. This method was used to compare the risks associated with nuclear power plants with other man-made disasters by US Nuclear Regulatory Commission [1], where the risk curves were plotted on log-log scale [7].

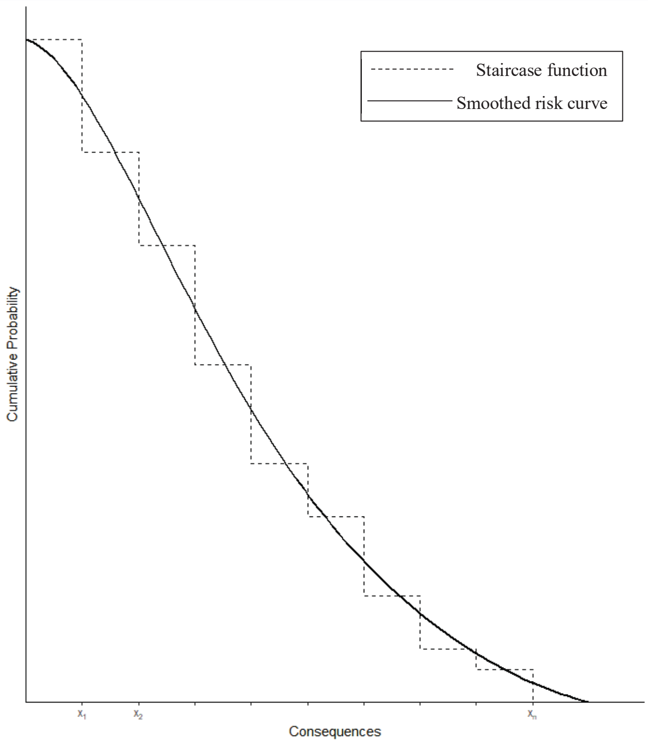

Figure 1: Risk curve resulting from plotting the consequences against the cumulative likelihood.

For completeness, Kaplan and Garrick [7] then introduce a final s_{N+1} scenario that acts as an "other" category, containing all possible scenarios that are not explicitly stated in the N scenarios that answer Question 1. This guides the assessor to consider the limitations of the assessment and give thought to events not listed as one of the N possible scenarios. Kaplan and Garrick [7] consider the "other" category of s_{N+1} as containing events that have not yet occurred. The fact that these events have not yet occurred in the assessed system, or any similar systems is a piece of knowledge that can be treated as evidence when applying Bayes' theorem to assign a likelihood.

Once the list of possible scenarios is completed, the associated likelihood of each is then calculated. The likelihood of a scenario can be expressed in one of three ways [23]. The first is as a frequency. This applies to events that are recurrent and the rate of occurrence is known. The second method for expressing the likelihood is as a probability. This is used when the event is not recurrent and thus there is no frequency of occurrence. The probability instead expresses the degree of belief that the event will occur given the knowledge and information available at the time of the assessment. This interpretation of probability is often referred to as subjective or Bayesian probability [24-26]. The final way in which the likelihood can be expressed is as a probability of a frequency. When the event is recurrent and the frequency of occurrence is unknown but there is some information and knowledge available to assess the frequency, then the likelihood is stated as a probability of the frequency.

When the likelihood is considered as a probability of a frequency, which Garrick [23] suggests as the preferred representation, the triplet expressing the quantitative definition of risk instead can be expressed as

$$R = \{\langle s_i, p_i(\phi_i), x_i \rangle\} \tag{2}$$

where $p_i(\phi_i)$ is the probability density function that expresses the assessor's state of knowledge of the frequency, ϕ_i. There is also uncertainty in the consequences associated with each scenario. The risk is being assessed for some time in the future and so the outcome cannot be known, which also results in uncertainty in the consequence of each scenario [7]. A joint distribution of the uncertainty in both the frequency and consequence can be used giving the quantitative definition of risk as

$$R = \{\langle s_i, p_i(\phi_i, x_i) \rangle\},\ i = 1, 2, \dots, N. \tag{3}$$

The risk is now communicated as a series of risk curves. This allows the uncertainty in both the frequency and magnitude of the consequences to be explicitly displayed within the results. Each curve represents a chosen fractile of the probability distribution of the of the consequence or loss level shown on the horizontal axis [27].

In practise, tools such as event tress and fault trees are used to quantify the risk. As discussed in Section 1, fault trees begin with a top event representing system failure which is then broken down into the preceding intermediate events that need to occur within the system so that the end state is reached [6]. They typically include "AND" and "OR" gates, with other, less common, gates also used when needed. From a fault tree, the minimum cut sets related to the end state can be found. A minimal cut set in the context of fault tree analysis provides the combination of the minimum number of events that need to occur such that the associated top event will be reached.

An event tree begins with an initiating event, such as a hurricane, and follows a path through the intermediate stages of the system to reach the end state, resulting in the associated consequence. Each branch in the event tree has an associated probability that the intermediate event will occur [6]. A simple example of an event tree is shown in Figure 2 where each intermediate event either occurs or does not.

The likelihood of an end state can be found by multiplying the frequency of the initiating event with the string of conditional probabilities of all intermediate events that result in that end state. For example, the likelihood of reaching the end state with consequence C_3 is

$$\phi(ES_{C_3}) = \phi(IE)\ \phi(A|IE)\ \phi(\bar{B}|A\ IE)\ \phi(C|\bar{B}\ A\ IE) \tag{4}$$

where $\phi(IE)$ is the frequency of the initiating event, $\phi(X|Y)$ is the frequency of the intermediate state X conditional on Y, and ES_{C_3} is the end state with consequence C_3. The expected consequence of the initiating event can be found by summing over the products of the likelihood and associated consequences of each end state. Once the expected consequence for each initiating event is calculated and ranked in order severity, the risk curve can be produced.

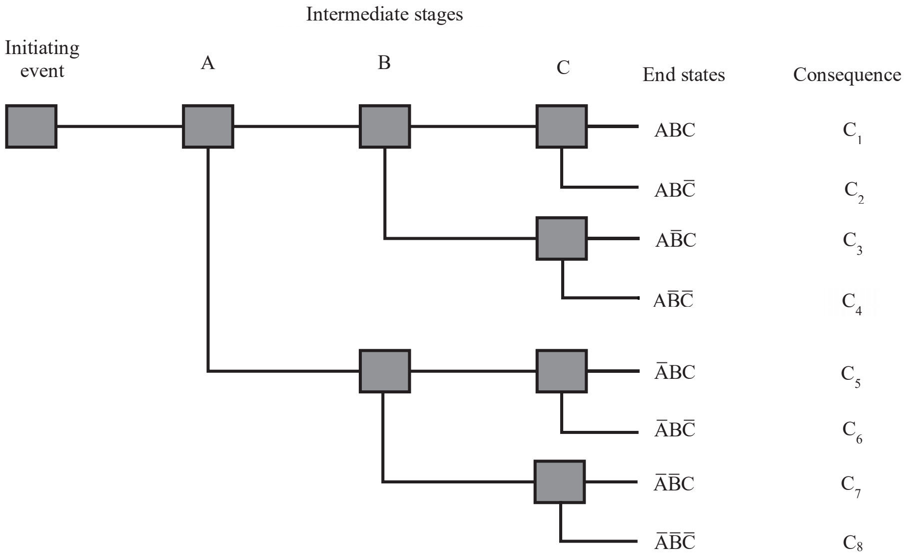

Figure 2: Example of an event tree.

When the frequency of the initiating event and the intermediate states are unknown, the likelihood is interpreted as probability of frequency. The severity of the consequences are also unknown and also are given as a probability. This instead results in a family of risk curves as previously discussed.

State enumeration and Monte Carlo simulation are common methods to analyse combinations of component failures during a risk assessment. Both methods enable the user to select the number of component states to be analysed. For simple assessments, the components are considered as only functional or failed. For more complex analysis, the component states can specify the level of functionality for components that can be partially functional. Some refer to the two methods separately [5, 28] while others use state enumeration as a blanket term which encompasses system state selection methods, which are referred to as Monte Carlo simulation and contingency enumeration [29].

State enumeration (or contingency enumeration) is used in practise when either the system being analysed, or the set of system states to be assessed are relatively small in size. A predetermined list of system states are used to analyse the system [30]. The probability of the system being in these specified states is calculated before assessing the consequences and risk associated with each state. A similar process is followed when using Monte Carlo simulation, but rather than a predetermined list of system states, system states are sampled based on the joint probability distribution of the component states [29], after which the consequences and risk associated with each state is calculated. When analysing a large system or evaluating a high order of contingencies, Monte Carlo simulation is the preferred method [29].

3 Infrastructure PRA formulation

In the most basic understanding, an infrastructure is a system of components that are, in the simplest realisation, either functioning or not. Once an initiating event has occurred within an infrastructure, the intermediate stages can then be thought of as the state change of components from the functional state to the non-functional state. Each component changes state depending on the initiating event and previous intermediate stages of the infrastructure. The end state will then be the combination of all components that have changed from the functioning to the non-functioning state, and the associated consequence of the component failure combination can be assessed.

To put this in context of the risk triplet, start with the consequence of a scenario s_i. The consequence is dependent upon the end state of the system, which can be expressed as $x_i(c_i)$ where $c_i = (c_i^1, c_i^2, \dots, c_i^N)$ is a vector of the component states for the n components within the system. Each c_i^j is binary expressing the state of the component j as functional (0) or non-functional (1), though this could be extended to multiple state components. The scenario, s_i, that results in consequence c_i is the occurrence of the initiating event, intermediate states and the end state of the system that results in consequence c_i. That is, the number of scenarios, N, would be equal to the number of possible end states. The event tree example shown in Figure 2 shows eight possible scenarios. The likelihood of scenario s_i is the joint likelihood of the initiating event occurring and the end state reached by the system. This can be expressed as $l_i = l(IE_i)l(c_i)$.

The main difficultly in performing PRA for infrastructure systems is the sheer size of the system. The number of components that are potentially affected when an initiating event occurs is vast in a large system such as an electrical power system. For example, the Pacific Gas and Electricity (PG&E) company in California provides electric power to 5.4 million customers over with over 120,000 circuit miles of power lines over an area of 70,000 square miles [31]. The number of components in such a system is likely in the millions, although a full enumeration has not been carried out for a system such as this.

For cases when the system being assessed is small, there may exist a workable number of minimal cut sets that can be used, reducing the complexity of the analysis. However, finding these minimal cut sets can also be challenging depending on the number and/or functionality of the components included within the system model. For larger systems, there may also exist a workable number of minimal cut sets, but even finding the minimal cut sets can have a large computational burden.

Now that a formulation of PRA for infrastructure systems has been developed, this can be applied to an infrastructure system to investigate the feasibility of performing PRA for infrastructure systems.

4 Infrastructure PRA example

To aid in the discussion of the feasibility of PRA for infrastructure, an example of applying the formulation expressed in the previous section to an infrastructure system is first completed. The PRA formulation will be applied to the virtual water system of Micropolis [32].

4.1 Micropolis water system

Micropolis is a virtual city developed by Brumbelow et al. [32] to aid infrastructure research. The aim of developing Micropolis is to provide open access data for infrastructure systems of a city without the need of data from real infrastructure systems. For our purposes, the water system of Micropolis will be used to illustrate how the PRA formulation from the previous section can be applied to an infrastructure system.

The water system of Micropolis has been modelled as if it has developed and expanded over a number of years. The “oldest” parts of the system are constructed as if it was built in 1910, with expansions and rehabilitations completed in 1950 and 1980. This results in an array of pipe materials and diameters. The primary input to the water system is from a surface reservoir, with the older source well now used as a back-up water supply. A water tank is also present in the system and is located in the centre of the city. The end users of the system are both residential and commercial buildings which have different demand patterns throughout a 24-hour period. The water system available from Brumbelow et al. [32] is modelled using EPANet [33]. The water distribution network of Micropolis can be seen in Figure 3.

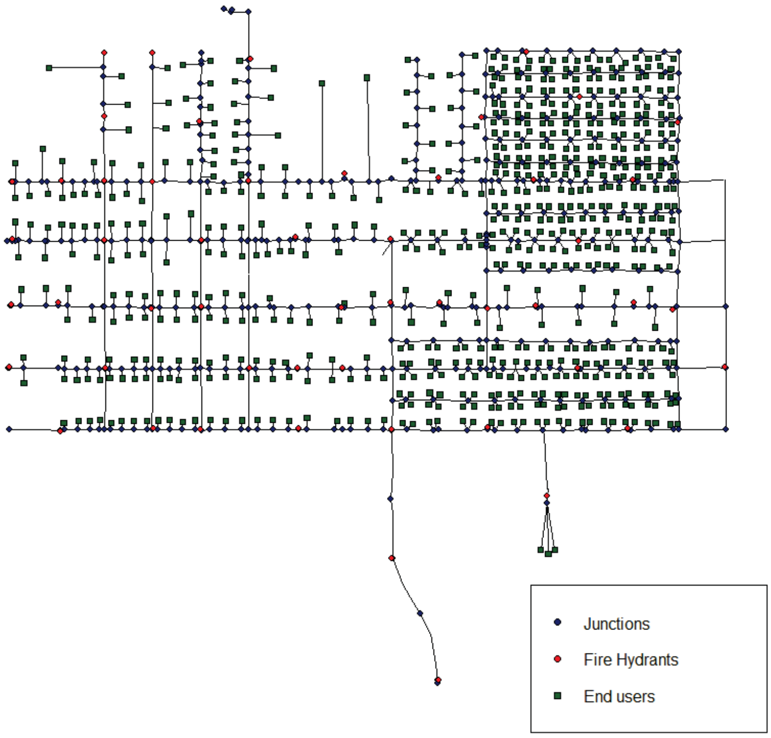

Figure 3: Distribution network of Micropolis water system.

4.2 PRA of Micropolis water system

To illustrate the PRA formulation provided in Section 3, an earthquake scenario was chosen to show the process involved in analysing one scenario within the PRA.

4.2.1 Simulation of earthquake scenario

To demonstrate the application of PRA, we used a single earthquake intensity scenario. To simulate an earthquake affecting the water distribution network of Micropolis the mean and standard deviation values for Peak Ground Velocity (PGV) were chosen to represent the PGV of an earthquake of magnitude 6 on the Modified Morcalli Intensity (MMI) scale [34]. Therefore, a normal distribution with mean of 5 and standard deviation of 1 was used to sample the PGV. The same PGV was then applied to all pipes in Micropolis given the small size of the city.

The probability of each pipe breaking given the PGV was then calculated. We used a model from ASCE [35] in which the probability of a pipe breaking depends on the length and the material of each pipe. First the failure rate per 1000ft is estimated for each pipe material, using the equation:

$$RR_{1000} = 0.0187 * K * PGV, \quad (5)$$

where K is adjustment factor depending on pipe material [35]. We are assessing the disruption to only the main pipes within the network, for which there are only three different types of materials in Micropolis. Table 1 shows the possible materials and the adjustment factor for each.

Table 1: Pipe material adjustment factor, K, used to calculate failure rate of water pipes.

Material	Adjustment factor (K)
Ductile iron	0.5
Cast iron	1.0
Asbestos cement	1.0

The failure rate per 1000ft is then adjusted for the length of each pipe, resulting in the failure rate for each pipe, RR. Given a Poisson distribution of the failure rate, the probability of at least one break in each pipe is

$$P(failure) = 1 - e^{-RR}. \quad (6)$$

Monte Carlo simulation was then used to find the state, failed or not, of each of the 651 main pipes within the network for 100,000 iterations. It is worth noting that the number of iterations to run was chosen arbitrarily for this example. For the purpose of presenting the example 100,000 iterations is relatively high number but is computationally inexpensive. When carrying out an actual PRA the number of iterations should be chosen based on convergence.

For each iteration, any failed pipes were assumed to be leaking 200 gallons per minute (gpm) and the simulation of the water system was run for 72 hours. In order to simulate a pipe leaking a demand of 200gpm was assigned to the end junction of the pipe. In the case where the pipe ended at a valve rather than a junction, the demand was assigned to the junction at the start of the pipe as a demand cannot be assigned to valves within EPANet. Although this is a somewhat simple method of simulating pipe leakage within EPANet, there exists no easily replicable method of simulating pipe leaks within a demand-driven hydraulic model like EPANet within the literature at this time [36-38]. For each simulated set of failed pipes, we then ran EPANet for a 72-hour run.

The consequences to the water system were measured as the number of terminal nodes that experienced insufficient pressure. Terminal nodes here refers to the system's end users, both residential and commercial buildings, as well as fire hydrants. There are 737 terminal nodes in the Micropolis water system network. For fire hydrant nodes, a failure was recorded when the pressure was below 20 psi as this is used as the standard in several U.S. states for baseline pressure needed for adequate fire-fighting [39]. For residential and commercial a failure was recorded when the pressure fell below 30 psi. Ghorbanian et al. [40] summarises current pressure standards for several countries, which range from 14 psi to 50 psi. 30 psi was chosen as a benchmark for buildings as this was roughly the median of the different countries pressure standards. It is worth noting that when the EPANet simulation of Micropolis is ran under normal conditions, only one pipe has a pressure below 20psi at 17 psi. The results of this Monte Carlo simulation can be seen in Figure 4.

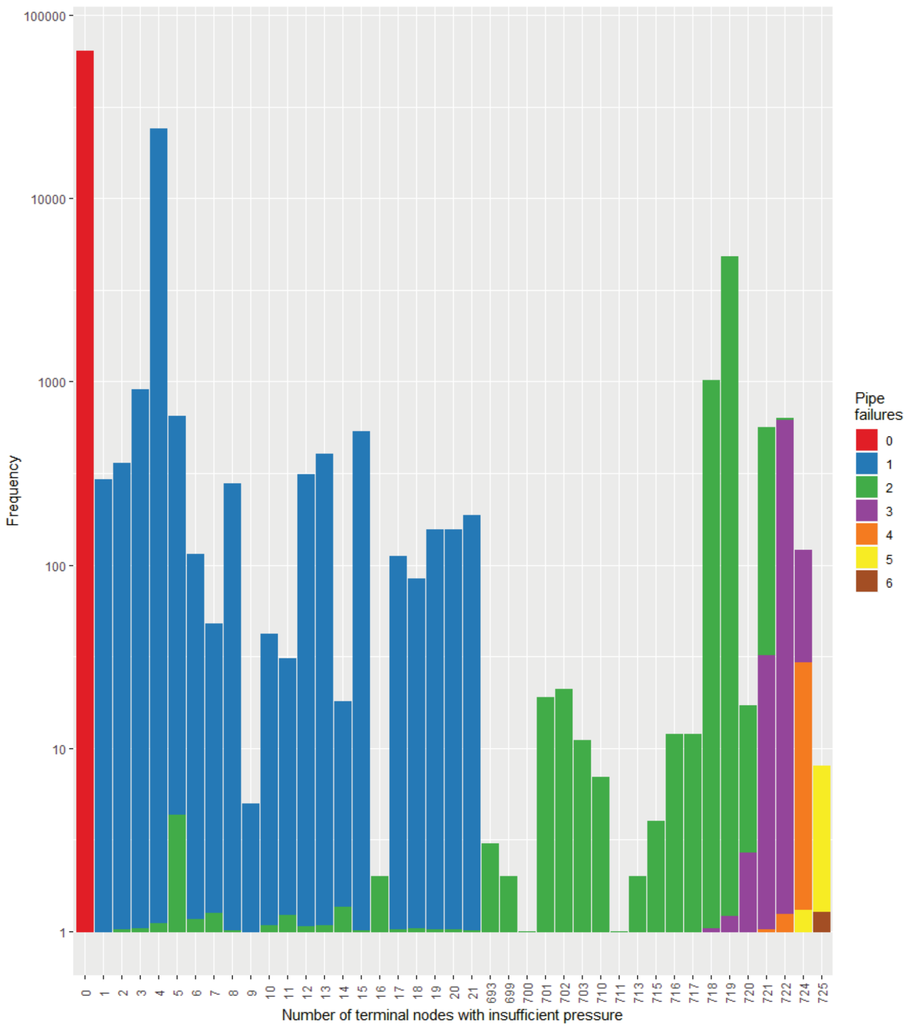

Figure 4: Results of the Monte Carlo simulation of 100,000 iterations showing the frequency of the number of terminal nodes had insufficient pressure on a log scale. The fill represents the number of pipes which failed due to the earthquake.

Figure 4 shows the frequency of terminal nodes which experienced insufficient pressure during the 72-hour EPANet simulation. It is worth noting that the frequencies are plotted on a log scale. For roughly two thirds of the 100,000 iterations (64,027) no pipes were affected by the earthquake and so there were no terminal nodes which experienced insufficient pressure. When pipe failures did occur due to the simulated earthquake, the majority of the simulations (24,004 of 35,973) resulted in 4 terminal nodes experiencing insufficient pressure. It is worth noting that there is a jump in the number of terminal nodes that experience insufficient pressure from 21 to 693, where no iterations resulted between 23 and 692 terminal nodes inclusively with significant loss of pressure during the simulation. This suggests there is a subset of pipe failures that have a relatively low effect on the water system and a subset of pipe failures that have a high impact on the water system.

4.2.2 PRA of earthquake scenario

The results of the Monte Carlo simulation of the effects of a magnitude 6 earthquake can also be presented as an FN curve, as shown in Figure 5. To complete the PRA of a scenario where an earthquake of magnitude 6 effects the Micropolis water system, the likelihood of this scenario occurring also needs to be calculated. However, as this is an illustration of how one would carry out PRA of infrastructure systems, and Micropolis is a virtual city, determining the likelihood of an earthquake of the given magnitude effecting the system is not particularly meaningful.

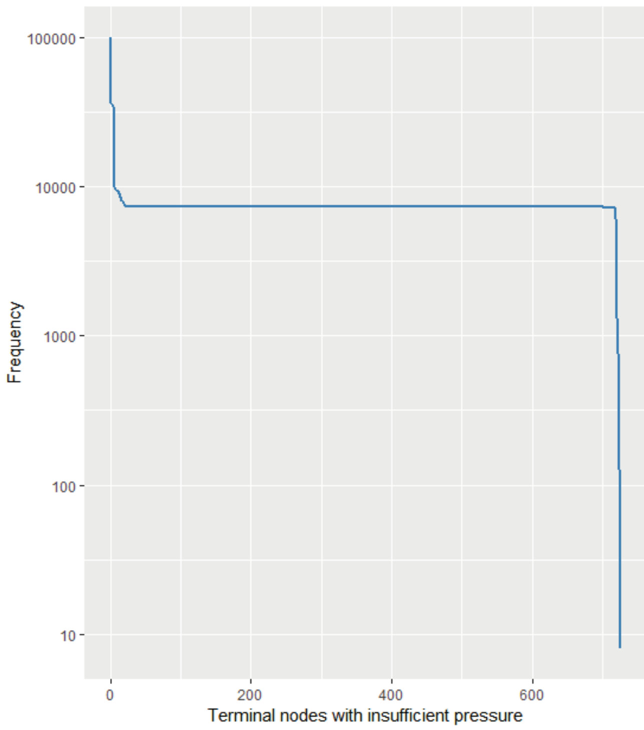

Figure 5: Cumulative frequency of terminal nodes with insufficient pressure due to an earthquake of magnitude 6 on the MMI scale, with a log scale on the y-axis.

To provide a full PRA of the water system of Micropolis, other scenarios must also be evaluated. These could include events such as a water tower leak, failure of components, such as pumps, improper treatment of water and so on. Earthquakes of different magnitudes could also be included. The likelihood and consequences of all scenarios would need to be assessed, as well as thinking about scenarios which have not yet occurred.

4.2.3 Complexity of infrastructure PRA

Even for a relatively small water system such as Micropolis the number of components within the systems is large. For the analysis of the magnitude 6 earthquake presented in Section 4.2.1

assumptions have been made which simplify the scenario to one which can be assessed, and the run times of the simulations are reasonable. For all scenario assessments within PRA, assumptions are made and these can often, although not intentionally, lead to results that can be misleading. There is a trade-off between the comprehensiveness of the analysis and the time available to perform the analysis as well as the level of information currently available.

Scenarios also need to be included which look at combinations of single scenarios which have the potential to occur at the same time. For example, if an earthquake does occur it could not only results in pipe breaks (as analysed above) but could also result in damage within the water treatment centre which results in a fire. There is also the possibility of the earthquake causing disruption to another infrastructure which the water system is dependent upon, for example the electricity power system. This could result in other components such as the pumps not functioning correctly and increasing the severity of the consequences.

PRA of an infrastructure is time consuming and requires large quantities of data. This can become expensive for infrastructure owners and managers. Depending on the procedures, many utilities do not keep the relevant data or do have the information available but it would need to be processed before being useful to the assessor. This again needs resources to be allocated that may not be available within the company's budget. Instead expert knowledge would be relied upon.

5 Comparison of infrastructure risk analysis methods

Although PRA is used within the nuclear power industry, other methods have developed which are more prevalent in other infrastructure sectors. This section aims to give a brief review of some of these methods and discuss which elements of PRA are covered and what would need to be included to better approximate PRA results. The methods chosen to compare with PRA are those which contain elements that can be related to PRA. There are other methods such as inoperability input-output methods which are also used to assess infrastructure but are not directly relatable to PRA.

The first method considered is *N-1* analysis, and the extension to *N-k* analysis. *N-1* analysis is common in the electricity sector of the USA due to regulations enforcing that generation and transmission systems should be able to function with the loss of one element, such as transformers or generators [17]. This has been extended to cases of *N-k* analysis where k components become non-functional simultaneously, or in a close time frame. This analysis allows the assessor to see which components, or combination of components are the most critical if non-functional and can provide direction on how to harden the system to ensure if these critical components are not functional that the system still performs as needed/expected.

In terms of PRA analysis, *N-k* analysis allows the consequences of system states to be assessed and easily compared. It contains elements of state (or contingency) enumeration, where the predetermined list of system states to assess is all possible combinations where k of the main components are non-functional. However, the likelihood of each component failure in the *N-1* analysis, or combination of component failures in *N-k* analysis is not considered. Components or combination of components which have large consequences when non-functional may be given focus when ideally, if the likelihood of failure was included, other components or combination of components which are more likely to fail should be given more attention. Hardening such components may lead to a better decrease in the overall risk of system.

Network models allow investigation of how initial failures or events within a system can internally cascade. The network is constructed such that the nodes represent components, or the important components, of the systems and the edges the connections between these components

[41]. It is usual for the edges to represent physical connections, such as pipelines as seen in Figure 3 where the nodes represent the end users and pipe junctions. However, the edges can also represent non-physical connections such as the sharing of information between two components.

Network models can be used to see the effect of a subset of the nodes and/or edges being non-functional, which is modelled by removing such nodes/edges from the network. These initial node or edge removals are commonly chosen either randomly or due to some characteristic, such as type of node, nodal degree (number of connections a node has) or spatial position [22, 42-44]. These two methods respectively represent either random failures, often attributed to the random failing of a component due to age etc., or targeted attacks, where the intention is to cause the greatest disruption possible when targeting a low percentage of nodes/edges within the system.

Some uses of network models include only the topology or structure of the network, whereas others also incorporate the flow of the infrastructure commodity within the network [41]. This could be the flow of water through a distribution system or electricity within a power system. This allows a more realistic assessment of how the consequences related to the system states assessed. Including the flow of water within a distribution system allows not only the nodes are not able to receive water to be identified, but also which nodes cannot receive water due to insufficient pressure within the system.

As with *N-1* and *N-k* analysis, network models allow different system states to be investigated but again the probability of these states occurring due to initiating events is not considered. When node/edge removals are randomly chosen, this is comparable with Monte Carlo simulation to find system states to investigate, however the probability of each node/edge failing is equal within the system. When the nodes/edges are chosen due to a characteristic, this is more in line with state enumeration, where the system states to be assessed are pre-determined.

Network models have also been used as a way to assess the cascading effects associated with interdependencies between infrastructures. As technology and society has developed, critical infrastructure systems have become more reliant on each other. Many systems require the input of electrical power to perform efficiently. For example, water distribution systems need electricity to run pumps and treatment plants and transportation systems need electricity to enable signals to function. The use of Supervisory Control and Data Acquisition (SCADA) systems within other infrastructures such as electricity plants to automate the rerouting of power transmission to prevent overheating of power lines is another example of these dependencies.

Johansson and Hassel [45] provide an example of an electric railway network and four systems it is dependent on to function. They describe two models used: a network model and a functional model. The functional model referred to is one that incorporates the flow of commodity and checks that it is sufficient for the nodes/edges to function within the system. The two models are used to find the vulnerability of the railway system to failures that occur within the systems it depends upon. Including interdependent systems allows the reason for initial failures, or first intermediate state, in one system to be seen, but as with independent network analysis, the probability of these failures occurring is still not considered.

Statistical learning theory is a method of assessing critical infrastructure with a focus on natural hazard disruptions. It involves using present knowledge to develop statistical models to estimate the impacts that natural events, such as hurricanes, have on critical infrastructure. The explanatory variables cover both aspects of the critical infrastructure system, the surrounding environment and characteristics of the natural hazard [10]. For example, Han et al. [46] developed a model to estimate the number of customers without power after a hurricane event in the Gulf Coast region. The model did not use a network of the power system, but instead a grid was superimposed over the assessed space and the number of customers, transformers, poles switches and miles of overhead lines for each grid was known. The model also used variables that characterised the hurricane and the area of each grid including land use, soil type and precipitation. The model was developed and trained on past hurricane events and the corresponding data.

Statistical learning theory methods of assessing infrastructure express the consequences of a given scenario. Therefore, they could be used to assess natural hazard scenarios within PRA, given that sufficient relevant data is available. The probability of the intermediate and end states are used within the model to arrive at the resulting consequences; however, the model does not explicitly state these. The method has been developed to be used when there is an indication that an event is occurring and thus does not explore the probability of the initiating event (such as a hurricane).

Winkler et al. [47] and Ouyang and Duenas-Osorio [48] have both used a hurricane model, developed using statistical learning theory, and a network model to assess electric power systems. The hurricane model is used to assign failure likelihood to components of the power network, which are used to choose which nodes, and edges fail. The performance of the electric power system is assessed after the disruptions have affected the network flow model. This combination of the two methods provides the likelihood of the first intermediate state of the system to be found. However, the likelihood of all proceeding intermediate and end states are assumed to be one, given the event occurs. In reality, this may not be the case. The probability of the scenario occurring, in these examples the hurricane, is also still not assessed.

6 Discussion

Although PRA gained popularity with the development of nuclear power system for assessing the risks associated with the systems in the 1970s, it is not commonly used to assess networked infrastructure such as water, power, and sewer systems. The two main reasons are resource and data availability. It takes considerable time and input from many people, both internal and external, to develop a full PRA for a given infrastructure system. This imposes high cost on an infrastructure management organisation. The complexity and size of the system means identifying those who have the knowledge needed to assess a certain area or subsystem of the infrastructure can be difficult. Collection of relevant data for the assessment can also be difficult. It can be expensive and time consuming to collate, although this is becoming easier with technological advancements. Knowing which information is needed is also challenging and may be a process of trial and error. Such impediments can deter organisations from investing in data collection. Therefore, many organisations do not have the data and experts needed to identify all states, assign probabilities to them and estimate their consequences.

Infrastructure systems are also becoming more complex as technology advances, particularly through more widespread adaption of automation and SCADA systems. These make the system more difficult to understand and model, which can also lead to an increase in the events that have not yet occurred, which are more complex to assess. As new technologies are developed and used, the more limited the assessors' knowledge of the system becomes and thus more uncertainty that is present in the analysis.

PRA also becomes even more complex when incorporating interdependencies within the analysis. The interdependencies between the different systems are especially noticeable when large natural hazards such as earthquakes and hurricanes occur. These large-scale scenarios have the potential to affect several systems at once, leading to larger consequences than when only one system is affected. Many infrastructure systems are privately owned and for safety and security reasons it is not common to willing share information with other systems. This makes assigning a likelihood of failure difficult when an event in a different infrastructure system that we have limited knowledge of is the initiating event of a scenario.

7 Conclusion

The use of PRA to assess the risk associated with an infrastructure system provides, in theory, a comprehensive assessment. The results show not only the consequences related to each possible scenario but also the associated likelihood. However, in practise performing a PRA for a full infrastructure system is very complex and expensive. This makes it unlikely to be fully implemented in practise.

The example using the Micropolis water distribution system demonstrates that even the analysis of a single scenario for a small, synthetic system is complex. Micropolis is a virtual city, where there is complete information available about the water distribution system. However, for real infrastructure systems such detailed information may not be available or easily accessible by the assessor. Even with access to the complete water distribution system data of Micropolis the assessment is complex. To reduce the complexity and allow for timely scenario assessments, assumptions have to be made and the level of detail at which to model the system is decided, both of which can influence the results. For the example presented in Section 4, only damage to main pipes was included in the model. This could be extended by also including damage to other component types such as the water tower and pumps but would add to the computational burden of the analysis. Such trade-offs and assumptions are common not just for PRA, but for all methods of risk analysis. However, due to the number of different scenarios assessed during PRA, this can be more time consuming than for other analysis methods.

Due to the intricacy of performing PRA for infrastructure systems, other methods such as network models or N-k analysis are more common when assessing such systems. These methods are less complex than PRA which is why they are preferred in practice. However, they tend to encompass an assessment of the system for only a handful of given events or scenarios and not all possible scenarios. They also often do not consider the probabilities of different damage scenarios. Different methods are favoured for different types of scenarios, which does not allow for an easy comparison of the results. However, the results for PRA are presented in such a way that allows for comparison of all possible scenarios.

Although practically implementing PRA within an infrastructure setting is not feasible, some elements of PRA that are not yet covered by other methods should be included into the analysis of infrastructure systems. The likelihoods associated with both the occurrence of a scenario and the resulting consequences need to be present within infrastructure assessments. Methods more common in infrastructure analysis tend not to include this aspect.

REFERENCES

[1] US Nuclear Regulatory Commission, *Reactor Safety Study. Wash 1400.* NUREG, 1975. **75**: p. 104.

[2] Apostolakis, G. and Kafka, P., *Advances in probabilistic safety assessment.* Nuclear engineering and design, 1992. **134**(1): p. 141-148.

[3] Bedford, T. and Cooke, R., *Probabilistic risk analysis: foundations and methods*. 2001: Cambridge University Press.

[4] Apostolakis, G.E., *How useful is quantitative risk assessment?* Risk Analysis: An International Journal, 2004. **24**(3): p. 515-520.

[5] Li, W., *Risk assessment of power systems: models, methods, and applications*. 2014: John Wiley & Sons.

[6] Holmberg, J., *Quantitative Risk Analysis*, in *Handbook of Safety Principles*, N. Moller, et al., Editors. 2018.

[7] Kaplan, S. and Garrick, B.J., *On the quantitative definition of risk.* Risk analysis, 1981. **1**(1): p. 11-27.

[8] Lindhe, A., Rosén, L., Norberg, T., and Bergstedt, O., *Fault tree analysis for integrated and probabilistic risk analysis of drinking water systems.* Water research, 2009. **43**(6): p. 1641-1653.

[9] ten Veldhuis, J.A., Clemens, F.H., and van Gelder, P.H., *Quantitative fault tree analysis for urban water infrastructure flooding.* Structure and Infrastructure Engineering, 2011. **7**(11): p. 809-821.

[10] Guikema, S.D., *Natural disaster risk analysis for critical infrastructure systems: An approach based on statistical learning theory.* Reliability Engineering & System Safety, 2009. **94**(4): p. 855-860.

[11] Ouyang, M., *Review on modeling and simulation of interdependent critical infrastructure systems.* Reliability Engineering & System Safety, 2014. **121**: p. 43-60.

[12] Newman, M., *Networks: An Introduction*. 2010: Oxford University Press.

[13] Erath, A., Birdsall, J., Axhausen, K.W., and Hajdin, R., *Vulnerability assessment methodology for Swiss road network.* Transportation Research Record, 2009. **2137**(1): p. 118-126.

[14] Sullivan, J., Novak, D., Aultman-Hall, L., and Scott, D.M., *Identifying critical road segments and measuring system-wide robustness in transportation networks with isolating links: A link-based capacity-reduction approach.* Transportation Research Part A: Policy and Practice, 2010. **44**(5): p. 323-336.

[15] Matisziw, T.C. and Murray, A.T., *Modeling s–t path availability to support disaster vulnerability assessment of network infrastructure.* Computers & Operations Research, 2009. **36**(1): p. 16-26.

[16] Matisziw, T.C., Murray, A.T., and Grubesic, T.H., *Bounding network interdiction vulnerability through cutset identification*, in *Critical Infrastructure*. 2007, Springer. p. 243-256.

[17] U.S. Department of Energy, *United States Electricity Industry Primer*, U.S. Department of Energy, Editor. 2015.

[18] Chen, Q. and McCalley, J.D., *Identifying high risk Nk contingencies for online security assessment.* IEEE Transactions on Power Systems, 2005. **20**(2): p. 823-834.

[19] Arroyo, J.M. and Fernández, F.J., *Application of a genetic algorithm to n-K power system security assessment.* International Journal of Electrical Power & Energy Systems, 2013. **49**: p. 114-121.

[20] Mori, H. and Goto, Y. *A tabu search based approach to (Nk) static contingency selection in power systems.* in *2001 IEEE International Conference on Systems, Man*

and Cybernetics. e-Systems and e-Man for Cybernetics in Cyberspace (Cat. No. 01CH37236). 2001. IEEE.
[21] Kim, D.-H. and Motter, A.E., *Fluctuation-driven capacity distribution in complex networks.* New Journal of Physics, 2008. **10**(5): p. 053022.
[22] LaRocca, S. and Guikema, S.D., *Characterizing and predicting the robustness of power-law networks.* Reliability Engineering & System Safety, 2015. **133**: p. 157-166.
[23] Garrick, B.J., *Chapter 2 - Analytical Foundations of Quantitative Risk Assessment*, in *Quantifying and Controlling Catastrophic Risks*, B.J. Garrick, Editor. 2008, Academic Press: Boston. p. 17-31.
[24] Singpurwalla, N.D. and Wilson, A.G., *Probability, chance and the probability of chance.* IIE Transactions, 2008. **41**(1): p. 12-22.
[25] Lindley, D.V., *The philosophy of statistics.* Journal of the Royal Statistical Society: Series D (The Statistician), 2000. **49**(3): p. 293-337.
[26] Aven, T. and Reniers, G., *How to define and interpret a probability in a risk and safety setting.* Safety science, 2013. **51**(1): p. 223-231.
[27] Paté-Cornell, E., *On "Black Swans" and "Perfect Storms": risk analysis and management when statistics are not enough.* Risk Analysis: An International Journal, 2012. **32**(11): p. 1823-1833.
[28] Mousavi, O.A., Cherkaoui, R., and Bozorg, M., *Blackouts risk evaluation by Monte Carlo Simulation regarding cascading outages and system frequency deviation.* Electric Power Systems Research, 2012. **89**: p. 157-164.
[29] Rei, A.M. and Schilling, M.T., *Reliability assessment of the Brazilian power system using enumeration and Monte Carlo.* IEEE Transactions on Power Systems, 2008. **23**(3): p. 1480-1487.
[30] Hua, B., Bie, Z., Liu, C., Li, G., and Wang, X., *Eliminating redundant line flow constraints in composite system reliability evaluation.* IEEE Transactions on Power Systems, 2013. **28**(3): p. 3490-3498.
[31] PG&E. *Company profile.* 2019 [cited 2019 23 May]; Available from: https://www.pge.com/en_US/about-pge/company-information/profile/profile.page.
[32] Brumbelow, K., Torres, J., Guikema, S., Bristow, E., and Kanta, L. *Virtual cities for water distribution and infrastructure system research.* in *World Environmental and Water Resources Congress*. 2007.
[33] Rossman, L., *EPANET 2 Users Manual*, O.o.R.D. National Risk Management Laboratory, US Environmental Protection Agency, Cincinnati, OH, Editor. 2000.
[34] Wald, D.J., Quitoriano, V., Heaton, T.H., and Kanamori, H., *Relationships between Peak Ground Acceleration, Peak Ground Velocity, and Modified Mercalli Intensity in California.* Earthquake Spectra, 1999. **15**(3): p. 557-564.
[35] ASCE, *Seismic fragility formulations for water systems.* Technical report, American Society of Civil Engineers, 2001.
[36] Javanbarg, M. and Takada, S. *Seismic reliability assessment of water supply systems.* in *Proceedings 10th international conference on structural safety and reliability, Osaka*. 2009.
[37] Yoo, D.G., Jung, D., Kang, D., Kim, J.H., and Lansey, K., *Seismic hazard assessment model for urban water supply networks.* Journal of Water Resources Planning and Management, 2015. **142**(2): p. 04015055.
[38] Klise, K.A., Bynum, M., Moriarty, D., and Murray, R., *A software framework for assessing the resilience of drinking water systems to disasters with an example earthquake case study.* Environmental Modelling & Software, 2017. **95**: p. 420-431.
[39] GLUMR Board. *Recommended standards for water works: Great Lakes--Upper Mississippi River Board of State Public Health Environmental Managers. Water Supply*

Committee. 2012 [cited 2019 29 August]; Available from: https://www.broward.org/WaterServices/Documents/states_standards_water.pdf.

[40] Ghorbanian, V., Karney, B., and Guo, Y., *Pressure Standards in Water Distribution Systems: Reflection on Current Practice with Consideration of Some Unresolved Issues.* Journal of Water Resources Planning and Management, 2016. **142**(8): p. 04016023.

[41] Ouyang, M., Hong, L., Mao, Z.-J., Yu, M.-H., and Qi, F., *A methodological approach to analyze vulnerability of interdependent infrastructures.* Simulation Modelling Practice and Theory, 2009. **17**(5): p. 817-828.

[42] Gallos, L.K., Cohen, R., Argyrakis, P., Bunde, A., and Havlin, S., *Stability and topology of scale-free networks under attack and defense strategies.* Physical review letters, 2005. **94**(18): p. 188701.

[43] Shao, S., Huang, X., Stanley, H.E., and Havlin, S., *Percolation of localized attack on complex networks.* New Journal of Physics, 2015. **17**(2): p. 023049.

[44] Johnson, C.A., Flage, R., and Guikema, S.D., *Characterising the robustness of coupled power-law networks.* Reliability Engineering & System Safety, 2019. **191**: p. 106560.

[45] Johansson, J. and Hassel, H., *An approach for modellng interdependent infrastructures in the context of vulnerability analysis.* Reliability Engineering and System Safety, 2010. **95**: p. 1335-1344.

[46] Han, S.-R., Guikema, S.D., Quiring, S.M., Lee, K.-H., Rosowsky, D., and Davidson, R.A., *Estimating the spatial distribution of power outages during hurricanes in the Gulf coast region.* Reliability Engineering & System Safety, 2009. **94**(2): p. 199-210.

[47] Winkler, J., Dueñas-Osorio, L., Stein, R., and Subramanian, D., *Performance assessment of topologically diverse power systems subjected to hurricane events.* Reliability Engineering & System Safety, 2010. **95**(4): p. 323-336.

[48] Ouyang, M. and Duenas-Osorio, L., *Multi-dimensional hurricane resilience assessment of electric power systems.* Structural Safety, 2014. **48**: p. 15-24.